

POLITECNICO DI TORINO

Collegio di Ingegneria Elettrica

**Corso di Laurea Magistrale
in Ingegneria Elettrica**

Tesi di Laurea Magistrale

Interface algorithms for a multi-site platform for real-time co-simulation of power systems



Relatore

prof. Ettore Bompard

Correlatori

prof. Antonello Monti
Marija Stevic, MSc

Candidato

Walter Fusto

Luglio 2017

To my family and friends

Acknowledgements

The aim of my thesis work was to find solutions to overcome issues when connecting two simulators geographically far one from another. Basically, it was about trying to make a long distance shorter, from Germany to Italy. And I like the idea to make countries closer, because it means also making people closer. I've been living 9 months in a foreign country and I met people from all over the world, I've been travelling to get to know new cultures and experience brand new things. But overall, I came to realize how amazing people can be, regardless of where they come from.

And of course, I managed to write my thesis in the meanwhile.

It wouldn't have been possible without the continuous and caring support of my family, my parents and my brother, the people I love the most in this world, without whom I wouldn't be the person I am today.

To my friends, the ones I've been knowing since I was a child and the ones I've met when I was older, you are one of the reasons why I am so thankful about my life, that you make so full.

To the people I met during those months abroad: I'm proud to call some of you friends by now. This moment is not a goodbye, it's the beginning of a connection I hope we'll never lose.

Last but not least, to my professors in Turin and in Aachen, for giving me the possibility to have such an important and great experience and for their support, and to my supervisor, for the motivational and inspiring abilities and aptitude in helping me in spite of the geographical distance.

Lo scopo del mio lavoro di tesi è stato trovare soluzioni per rimediare ai problemi che sorgono quando si collegano due simulatori geograficamente distanti l'uno dall'altro. Sostanzialmente, si tratta di rendere una lunga distanza più corta, dalla Germania all'Italia. E mi piace l'idea di rendere due paesi più vicini, perché significa anche rendere le persone più vicine. Ho vissuto per 9 mesi in un paese straniero e ho conosciuto persone provenienti da tutto il mondo, ho viaggiato per conoscere nuove culture e provare esperienze totalmente nuove. Ma in generale, sono riuscito a capire quanto le persone possano essere fantastiche, indipendentemente da dove provengano.

E ovviamente, sono riuscito a scrivere la mia tesi nel frattempo.

Non sarebbe stato possibile senza il continuo grande supporto della mia famiglia, i miei genitori e mio fratello, le persone che amo di più in questo mondo, senza i quali non sarei la persona che sono oggi.

Ai miei amici, quelli che conosco da quando ero un bambino e quelli che ho conosciuto quando ero più grande, siete una delle ragioni per cui sono così grato della mia vita, che rendete così piena.

Alle persone che ho conosciuto durante questi mesi all'estero: sono fiero di poter chiamare alcuni di voi amici ormai. Questo momento non è una fine, è l'inizio di una connessione che spero non perderemo mai.

Ultimi ma non meno importanti, ai miei professori, a Torino e ad Aachen, per avermi dato la possibilità di un'esperienza così importante e fondamentale, e alla mia supervisor, per il lavoro ammirevole e pieno di motivazione che ha svolto aiutandomi nonostante la distanza geografica.

A tutti voi: grazie mille.

Table of contents

Acknowledgements	II
Table of contents	IV
List of figures	IV
1. Introduction	1
1.1 Digital real-time simulation	1
1.2 Distributed co-simulation	3
1.2.1 System decoupling	4
1.2.2 Communication interface	4
1.2.3 Interface algorithms	5
1.3 Focus and contribution of the thesis	5
1.3.1 Thesis structure	7
2. Related work	9
2.1 Parallel real-time simulation	9
2.2 Power Hardware-In-the-Loop	10
2.3 Applications of Internet-distributed PHIL in automotive engineering	11
2.4 Energy conservation approaches	12
2.5 Bilateral teleoperation	14
2.5.1 Wave transformation	15
2.5.2 Direct force-reflection	16
2.5.3 Passivity control	17
2.6 Networked Control Systems	18
3. Background	21
3.1 PHIL interface algorithms	21
3.1.1 Ideal Transformer Method (ITM)	21
3.1.2 Time-variant First-order Approximation (TFA)	25
3.2 Bilateral teleoperation methods	28
3.2.1 Passivity formalism	28
3.2.2 Wave transformation	29
3.2.3 Main issues of the method	31
3.3 Representation of interface quantities	34
3.3.1 Dynamic phasors theory	34
3.3.2 Time-frequency interface quantities for co-simulation	36
4. Co-simulation interface algorithms	39

4.1	Co-simulation interface algorithm based on Time-variant First-order Approximation	39
4.1.1	Description of the modified algorithm in time-domain	40
4.1.2	Modification of the algorithm using dynamic phasors	41
4.1.3	Issues of the interface	42
4.2	Co-simulation interface algorithm based on Wave Transformation	44
4.2.1	Adaption of the interface to electrical systems	44
4.2.2	Modification of the method using dynamic phasors	47
4.2.1	Algebraic loop in the wave transformation-based interfaces	49
4.3	Implementation of the interfaces	49
4.3.1	Models used for simulation	50
4.3.2	Simulation case I: stability test using certain circuit parameters	51
4.3.3	Simulation case II: performance with large and variable interface time-delay	53
4.3.4	Simulation case III: performance using DC voltage sources	57
5.	Accuracy evaluation based on signal and energy residuals	60
5.1	Definition of metrics for co-simulation	60
5.1.1	Absolute signal and power errors	61
5.1.2	Relative signal errors: signal “residuals”	61
5.1.3	Power and energy residuals	62
5.1.4	Error estimation based on power and energy residuals	64
5.2	Accuracy evaluation of the interface algorithms	64
5.2.1	Implementation and suitability of the metrics	65
5.3	Steady-state accuracy evaluation of interface algorithms	69
5.3.1	Evaluation using a simple single-phase circuit	70
5.3.2	Evaluation using a three-phase power system	71
5.4	Transient state accuracy evaluation of interface algorithms	74
5.4.1	Evaluation considering single-phase transients	74
5.4.2	Accuracy considering three-phase transients	78
6.	Application to realistic power systems	81
6.1	Co-simulation of an HVDC Transmission Link	82
6.1.1	Description of the model	83
6.1.2	Simulation set-up	83
6.1.3	Simulation results	84
6.1.4	Accuracy evaluation	86
6.2	Co-simulation of a Transmission Network and a Distribution Network	89
6.2.1	Description of the model used for co-simulation	90
6.2.1	Co-simulation set-up	91
6.2.2	Simulation results	92
6.2.3	Transmission-distribution networks interaction	95
6.2.4	Accuracy evaluation	97
7.	Conclusions and future work	101
7.1	Conclusions	101
7.2	Future work	102

List of figures

Figure 1.1.1: Offline and real-time simulation [1]	2
Figure 1.2.1: Example of co-simulation [4]	4
Figure 1.2.2: Role of IA in a co-simulation set-up	5
Figure 2.1.1: Virtual decoupling in SSN	10
Figure 2.2.1: PHIL set-up for simulation	11
Figure 2.4.1: Different integration time-step introduce residual power in co-simulation, compromising accuracy and stability	13
Figure 2.5.1: Concept of teleoperation system [18]	15
Figure 2.5.2: Clarification of the two types of control architectures [19]	15
Figure 2.6.1: Single-loop NCS architecture	19
Figure 3.1.1: Original circuit used to illustrate PHIL IA	21
Figure 3.1.2: ITM-IV interface	22
Figure 3.1.3: Simulation results of a stable PHIL simulation using ITM-IV interface	23
Figure 3.1.4: Simulation results of an unstable PHIL simulation using ITM-IV interface	23
Figure 3.1.5: ITM-VI interface	24
Figure 3.1.6: Simulation results of a PHIL simulation using ITM-IV interface with a large time-delay	24
Figure 3.1.7: TFA-IV interface topology	25
Figure 3.1.8: TFA-VI interface topology	26
Figure 3.1.9: Simulation results of a PHIL simulation using TFA-IV interface with a small time-delay	27
Figure 3.1.10: Simulation results of a PHIL simulation using TFA-IV interface with a large time-delay	28
Figure 3.2.1: Wave transformation using x_1 and F_2 as inputs	30
Figure 3.2.2: Wave transmission with matched terminations	32
Figure 3.2.3: Algebraic loop arising at the connection between wave transformation and environment	33
Figure 3.3.1: Co-simulation interface based on ITM and using DP	36
Figure 3.3.2: Simulation result using ITM-IV interface with a large time-delay, using DP to exchange information over the communication	37
Figure 4.1.1: Modified TFA interface algorithm implemented on both sides of decoupled system for co-simulation	39
Figure 4.1.2: Simulation result of a simple voltage divider circuit using original TFA and modified TFA interfaces	41
Figure 4.1.3: Results of simulation of the simple voltage divider circuit using the modified TFA interface using DP, initialized for the first 0.2 s of simulation	44
Figure 4.2.1: WT-VI interface	45
Figure 4.2.2: WT-IV interface	46
Figure 4.2.3: Results of simulation using both WT-IV type and WT-VI interfaces, showing equal stability in both cases with parameters of the circuit that make ITM interface unstable	47
Figure 4.2.4: WT-IV interface using DP as interface quantities	47
Figure 4.2.5: Results of simulation of the simple voltage divider circuit using the WT-IV interface in time-domain with a large variable interface delay in communication	48
Figure 4.2.6: Results of simulation of the simple voltage divider circuit using the WT-IV interface with dynamic phasors, with a large variable interface delay in communication	49
Figure 4.3.1: Simple circuit A	50
Figure 4.3.2: Single line diagram of simple power system B	50

Figure 4.3.3: Definition of variables names for simulation results	51
Figure 4.3.4: Results of simulation of circuit A showing stability of wave transformation interfaces	52
Figure 4.3.5: Results of simulation of circuit B showing stability of WT and TFA interfaces	52
Figure 4.3.6: Artificial time-delay over simulation time. Initial value: $5 \cdot T_s$. At $t = 0.1$ s delay increases to $300 \cdot T_s$. At $t = 0.2$ s delay becomes variable	53
Figure 4.3.7: Results of simulation for circuit A using TD interfaces, with a variable time-delay over the simulation time	54
Figure 4.3.8: Simulation results of circuit A with WT interface considering only a large interface time-delay (15 ms) and an adjusted wave impedance ($b = 10 \Omega$)	55
Figure 4.3.9: Results of simulation for circuit A using DP-based interfaces, with a variable time-delay over the simulation time	55
Figure 4.3.10: Results of simulation for circuit B using TD interfaces, with a variable time-delay over the simulation time	56
Figure 4.3.11: Results of simulation for circuit B using DP-based interfaces, with a variable time-delay over the simulation time	57
Figure 4.3.12: Results of simulation for circuit A using DC voltage source and a fixed time-delay $\Delta T = 15$ ms	58
Figure 5.1.1: Explanation of defining relative errors between coupling variables for a co-simulation set-up	62
Figure 5.2.1: Simulation results for the simple voltage divider circuit using several IAs	66
Figure 5.2.2: Absolute signal errors for the simple voltage divider circuit using several IAs.	66
Figure 5.2.3: Absolute power errors for the simple voltage divider circuit using several IAs	67
Figure 5.2.4: Signal residuals for the simple voltage divider circuit using several IAs.....	68
Figure 5.2.5: Power residuals for the simple voltage divider circuit using several IAs.....	69
Figure 5.2.6: Energy residuals (top) and absolute energy errors (bottom) for the simple voltage divider circuit using several IAs.....	69
Figure 5.3.1: Signal residuals for circuit A in steady state, with two different levels of time-delay	70
Figure 5.3.2: Power residuals for circuit A in steady state, with two different levels of time-delay	71
Figure 5.3.3: Energy residuals for circuit A in steady state, with two different levels of time-delay	71
Figure 5.3.4: Signal residuals for circuit B in steady state, with two different levels of time-delay	72
Figure 5.3.5: Power residuals for circuit B in steady state, with two different levels of time-delay	73
Figure 5.3.6: Energy residuals for circuit B in steady state, with two different levels of time-delay	73
Figure 5.4.1: Waveforms of the integrated circuit A to show transients in simulation scenario I	74
Figure 5.4.2: Signal residual errors for circuit A in simulation scenario I.....	75
Figure 5.4.3: Power residual errors for circuit A in simulation scenario I.....	75
Figure 5.4.4: Residual energy and absolute energy errors for circuit A in simulation scenario I	76
Figure 5.4.5: Signal residuals for circuit A when a short-circuit occurs in the decoupling point	77
Figure 5.4.6: Power residuals for circuit A when a short-circuit occurs in the decoupling point	77

Figure 5.4.7: Energy residuals for circuit A when a short-circuit occurs in the decoupling point	78
Figure 5.4.8: Signal residuals for circuit B with a voltage source slow frequency modulation transient	79
Figure 5.4.9: Power residuals for circuit B with a voltage source slow frequency modulation transient	79
Figure 6.1.1: Single-line diagram of the HVDC transmission link model.....	83
Figure 6.1.2: Results of simulation of HVDC link showing DC voltages and currents in the decoupling point.....	85
Figure 6.1.3: Zoomed results of simulation of HVDC link showing AC voltages and currents in buses 1 and 2 during the voltage amplitude transient	85
Figure 6.1.4: DC signal residuals for simulation of the HVDC transmission link using a small interface-delay.....	86
Figure 6.1.5: DC power residuals in steady state for simulation of the HVDC transmission link using a small interface-delay.....	87
Figure 6.1.6: Energy residuals in steady state for simulation of the HVDC transmission link using a small interface-delay.....	87
Figure 6.1.7: AC signal errors for simulation of the HVDC transmission link using a small interface-delay.....	88
Figure 6.1.8: AC power errors for simulation of the HVDC transmission link using a small interface-delay.....	88
Figure 6.1.9: AC energy residuals for simulation of the HVDC transmission link using a small interface-delay.....	89
Figure 6.2.1: Topology of European Transmission Network Benchmark used for co-simulation [40].....	90
Figure 6.2.2: Topology of European Distribution Network Benchmark used for co-simulation [40].....	92
Figure 6.2.3: Coupling variables and active powers in the decoupling point using ITM-TD interface, with no additional interface delay	93
Figure 6.2.4: Coupling variables and active powers in the decoupling point using ITM-TD interface, with an additional 15 ms interface delay.....	93
Figure 6.2.5: Coupling variables and active powers in the decoupling point using ITM-DP interface, with no additional interface delay	94
Figure 6.2.6: Coupling variables and powers in the decoupling point using ITM-DP interface, with an additional 250 us interface delay.....	94
Figure 6.2.7: Coupling variables and powers in the decoupling point using ITM-DP interface, with an additional 15 ms interface delay.....	95
Figure 6.2.8: TN-DN interactions when generator in bus 11 of TN is disconnected at $t = 4$ s	96
Figure 6.2.9: Voltage profiles of transmission network buses when generator in bus 3 of TN is disconnected at $t = 4$ s	97
Figure 6.2.10: Frequency responses of transmission network buses when generator in bus 3 of TN is disconnected at $t = 4$ s	97
Figure 6.2.11: Residual powers using ITMTD and ITMDP interfaces with various levels of delay (top); zoom of figure to show improvements in accuracy using DP with large delay (bottom).....	98
Figure 6.2.12: Residual energies using ITMTD and ITMDP interfaces with various levels of delay	99

1. Introduction

1.1 Digital real-time simulation

A simulation is a process executed to study the behavior of a system in certain conditions, based on reproduction of that system, or of the environment where it is supposed to operate, by the use of models. Executing a simulation in discrete time and with constant step duration, it means that time moves in steps of identical duration: it is usually called fixed-time step simulation. Of course, other simulation methods that use variable time-steps exist and are more appropriate for non-linear systems and high frequency dynamics issues, but they are not suitable for real-time simulation.

During a fixed-time step simulation, the amount of real time required to calculate functions and solve equations representing a system at a certain time step might be shorter or longer than the duration of the simulation time step. For a real-time (RT) simulation, the simulator must precisely compute variables and outputs within the same length of time that the physical system would. In fact, the required time to calculate the solution at a given time-step has to be shorter than the time-step duration itself, as shown in Fig. 1.1.1, where simulation time is compared to computation length, for both offline and real-time simulations. If the simulation is to be performed off-line, the aim is to get results as fast as possible: thus, any idle-time before or after any simulator operations is used to compute results of the following time step. In real-time simulation, instead, the simulator waits until the next time-step to begin a new calculation and idles are lost. If operations are not all completed within the fixed time-step, the real-time simulation is referred as an “overrun” (Figure 1.1.1(b) is an overrun case).

Based on these definitions, it can be said that a real-time simulator is performing as expected if the equations and the states of the simulated system are solved accurately without the occurrence of overruns.

More in detail, for each time-step the simulator executes the same series of tasks: reading of inputs and output generation, model equations solution as a function of the previous time-step, exchange of results with other simulation nodes, and waiting for the next time-step. In other words, the state of externally connected devices is sampled once at the beginning of every time-step and, as a consequence, the state of the simulated system is sent to external devices only once per time-step. Therefore, the use of a discrete time-step solver is a constraint of today’s real-time simulators and it can be a major problem when simulating non-linear systems.

Lately, real time-simulator manufacturers have found solutions to timing and stability problems, which typically are known as discrete-time compensation techniques and normally implicate time stamping and interpolation algorithms. Basically, simulators benefit of advanced I/O cards running at sampling rates significantly faster than fixed-step simulation. The cards, thus, acquire data more often than the simulation, and can extract changes in the state between simulation steps. Then, when the new time-step begins, the I/O card gives the simulator information on state and timing, as when the state change has happened. Therefore, the simulator can compensate for the timing error. [1]

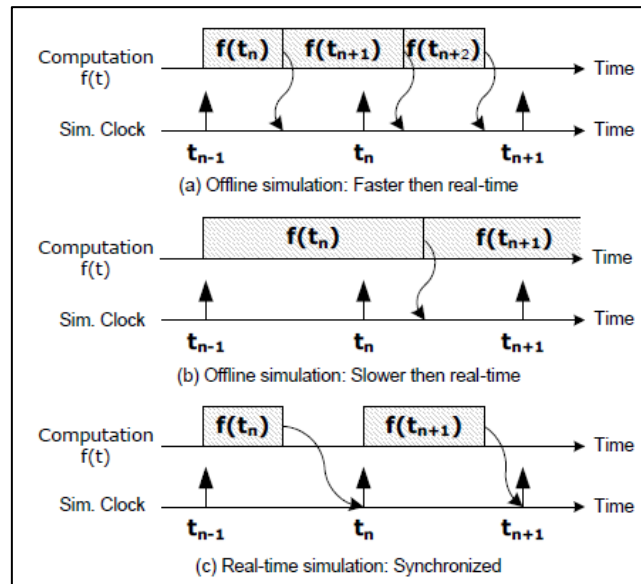


Figure 1.1.1: Offline and real-time simulation [1]

One might wonder why real-time simulation is needed. Actually, there are several applications that have also changed the role simulation itself has compared to the past. The possibility to represent a complete large system or an environment, made the simulation become the model to pursue during the designing phase of a project. Two main categories of real-time simulations for electric power systems can be distinguished:

- Entirely digital real-time simulations, in which no physical device is connected to the simulator and the entire system is modelled. They are usually used to understand the behaviour of a system under certain circumstances.
- Power Hardware-In-the-Loop simulations, used to test a physical device prototype before actually connecting it to the real network or to other already existing devices, reducing this way the risk. [2]

Simulating electrical networks in real time was the first and only way, using analog real-time simulators with actual devices. Then, the complicated devices such as machines were simulated with digital simulators connected to the analog part. Eventually, fully digital simulations started by the end of the 1990s. The first applications of RT simulation were typically focused on transmission grid, such as protection systems and HVDC. Lately, distribution grids have been simulated because of the increasing interest in micro grids and smart grids, although these are much more difficult to simulate. [3]

The computing capability of a real-time simulator has to be quite high, in order to maintain the model solution fast enough to guarantee a real-time execution. The complex interconnected nature of current power systems requires simulation of a large-scale system maintaining a certain level of detail of the models. Examples of such systems are multi-terminal HVDC grids that connect offshore wind-farms and onshore AC systems.

Moreover, correct time-step length has to be determined to represent truthfully the system response over the range of frequencies of interest. One has to solve a grid-scale model within 50 μ s or less to simulate transients of up to 3 kHz with high fidelity. For higher frequency applications (such as power-electronic systems operating with high switching frequency) smaller time steps are necessary.

Therefore, there could be different purpose to extend real-time simulation to a co-simulation, which means dividing the system in different subsystems in order to:

- Increase the maximum network size that can be simulated: a real-time simulator is configurable to be scalable: the intensification of computing power is made by adding rack-mount units that require data communication between racks. [2]
- Simulate both fast and slow subsystem transients: a multi-rate co-simulation approach is possible.

In the context of real-time simulation of electric power systems, co-simulation is especially challenging due to the very small time-steps used for EMT simulation: further methods to simulate the entire system in real time become necessary.

1.2 Distributed co-simulation

As mentioned in the previous section, a model of the system under study can be split into subsystems with the aim to allocate to multiple computation units to reach parallel computation of system solution. One of the first approaches to achieve parallel computation, is to take advantage of the natural propagation delay of travelling waves to divide the network model at transmission line where the propagation time exceeds the time step of the simulation. This method necessitates the modelling of transmission lines based on the distributed parameters. In most cases, the decoupling has to be done manually by the operator, but some latest solutions from vendors provide automated decoupling in the simulation environment [4].

The computational cores can be interconnected in several combinations, such as:

- Multiple cores/units of the same simulator
- Different types of simulators

A motivation to run a co-simulation using two different simulators is to exploit available model libraries and simulation resources. Furthermore, concurrent and efficient modelling across different applications is supported.

The connection can be made in a local area via Local Area Network (LAN) or point to point connection via optic fiber, or in distant geographic locations through Wide Area Network (WAN). [4] The idea of co-simulation is shown in Figure 1.2.1.

So one can distinguish between locally distributed and geographically distributed co-simulation. This further extension of co-simulation that allows having a virtual environment, where different computers located in different laboratories can execute a simulation at the same time, has other advantages, besides the possibility to extend network size in simulation:

- Opportunity to share hardware and software facilities for simulation
- Sharing of expertise of various research fields: different laboratories with available equipment may benefit the know-how of another lab in collaboration.
- Ensuring security of confidential data: it is easier to simulate locally and exchange interface quantities and results via real-time co-simulation.

Although multi-site located co-simulation shows many advantages, many issues remain challenging. The main ones will be recalled in the following paragraphs.

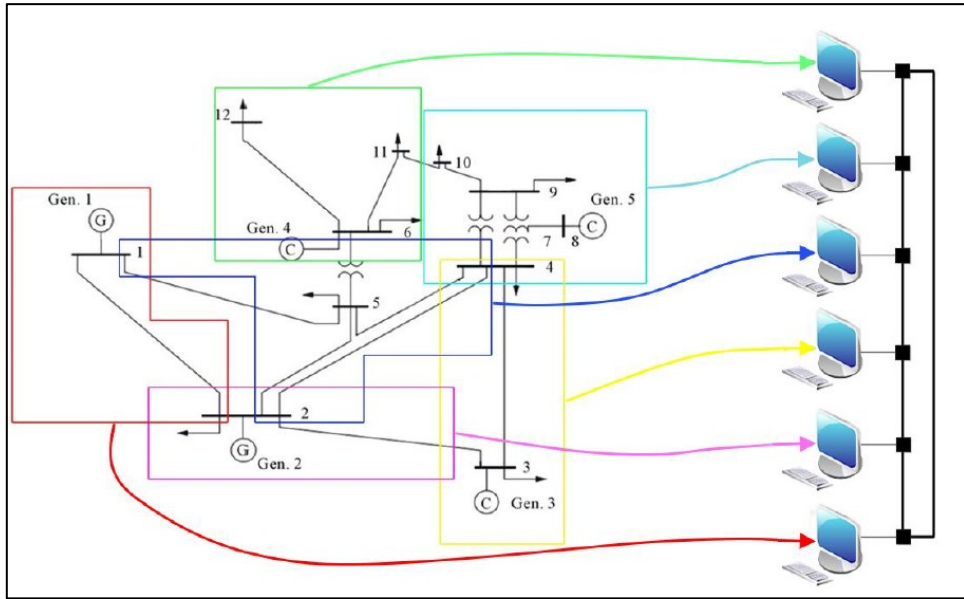


Figure 1.2.1: Example of co-simulation [4]

1.2.1 System decoupling

The whole network has to be decoupled in certain points and every portion has to be assigned to a simulator for simulation. In a power system aspect, this is a significant challenge: finding the optimal decoupling points and information to be exchanged between subsystems.

Regarding the optimal point, it can affect the simulation results in terms of accuracy and stability: it is thus reasonable, to turn this selection into a design decision, and a metric to evaluate a system *distortion* can be defined in order to understand the conditions under which the coupling point is not disturbing the co-simulation. [5]

The main idea behind this approach is to separate the two subsystems allowing them to communicate to each other finding a separation scheme so that distributed co-simulation can provide sufficient accuracy. It is, in other words, a concept of sensitivity of the desired dynamics to the remote system dynamics.

1.2.2 Communication interface

There are plenty of different methods to exchange information under either implementation or investigation. A common one is exchanging current and voltage quantities among the two real time simulators located in geographic distance. Instantaneous values could be delivered in case of connection within very short distance, even though this is never used across long distance over Wide Area Network, because it would give unacceptable results. It is significant how elaborating these values using other methods would give better results.

One of the approaches is transforming quantities to their time varying Fourier coefficients for a fundamental frequency phasor (magnitude and phase information) in one side and send to the other side where an inverse transformation is applied. In a more sophisticated way, an interface with higher components of dynamic phasors might be used. Fourier coefficients with higher order harmonics are captured in one side and sent to the other side for an inverse transformation.

Besides the choice of the type of quantities to send through the interface and their representation, the communication itself causes several issues. First of all, connecting two different simulators

implies a time-delay. Regardless of how large the delay will be, it causes inaccuracy in simulation of system values and, in some cases, instabilities of the simulation itself, even though the original system is stable. Using the Internet as the medium for co-simulation, introduces more challenges. Time delay is much larger than in a locally distributed simulation, and most of it is due to routing and processing in the network. In terms of multiple of simulation time-steps, if in locally distributed co-simulation delay is about 1-5 times the simulation time step, in geographically distributed it will be around 300 times the time step, for a time-delay of 15 ms and a typical time step of 50 μ s. Then, a packet jitter exists, which means a variation in latency as measured in the variability over time of the packet latency across a network. In other words, that implies a variable and unpredictable time delay. Finally, an inherent packet loss is present over the internet, i.e. not all the packets arrive to their destination [6].

1.2.3 Interface algorithms

Although many differences exist, some issues of co-simulation are related to power Hardware-in-the-loop simulation, especially when considering the power interface. The so-called interface algorithms define three important characteristics: types of signals being exchanged (voltage, current, power, etc.), how the signals are transmitted (amplification, filtering, etc.) and the methods to compensate the time-delay. Various types of IA are available in literature [7], where considerations regarding both stability and accuracy of simulation are addressed.

It has been shown, how an inappropriate choice of interface algorithm (IA) for a certain simulated system can lead to instability, regardless if the real system is stable or not. Moreover, even a stable simulation does not imply accuracy. Therefore, a proper choice of IA should also take into account accuracy of results. It is also important to highlight how an IA has to be implemented on the two decoupled systems paying attention to a proper choice of decoupling variables, i.e. sending a voltage rather than a current, or a certain voltage rather than another voltage from a circuit to another can make the simulation unstable.

Generally, an IA has to be considered as a separated element connected to the two decoupled systems, as shown in Figure 1.2.2.

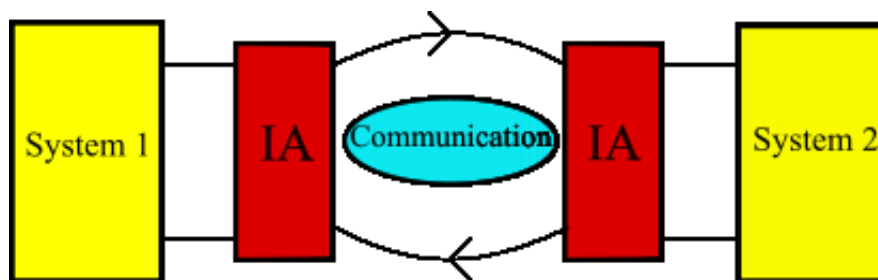


Figure 1.2.2: Role of IA in a co-simulation set-up

1.3 Focus and contribution of the thesis

To sum up, geographically distributed real-time co-simulation is a promising concept for simulation and, consequently, designing, operation and maintenance of power systems. The main aim of this thesis is the development of interface algorithms for this type of simulation set-up in order to ensure accuracy of simulation and provide stability.

The work that led to getting this achievement started from reviewing related contributions from similar fields. In this initial phase, several approaches found in literature have been analyzed, trying to determine similarities and differences. The purpose was to understand properly which issues actually arise in distributed co-simulation for power systems.

Starting from these already existing works, the next step was to evaluate the applicability of such solutions for the experimental applications proposed for this thesis, i.e. running co-simulations between two real-time simulators that are physically far from one another. Among those procedures, two approaches have been furtherly studied and, later on, implemented with the simulators Graphical User Interface (GUI), in order to execute the co-simulation tests.

Originally proposed as an interface algorithm for PHIL simulation background, the Time-variant First-order Approximation (TFA) interface, which is a predictive algorithm based on previous states of the system, has been studied and adapted to co-simulation. Then, an interface derived from teleoperation application, the so-called Wave Transformation (WT) interface, has been taken into account.

After a first evaluation of applicability regarding actual improvements in accuracy and stability, the next step was to modify such interfaces acting on the exchanged quantities during the simulation. In detail, the dynamic phasors theory has been considered, exploring the improvements in terms of delay compensation given from using the time varying Fourier coefficients instead of the instantaneous values in the communication interface. Therefore, the two mentioned interfaces have been implemented and tested integrating a dynamic phasors transformation before sending the quantities from one simulator to another and inverse transformation when they arrive to the other simulator.

These first tests have been done offline using SimPowerSystem toolbox from Simulink/MATLAB, on both simple single-phase circuits and simple three-phase power systems, showing improvements in terms of accuracy for the WT interface, which is known to suffer from accuracy issues, since often stability is the main aim of telerobotics operation. Regarding the TFA method, instead, the algorithm has been derived in the dynamic phasors domain using a discrete approximation. Since complex numbers are used for computation, a modification of the algorithm is necessary.

Later, the newly tested interface algorithms have been used for some practical applications, using real-time distributed co-simulations, using different simulation set-ups:

- Multi-core parallel co-simulation using OPAL-RT
- Locally distributed co-simulation using both RTDS and OPAL-RT
- Geographically distributed co-simulation using RTDS, located at RWTH Aachen University (Germany) and OPAL-RT, located at Politecnico di Torino (Italy).

The teleoperation WT interface has been tested using DC systems. After some evaluating tests on simple DC circuits, a multi-core parallel co-simulation of an HVDC Transmission link has been run on OPAL-RT.

The last two types of co-simulations have been used, then, to simulate two entire power networks, in particular two benchmark models introduced and modeled in [9]:

- An high voltage transmission network modelled using the GUI RSCAD of RTDS
- A medium voltage distribution network modelled using Simulink and simulated in OPAL-RT

The aim of these simulations was to evaluate both stability and accuracy of the new interfaces. One of the reasons itself that lead to use distributed co-simulations is the impossibility to simulate a whole system in the same simulator. Consequently, to evaluate accuracy of simulations there is no original integrated system that can be used as a reference for evaluation. Starting from this observation, a new metric based on the concept of energy residuals, i.e. energy wrongly introduced in co-simulations because of imperfect time synchronization of the simulators and non-ideal communication events (time-delay, sampling, etc.), has been adopted to evaluate the interface algorithms.

Furthermore, the tests executed during the work for the thesis, have shown evidence that some interfaces are more appropriate than others are for certain types of systems and different conditions of the systems (e.g. transients, faults, AC or DC systems, etc.). Thus, an empirical evaluation of region of application of interfaces has been done.

1.3.1 Thesis structure

The thesis is structured as follows. Chapter 2 contains the bibliographical review of works existing in literature somehow related to real-time geographically distributed co-simulation, in order to highlight similarities and differences and to focus on the correct path to follow from the very beginning.

In chapter 3, two fields among those works have been further reviewed to investigate applicability and feasibility for the case under study. Thus, the concept of interface algorithm is introduced, and two methods derived from Power Hardware-in-the-Loop simulation have been implemented for a simple electric system to show basic characteristics. Additionally, a method introduced for bilateral teleoperation is presented. Finally, the representation of interface quantities during a co-simulation is taken into account, reporting the dynamic phasors concept and its application on co-simulation for time delay compensation.

Chapter 4 contains the main contribution of the thesis, which is the development of interface algorithms to co-simulation. The Time-variant First-order Approximation algorithm is adapted to a simulator-to-simulator set-up and then modified into dynamic phasors domain. The Wave Transformation interface is applied to electric power systems and further changed using dynamic phasors for the communication interface.

Chapter 5 addresses the issue of evaluating accuracy of a co-simulation, since no original system dynamics are available to use as reference, otherwise there would be no need to run a co-simulation in the first place. To overcome this issue, a metric based on the concepts of residual power and energy is developed, proving its efficiency when compared to standard absolute error. Furthermore, the metric is used to evaluate the newly tested interface algorithms.

In chapter 6, finally, the developed interface algorithms are applied to realistic power systems models, using actual co-simulation set-ups. In particular, the Wave Transformation interface is used to simulate a power system containing an HVDC transmission link. The interfaces based on dynamic phasors, instead, are used to co-simulate an high voltage transmission network and a medium voltage distribution network.

2. Related work

The challenges regarding geographically distributed real-time co-simulation have common aspects with some other problems.

Moreover, other topics have been helpful to understand better some issues and to develop different approaches to solve them during the research.

Narrowing down the issues concerning the problem faced in this thesis, may help to understand the correct path to take from the very beginning. Therefore, a brief overview of the mentioned related problems will follow.

2.1 *Parallel real-time simulation*

The increasing complexity of power systems, due to higher interconnection, more utilization of power electronic devices and larger penetration of distributed renewable generators, require more attention on planning, protection and control, with consequent more demand on system simulators. Presence of a wide range of dynamics, including ultra-fast transients concerning power electronic converters and AC circuits with very short lines, call for smaller simulation time-steps. Moreover, time domain analysis of power systems has become an important focus in terms of real-time simulation, but the continuous expansions of networks creates new problems.

For all these reasons, modelling and simulation of large-scale systems requires vast computational resources. One of the possible solutions to overcome this major issue is to exploit parallel computational architectures on multi-unit processors of simulators. [8]

In order to address simulation of different transient speeds and different system sizes, several types of solvers characterized by solution algorithms may be used. One of these types of solution methods for real-time simulation of power systems is ElectroMagnetic Transient (EMT). For the purposes of this thesis, solution methods used in SimPowerSystems for Simulink from the Mathworks, in ARTEMIs solvers used in the eMEGAsim simulator of Opal-RT and in RTDS simulator from RTDS technologies are interesting, since they are used to generate results. In addition, the concept of parallel multi-units simulation itself is similar to co-simulation idea.

RTDS simulator uses a traveling wave property of long transmission lines for decoupling of the system. Modular units called racks, each of them containing different digital signal processors, compose its whole hardware.

SimPowerSystems solvers are state-space based ones, but they are not suitable for real-time simulation. The ARTEMIs solver of OPAL-RT overrides Simulink native solvers with two kinds of solvers:

- 1) State-space solvers with pre-computation of all matrix variations due to switches
- 2) State-Space-Nodal (SSN) solver: classic branch equations of the network are represented by state-space equations. The idea behind SSN is to add virtual nodes in the system of equations to have a virtual decoupling: this allows getting many zeros in

matrix sets, which allows decoupling of matrices and utilizing parallel computation which increases the overall speed of calculation, as shown in Figure 2.1.1. [9]

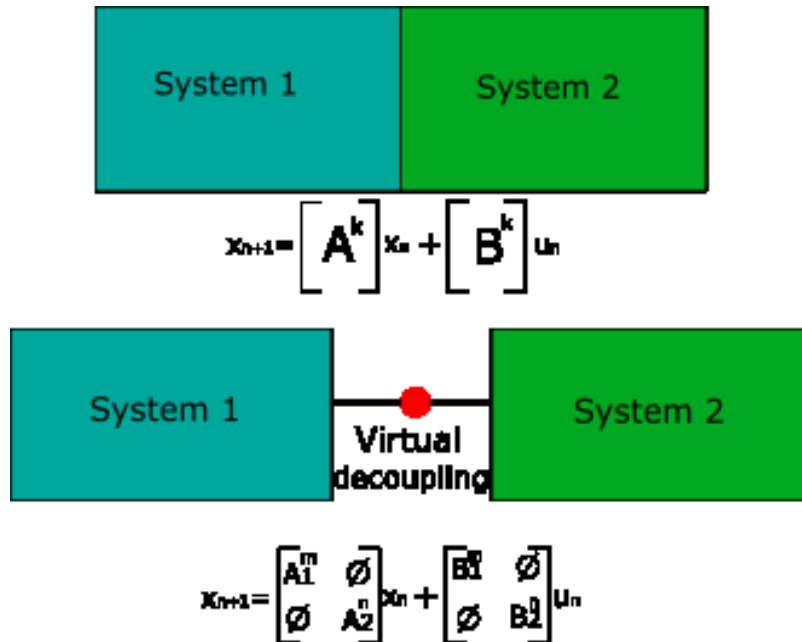


Figure 2.1.1: Virtual decoupling in SSN

Thus, parallel simulation is related to the focus of this thesis in two major ways:

- The simulators used to generate results and get conclusions for the thesis are based on this type of solution methods themselves
- SSN solver is based on a decoupling idea, like distributed simulation. Transmission lines models are used to separate state-space equations, exploiting natural propagation delay of the lines.

2.2 Power Hardware-In-the-Loop

Hardware-in-the-loop simulation means that a part of the system in the simulation is an actual physical device connected to a simulated large system [11]. This is particularly useful when one needs to make some testing in a realistic condition even before the real system has been completed or the model of the physical device is not available or it is not accurate enough. Thus, costs and investment risks are minimized, since every kind of condition can be imposed to the system and there are bigger possibilities to discover unexpected drawbacks of the device itself. What is more, the response of the system to the new device can be tested: if the simulated system is the electrical network, the risk to damage the network by connecting a new element can be avoided.

The set-up for an HIL simulation consists of three elements: the physical device (Hardware under Test – HuT), the Virtually Simulated System (VSS) and an interface between the two. The HuT can be either a controller or a power device. In the first case, called Controller HIL (CHIL), interfacing signals are low voltages and currents: then, only Analog/Digital Converters are enough for communication. In the second case (Power HIL – PHIL), instead, power amplification and conversion devices are necessary, like actuators, voltage converters and sensors: a power interface is needed (Figure 2.2.1).

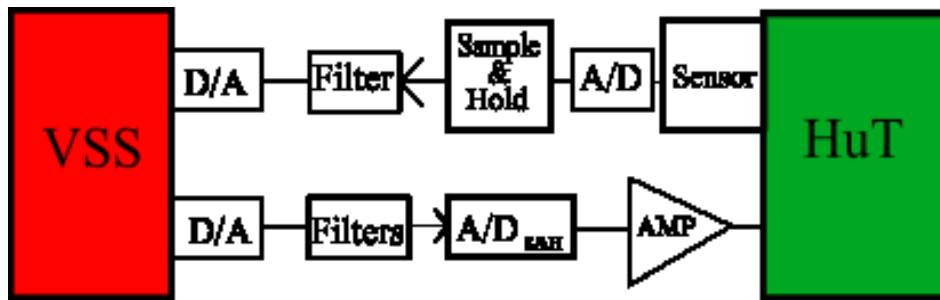


Figure 2.2.1: PHIL set-up for simulation

This interface should have ideally no time-delay, unity gain and infinite bandwidth, even though actually such a result is not possible. This issue is similar to geographically distributed co-simulation interface, meaning that it is important to reduce errors in the interface as much as possible; otherwise, results of simulation are compromised. On the other hand, the reasons why the interface is not perfect are different, since in distributed co-simulation the main problem is time-delay that has normally an order of magnitude around tens of milliseconds. In PHIL, instead, A/D conversion and dynamic of a power amplifier are usually the major issues. In other words, the main difference is that in distributed co-simulation there is no physical device connected to the virtual simulated system, so the problems regarding this connection disappear.

Another mutual concern between these types of simulation is the evaluation of accuracy: the problem is basically that the original system, which can create the correct results, is not available. Otherwise, there would be no need to execute a PHIL or a distributed co-simulation in the first place, because both are performed when it is not possible to simulate the entire system, even if for different reasons. [10]

Stability of simulation has to be addressed as well, since it is a necessary condition to perform an accurate simulation. Even regarding this topic, stability must be guaranteed in PHIL and co-simulation but causes of instability are not the same. In PHIL, the closed-loop system containing the simulator, the power interface, the HUT, samplers and sensors must be taken into account when evaluating stability, using basic criteria of stability for dynamic systems, whereas in co-simulation the closed-loop chain is less complex.

Moreover, sometimes it is indispensable to move subsystems from hardware to software or vice versa to assure stability, meaning that the decoupling point of the system must be changed: this is also important in co-simulation. [11]

Finally, a major part of stability and accuracy depends on the interface algorithm chosen for the simulation. In [10], several IA are tested on the same circuit to prove how performance of the simulation can be considerably affected in terms of accuracy and stability. Moreover, an analysis based on transfer functions evaluation of the various IA is done, in order to justify which interface is better than another is. In this thesis, a first approach to IA starts by implementing IAs used in PHIL for electric power systems, but only some of them will be furtherly examined in depth and modified for the case under study in the next chapters.

2.3 Applications of Internet-distributed PHIL in automotive engineering

An extension of PHIL idea is to connect different HIL setups to furtherly exploit the benefits of HIL simulation. If the laboratories are geographically separated, it is necessary to create a virtual coupling using a communication channel. The Internet is usually the most attractive way to communicate in long distance, because of its spread, but it also comes with inherent

drawbacks. Delays, jitter and packet loss, indeed, affect simulation results. A common application of this extension of PHIL is automotive engineering. Work has been done to improve this method in several ways [13].

The literature shows several techniques to overcome typical issues of this kind of PHIL simulation, and they can be classified into three groups, which will be listed in the following, highlighting feasibility for power system co-simulation:

- 1) Direct transmission of coupling variables. It is possible for co-simulation as well. It is, in fact, the easiest implementation, because no transformation or filtering is applied. The major weakness is that accuracy and stability are not guaranteed, especially with increasing and variable time-delay.
- 2) Prediction and filtering methods based on observers. In this arrangement, each of the two systems owns a detailed dynamic model of the other one. Thus, interactions happens with the models rather than with the other system, while the Internet ensures that the observer states stay close to those of the remote site. Main disadvantage of this method is the necessity to have an accurate model of the remote system, which is in contrast with one of the reasons of why Internet-distributed geographically co-simulations are executed. Some research in this field pursuing the aim to eliminate the need for detailed models has been done. [14]
- 3) Improvement of coupling fidelity without information about the system dynamics. This approach overcomes the need for knowledge of the monolithic system dynamics when evaluating accuracy of simulation. Thus, a metric based on relative errors between instantaneous values of coupling variables can be derived, and this information can be used to implement various algorithm that enhance fidelity of simulation. An off-line iterative learning control approach has been developed [15], whereas a coupling methodology based on polynomial extrapolation techniques of low order together with error correction methods has been tested by research project “Advanced Co-Simulation Methods for Real-Time Applications” [16]. The main concept of using a metric that does not require original system knowledge can be adapted to power systems co-simulation, but both the approaches used to improve actually fidelity require a connection between real-time and off-line simulations, which is different from the work present in this thesis. As a matter of fact, in [15] the results of the iterative learning control are influenced offline to improve fidelity.

2.4 Energy conservation approaches

The reduction of simulation accuracy and threatening to its stability when simulators are coupled based on a virtual power interface has been studied using the power bonds theory [17] [18]. Usually, time synchronization of simulators involved in a co-simulation is not assured, and since in those works the objective was not geographically distributed co-simulation, time-delay is not the main issue, but synchronization is more challenging. Therefore, the problem is that time moves forward independently of each other, with coupling variables sampled at discrete time points. The major disadvantage of this approach is that simulation inputs are, generally, unknown during the time integrations inside the simulators and they have to be approximated.

This can be better explained using the power bond concept: a power bond is defined by two power variables, a flow and an effort, whose product is a physical power: thus, using power bonds as coupling variables allows to have direct access to powers and energy values during

co-simulations. Considering two systems coupled in co-simulation, because of different time integrations of the simulators, power in one system is generally different from power in the other one. This is a problem because, substantially, conservation of energy is not maintained.

In literature, this issue is defined with introducing a residual energy that is added to the energy flow in the co-simulation, and it results with distorting system dynamics and accuracy of simulation, with also possibility to lead to instability [17]. This concept is illustrated in Figure 2.4.1.

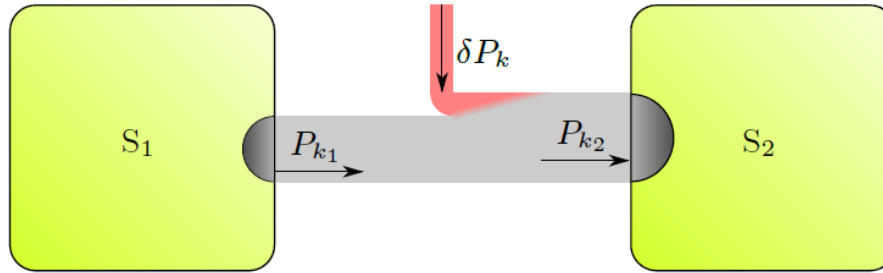


Figure 2.4.1: Different integration time-step introduce residual power in co-simulation, compromising accuracy and stability

This concept is used in different ways to improve co-simulation results:

- ECCO (Energy Conservation-based Co-simulation method): an adaptive control of the co-simulation time-step
- NEPCE (Nearly Energy Preserving Coupling Element): correction to the power flow between simulators to compensate for residual power introduction

Besides these methods, in [17] another related notion that is also useful for the purposes of this thesis is introduced. As mentioned, using power bonds as coupling variables quantifies residual energies as errors added in the simulation. For this reason, residual energy are suitable as metrics for accuracy evaluation of a co-simulation.

As it will be more in detail explained in the following chapters, residual energies can be used as error estimators in co-simulations, having multiple advantages compared to absolute errors and to quantities not related to power or energy variables:

- If a co-simulation is executed, one of the main reasons is that the original integrated system cannot be simulated as a monolithic model. Thus, there is no exact solution to compare results of the simulation. The use residual power is expressed as:

$$\delta P_k = (P_{k1} - P_{k2}) \quad (2.1)$$

for the power bond k between decoupled systems 1 and 2.

Eq. (2.1) is in general different from zero, violating conservation of energy. This itself is a measurement of error: there is no need to know the solution of the integrated system, but only the local errors compared to power outputs of a power port.

- As the already mentioned NEPCE, several methods that correct power flows online during the simulation exist in literature for various approaches. Therefore, knowing the exact amount of exchanged energy for every time-step can help to improve the simulation itself.

- Using power variables offers a more holistic approach, considering immediately energy conservation. In addition, the problem related to the different units of measurement of the coupling variables (e.g. voltage and current) is indeed resolved.

2.5 Bilateral teleoperation

Teleoperation means operation of a device at a distance. It is a field of robotics, consisting of the development of methods and solutions to allow a human operator to control a robot located in a remote environment that, for reasons of safety or inaccessibility, a human operator cannot reach. In particular, basic elements of a teleoperation system are the master and the slave robots. In unilateral teleoperation, the operator moves the master and the slave follows the motion of the slave. In bilateral teleoperation, instead, when the slave is in contact with the environment, reflects back the contact force to the master, which is reflected to the operator.

As a matter of fact, several issues show up when trying to implement a bilateral teleoperation control, since a certain level of accuracy, which is in teleoperation more commonly called “transparency”, is required in order to execute commands with precision. Moreover, as it can be seen in Figure 2.5.1, a teleoperation system is a closed-loop system, thus stability problems arise as well. Especially when the communication channel is considered, it is likely to have time-delays.

What bilateral teleoperation methods try to address has many similarities with distributed co-simulation, meaning that in both cases the main idea is to synchronize two physically distant decoupled subsystems, in order to preserve accuracy and stability of the whole system. The main idea is, like in other typical control strategies of PHIL (the so-called interface algorithms), to send a reference signal from one side, which in telerobotics is usually a velocity or force signal, to the “remote” side, which sends back a feedback signal to the local side.

However, substantial differences exist. In teleoperation theory, one of the systems is a human operator, who sends a reference signal that is executed by the robot on the other side. The feedback signal is received by the operator who uses it to have an idea of what happens in the remote environment. The feedback signal is typically a force feedback, which is not necessarily an ideal representation of the remote environment in order to achieve a bilateral teleoperation with suitable performance. In distributed co-simulation, the feedback signal must be accurate and perfectly executed by the other system, since two subsystems are naturally interfaced in the monolithic system and conservation of energy must be ensured.

Control architectures for bilateral teleoperation can be classified on the basis of several aspects, such as number of communication channels, types of variables used for communication (e.g. position, force, velocity, etc.) or, like in [19], on their main goal.

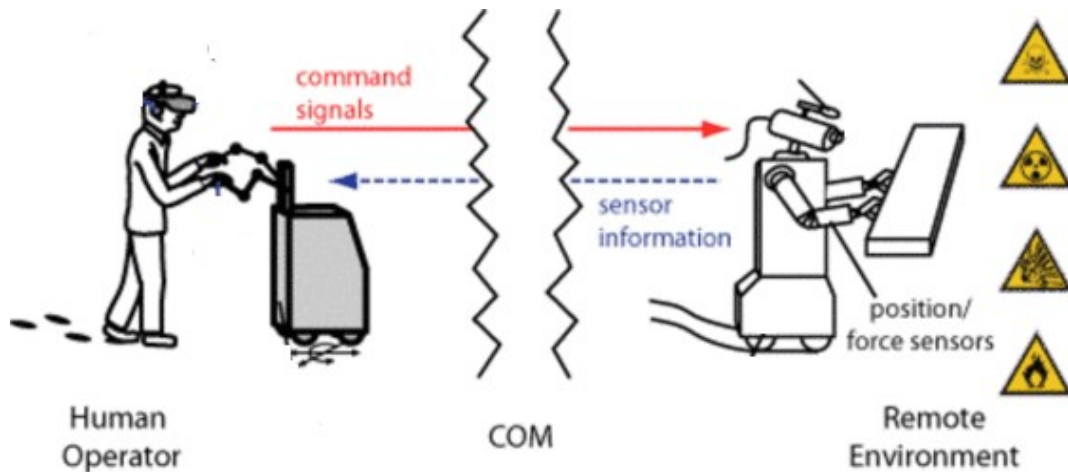


Figure 2.5.1: Concept of teleoperation system [18]

In other words, two categories of teleoperation control architectures are distinguished:

- 1) Bilateral motion synchronization: both ends try to reach synchronization using a virtual connection between the *master* and the *slave*, which represent respectively the human operator and the robot (Figure 2.5.2a).
- 2) Direct force-reflection: the slave is controlled by a virtual operator and the master is controlled by a virtual environment (Figure 2.5.2b).

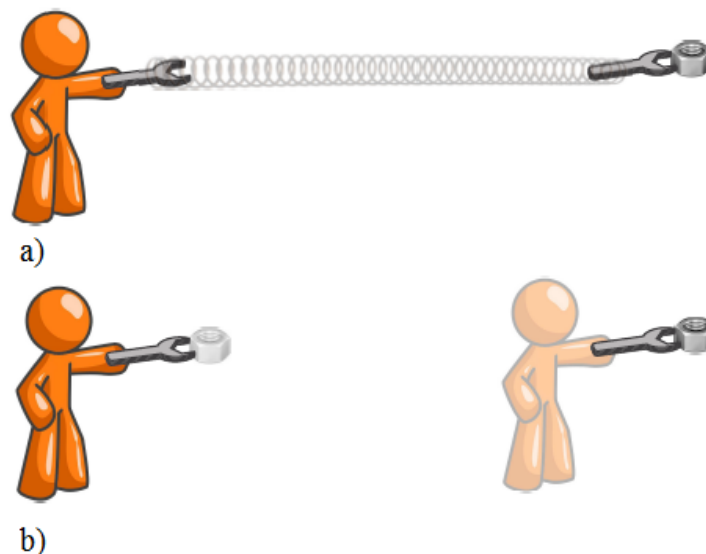


Figure 2.5.2: Clarification of the two types of control architectures [19]

Besides this basic distinction, many control architectures variants have been implemented and studied in literature for both cases. Here follows a literature review of the main ones.

2.5.1 Wave transformation

One of the most common bilateral synchronization methods is based on the passivity formalism, which is based on an easy way to verify the stability of a nonlinear system. In simple terms, a system is said to be passive if the power entering the system is either stored or dissipated and, using theory of stability of nonlinear systems, it can be proved that, without external inputs, a passive system is stable. One can notice comparisons with energy conservation-based

approaches: if conservation of energy is violated, stability and accuracy of the system might be compromised. In a teleoperation system though, wrongly added energy can be stored, violating conservation of energy without jeopardizing the stability of the operation.

On this basis, a teleoperation system that reproduces physical systems and thus follows passivity theory has been widely implemented and used in telerobotics: the method called either wave scattering or wave transformation [20]. It is strictly related to the passivity theory and essentially divides the power flow of the system in two subsystems, which are connected through input and output waves. Therefore, physical quantities such as velocity and force or, for electric systems, current and voltage, are transformed into wave variables through the use of a wave impedance, whose correct tuning is fundamental for reproduction of original system behavior.

Deriving the equations of such a variables transformation, it is proved that passivity of the system is assured, theoretically, if the energy delivered by the output waves has a boundary represented by the energy that input waves give. Using wave variables instead of power variables, then, a passive communication regardless of time-delays is automatically achieved. However, several issues arise in actual application. For instance, when considering variable time-delay or discrete time-steps in communication, or even a proper choice of wave impedance can be critical, but much research has been done to overcome these issues, proving that this method is nevertheless promising for real applications.

In [22], wave transformation is generalized and a linear matrix composed by a rotation matrix and a scaling matrix is used instead of a simple wave impedance to get the wave variables.

Different values of wave impedance are used in [23], automatically tuning the wave impedance online based upon sensing whether the slave is in free space or in contact with the environment. In electric domain, that would mean to define different values of impedance for zero-current and zero-voltage operation of the remote circuit but, since time constants of electric systems are smaller than mechanical systems, this type of control is not easily implementable. Moreover, this dynamically variable wave impedance control scheme requires the slave to be controlled by a PD controller, which creates further issues in implementation for power systems. In this thesis, other solutions to overcome the tuning of wave impedance will be adopted.

As mentioned earlier in this chapter, large time-delays in communication (e.g. over the Internet) are a serious risk that can lead to instability of simulation. Even though wave transformation theory assures passivity for ideally any time-delay, experimental results have shown that increasing the delay increases the quantity of exchanged information. Therefore, a phenomenon that resembles wave-reflections can arise, leading to decreasing the fidelity of the simulation. In [24], a predictor-based method is proposed to solve such issues, using a correction algorithm to modify the returning wave variable to maintain passivity. This can be implemented with any control architecture and does not require wave transformation.

2.5.2 Direct force-reflection

One of the main issues of motion synchronization techniques is the trade-off between transparency and stability of the communication. In fact, many control strategies tend to focus on maintaining stability at the expense of accuracy. Direct force-reflecting control architectures have more potential to have precise reference tracking and force reflection, particularly in delayed operation. In contrary to bilateral motion synchronization, such schemes are not passive: for this reason, they have not been studied in this thesis.

Since they have been created for mechanical applications, these strategies are normally based on a position-force control scheme, which in electrical domain would mean to control the integral of current. In addition, this type of architecture changes from a bilateral type to a unilateral structure online, meaning that the control law changes whether the remote side is in zero-force condition (free motion) or in contact. In the first case, no movement feedback quantities are sent to the master controller, then stability is assured even with delayed communication. In the second case, instead, force is reflected to the operator and, since dynamics change significantly, controlling the effect of such a change is much harder than in bilateral synchronization, especially in presence of time-delays. These problems have been addressed by Heck in [19], where some solutions have been proposed.

These issues become even more challenging in electric domain, because of the already mentioned smaller time constants and their consequent faster transients. This is why bilateral synchronization methods are the only architectures that will be furtherly explored for the aims of distributed co-simulation of power systems.

2.5.3 Passivity control

Recalling the problems of loss of stability due to time-delay, to the use of discrete time-steps and consequent quantization and, generally, the critical trade-off between transparency and stability, some attempts to perform an accurate teleoperation without jeopardizing stability have been proposed.

As it has been shown in the previous paragraphs, certain teleoperation control architectures are based on the definition of a virtual damping element (e.g. wave impedance in wave transformation) that assures stability, although can lead to inaccurate execution of the required signals.

In [25], a time-domain passivity control approach has been proposed. In simple terms, a passivity observer (PO) and a passivity controller (PC) are defined: the PO checks, for every time-step of simulation, if energy at the power port of the system is positive. If it is negative, that means that the system generates energy and thus passivity condition is violated. If this second condition happens, the PC is activated: it is substantially a dissipative element connected to the system that, with a certain compensation algorithm, brings the system to passivity condition again. Unfortunately, this approach has the major disadvantage of causing a strong force change (or voltage, in electric domain), when the PC begins its compensation. An improvement in this sense has been done in [25], where the passivity control is implemented on power rather than on energy. Therefore, the PC is activated more softly and the PO does not require time integration for calculation of energy, decreasing the inevitable related errors.

A further extension has been done in [26], where the passivity control was extended to a two layer approach. In a top layer, named Transparency Layer, any control architecture can be implemented. In the bottom layer (Passivity Layer) passivity is enforced, varying a damping element of the master controller, so that the operator can give energy to both master and slave. This distribution of energy is governed by a synchronization of the passivity layers only. In this way, two different communication channels exist, so that information related to exchanged energy is totally separated from information regarding the generic control strategy, allowing an almost completely independency from time-delay.

In a similar fashion, but specifically designed for direct force-reflecting bilateral teleoperation, another two-layer architecture has been proposed in [27]. The main difference is that in this case, synchronization is not proper of force-reflecting architectures. Therefore, the passivity

layer is here implemented on the controllers of master and slave using a *duplicate* of the energy applied by the operator and the environment, and the damping elements of both controllers are varied when passivity condition is not respected.

Overall, passivity control offers some methods that can be adapted to distributed co-simulation of power systems. In fact, the general idea of power monitoring is similar to the residual energy strategies introduced in paragraph 2.4.

2.6 Networked Control Systems

Networked control systems (NCSs) are physically distributed systems where communication between elements such as sensors, actuators and controllers is based on a shared network with limited digital bandwidth [29]. They present the main advantage of allowing flexible architectures and low installation costs. Consequently, NCSs have applications in a wide range of areas, such as distributed control of production plants, mobile networks and haptic collaboration over the internet.

Nevertheless, sharing a network rather than using dedicated connections creates new issues. In [29], a systematic list of challenges inherent NCS is presented, highlighting the principal differences to other control systems. For the purposes of this chapter, a further distinction from distributed co-simulation will be made.

A first observation refers to the communication channel itself, which like any other network has a limitation in quantity of information that can be transported per unit of time. The problem is to determine the minimum rate necessary to make a closed loop system with a finite capacity channel stable. Even though this is a constraint on the stability, one should actually consider the transmitted data and not the single bits: thus, a certain number of so-called *packets* can be sent through the communication channel but each of them can contain a very large number of bits. This consideration is taken into account for the following comments.

Similarly to real-time co-simulation, the communication is in discrete time, but for a different reason. In NCSs, continuous signals must be sampled to be transmitted over the network, and eventually they must be decoded. In co-simulation, instead, sampling is introduced by digital real-time simulator. When considering geographically distributed co-simulation over the Internet, another similarity of the two structures is inherent time-delay. As a matter of fact, highly variable network conditions make the delay unpredictable. In NCSs, there is another component of time-delay, that is the network access delay: the time that a shared network needs to accept receiving data. This happens because in NCSs participants of the shared network may be required to collaborate in every moment.

Another comparison of NCS to geographically distributed co-simulation is the possibility that some data is lost during the communication, so that a packet loss or dropout happens. In NCSs, this can create problems regarding state estimation of a remote plant, and a possible solution is in the algorithm for state estimation itself. In fact, two possibilities may occur:

- 1) Every measurement is sent through the channel, with the chance that it might not arrive to the remote estimator because of network congestion
- 2) Measurements are processed locally and they are sent through the channel only if it is estimated that the network is not too busy and it can transmit the data.

The second approach shows of course more advantages and its development was possible thanks to the increasing number of smart sensors.

Although the system architectures of NCSs may resemble the ones of co-simulation or, generally, HIL simulation, another similarity is again in the communication channel, which is unique for both direction of communication, as shown in Figure 2.6.1, and a multiple number of users can theoretically share it.

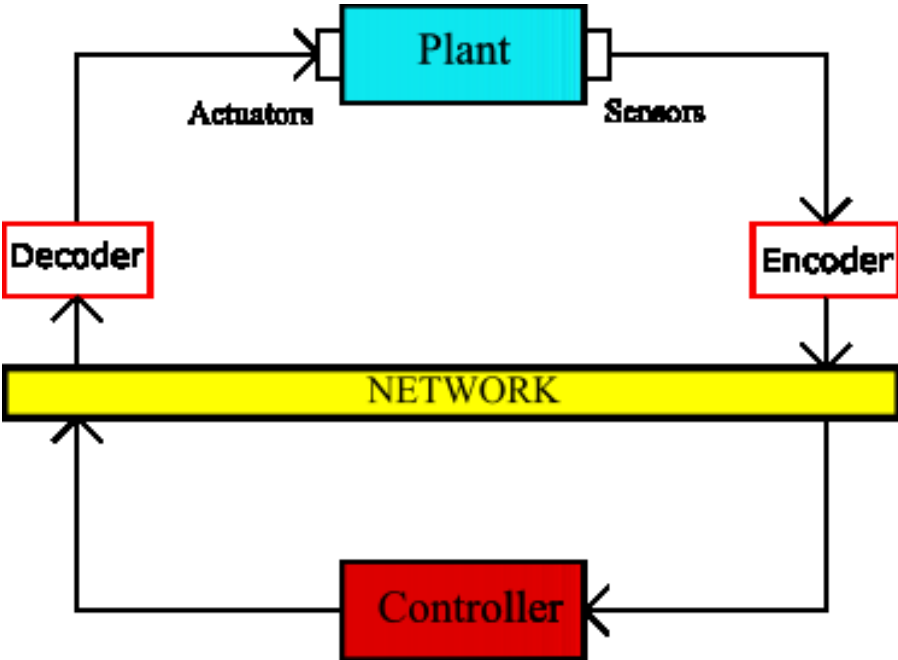


Figure 2.6.1: Single-loop NCS architecture

Finally, the main difference between co-simulation and NCS is the requirement of conservation of energy. In fact, this is not considered in NCS, since there is no monolithic system as in a co-simulation set up. Thus, an acceptable performance in terms of exchanging information is enough in NCS, whereas accuracy is one of the main objectives of co-simulation.

3. Background

The literature review in chapter 2 introduced related work that considers similar issues as in real-time geographically distributed simulation. Particularly, some of these approaches identify similar issues useful to understand more properly the problems of the co-simulation; others present instead actual solutions that can help improve it.

Among those, two approaches available in literature will be further explored, with the purpose to adapt for the solution of co-simulation of power systems. Furthermore, to improve them, acting on the type of variables exchanged in co-simulation.

Dynamic phasors concept will be briefly introduced at the end of this chapter, together with a reference to previous work present in literature regarding the use of dynamic phasors in real-time co-simulation of power systems.

3.1 PHIL interface algorithms

In a PHIL simulation, the interface algorithm defines the interface of two decoupled systems, i.e. which signals are exchanged between the VSS and the HuT and how such signals are handled. A systematic evaluation of the main IAs is used in literature in [11]. Here, some of them will be shortly recalled, based on a simple voltage divider circuit shown in Figure 3.1.1 and will be used as the original system simulated in PHIL.

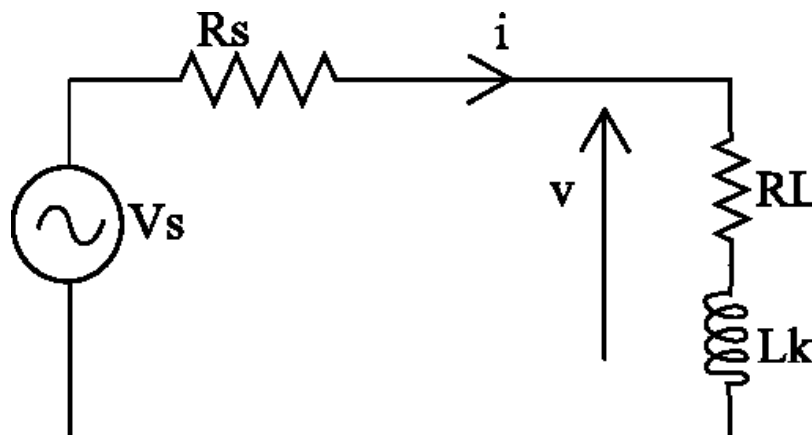


Figure 3.1.1: Original circuit used to illustrate PHIL IA

3.1.1 Ideal Transformer Method (ITM)

In order to clarify the IA concept, the most conventional interface algorithm using a simple example is introduced. In the PHIL simulation set-up, we can consider that the impedance load $Z_L = R_L + L_k$ is the HuT, whereas the voltage source and its series resistance R_s are the VSS.

The ITM method consists of replacing the two ends of the decoupled system with ideal controlled sources. On one side a voltage source is used, while the other side will have a current source. A proper choice of the types of sources can lead either to stability or to instability of the

simulation, even if the original circuit is stable, such as the simple voltage divider in Figure 3.1.1.

Let us consider the causality with current source in VSS and voltage source on the HuT side, the so-called IV set-up (Figure 3.1.2).

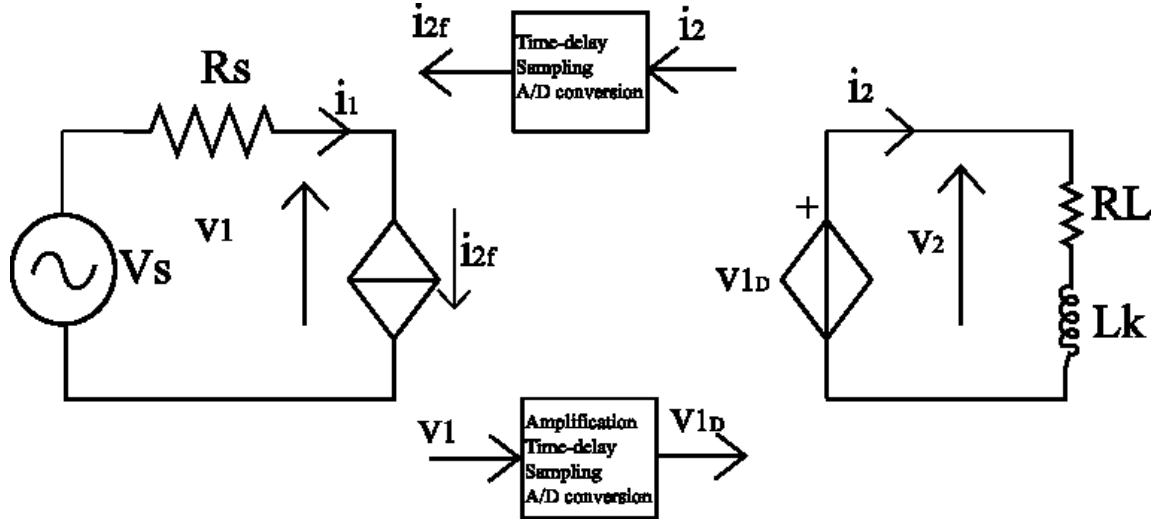


Figure 3.1.2: ITM-IV interface

In this arrangement, v_{1D} is the simulated voltage v_1 that is amplified in order to be connected to a power device, sampled and of course subject to delay, before being utilized to command the controlled voltage source of the HuT. The ideal case would be an interface with unity gain, infinite bandwidth and no time delay in order to have an identity between the HIL system and the original system [11]. However, such an interface is not achievable in practical applications.

Thus, errors are always present in this process, and they are amplified as well as signals. The current i_2 , measured on the physical HuT, will be converted in digital form and fed back to the simulator, preserving such errors. Then, its value is used in the simulator to compute the next time-step state of the system.

In particular, it can be proved that for ITM interface, the error is fed back to the simulator amplified by a factor $-(Z_S/Z_L)$, being Z_S and Z_L the source and load impedances, respectively. Therefore, if $Z_L > Z_S$, such error decreases because the factor is smaller than one and consequently the PHIL simulation is stable. Since the main topic of this thesis, is not PHIL testing, it will not be executed to demonstrate how it works. Nevertheless, it is possible to simulate both the hardware and the rest of the system in a pure simulation environment, using MATLAB/Simulink.

The system described in Figure 3.1.2 is thus simulated, selecting values for parameters of the circuit in order to have $Z_L > Z_S$, i.e. a stable simulation using ITM interface. Furthermore, an ideal unity gain is supposed for the amplification and the interface introduces a time delay of $\Delta T = 250 \mu s$ that, considering a time-step for simulation $T_s = 50 \mu s$, corresponds to 5 time-steps. Hence, choosing parameters shown in Table 1 and considering also a 5th harmonic component with amplitude of 0.1 p.u. added to the voltage source V_s , waveforms of the PHIL system quantities v_1 , v_2 , i_1 and i_2 can be generated and compared to the original waveforms i and v (refer to the Figure 3.1.3).

A sampling rate of 5 time-steps has been used as well, as it can be seen from the results, which show some inaccuracy because of time-delay and the above mentioned sampling. However, waveforms are reproduced with a certain fidelity and the simulation is stable.

Table 1: Values of original circuit for PHIL stable simulation using ITM-IV interface

R_s	R_L	L_k	V_s
2Ω	5Ω	1 mH	$220 V_{pk}$

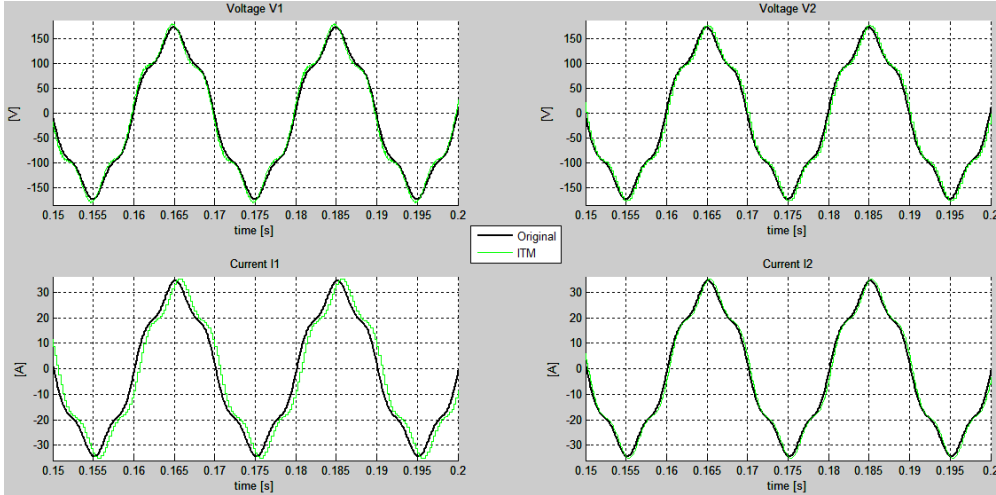


Figure 3.1.3: Simulation results of a stable PHIL simulation using ITM-IV interface

On the other hand, if the error oscillates with increasing amplitude, the simulation becomes unstable. Thus, stability of co-simulation depends on the IA but also on system parameters and dynamics. As example, maintaining the same IA topology used in the previous simulation, but setting parameters of the circuit so that $Z_L < Z_S$ (Table 2), results of simulation are shown in Figure 3.1.4.

Table 2: Values of original circuit for PHIL unstable simulation using ITM-IV interface

R_s	R_L	L_k	V_s
5Ω	2Ω	1 mH	$220 V_{pk}$

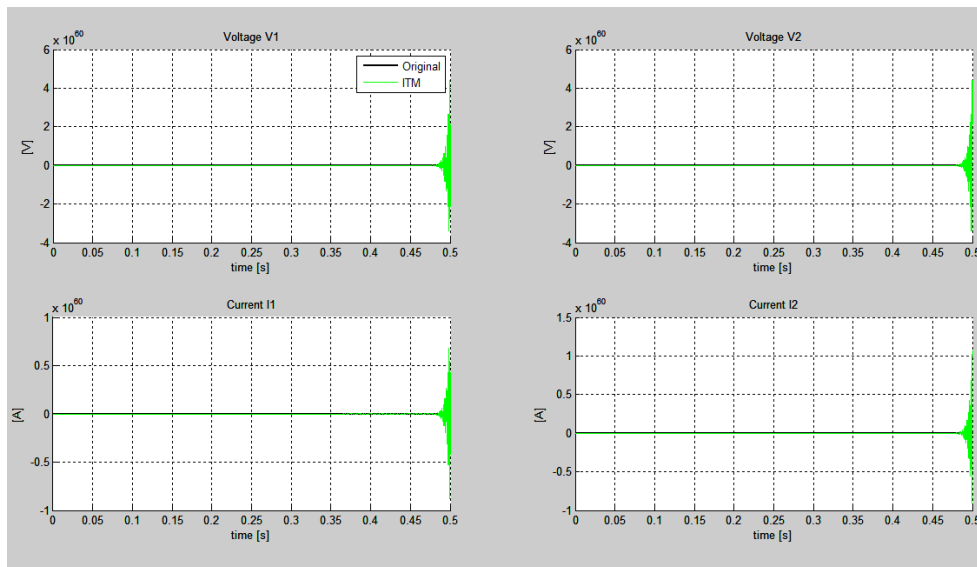


Figure 3.1.4: Simulation results of an unstable PHIL simulation using ITM-IV interface

It is important to highlight that if the system parameters make the simulation unstable, the IA can be implemented using a different topology, i.e. with voltage source in VSS and current source in HuT (Figure 3.1.5). Following the same logic to derive the amplitude of error, in this case it will be amplified by a factor $-(Z_L/Z_S)$. Thus, using parameters of the circuit shown in Table 2 allow this time to get a stable simulation.

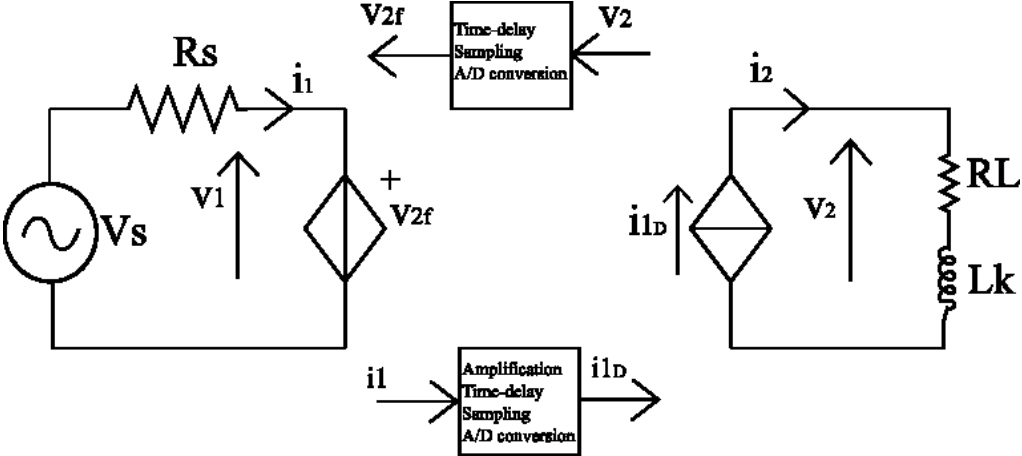


Figure 3.1.5: ITM-VI interface

Although it might show problems of stability with certain characteristics of the system, the implementation of the ITM interface is straightforward and, generally, quite accurate with small values of interface delay. In fact, larger values of such delay compromise accuracy and might jeopardize stability of the simulation itself. The same simulation with results represented in Figure 3.1.3 (so that ITM-IV interface allows a stable simulation), is repeated with an interface delay of $\Delta T = 15 \text{ ms}$, i.e. $300 \cdot T_s$, and accuracy of simulation is much lower, as shown in Figure 3.1.6.

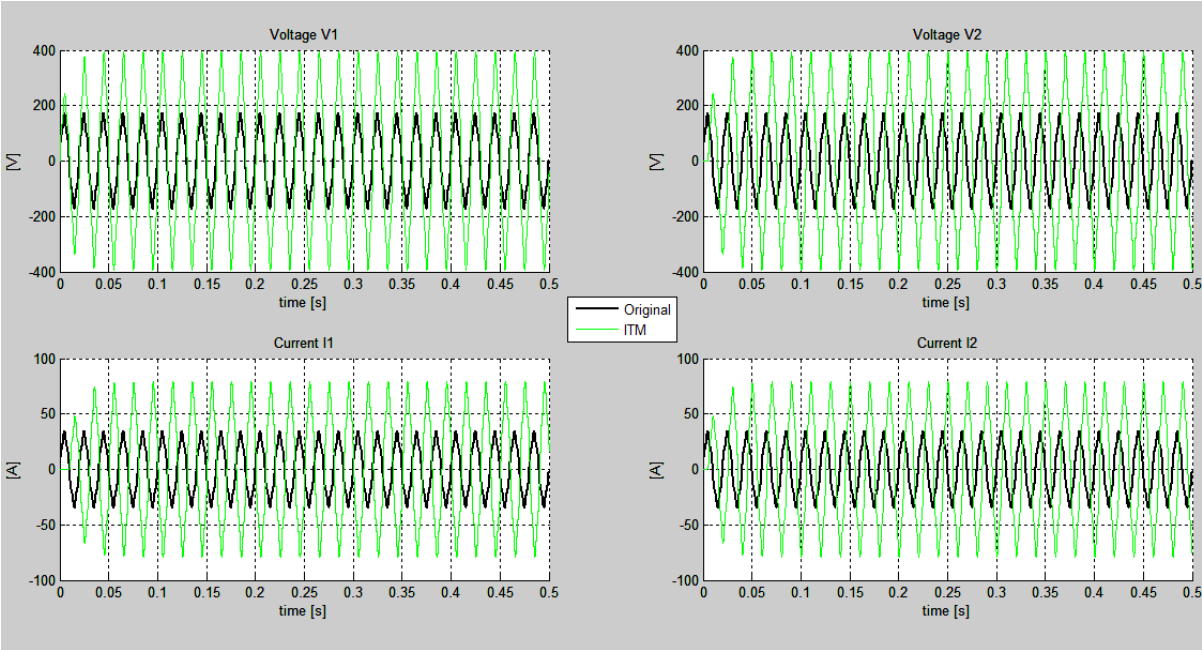


Figure 3.1.6: Simulation results of a PHIL simulation using ITM-IV interface with a large time-delay.

Therefore, it is possible to notice how accuracy decreases with larger time-delay. This issue is because instantaneous values of variables of both VSS and HuT are exchanged during a PHIL simulation. Thus, they are very sensitive to time-delay and, in general, to imperfections of the power interface.

3.1.2 Time-variant First-order Approximation (TFA)

The TFA method was presented in [30]. The basic idea is that the HuT can be approximated as a first order linear system, i.e. RL or RC circuit. Then, the topology of the decoupled system is similar to the ITM one, but the feedback variable is not just measured and sent back to the simulator, as shown in Figure 3.1.7, that illustrates a TFA interface applied to the same circuit of Figure 3.1.1.

An algorithm based on the previous values of the system itself is applied to compute the correct value of the variable, in order to compensate delay caused by the power interface. Results of such algorithm are values of an equivalent conductance or resistance and an equivalent current or voltage, depending on the topology of the algorithm.

In Figure 3.1.7, the TFA-IV topology is reported, which is derived supposing an inductive load for the HuT. The dual interface, instead, is derived considering a capacitive load, and it is shown in Figure 3.1.8.

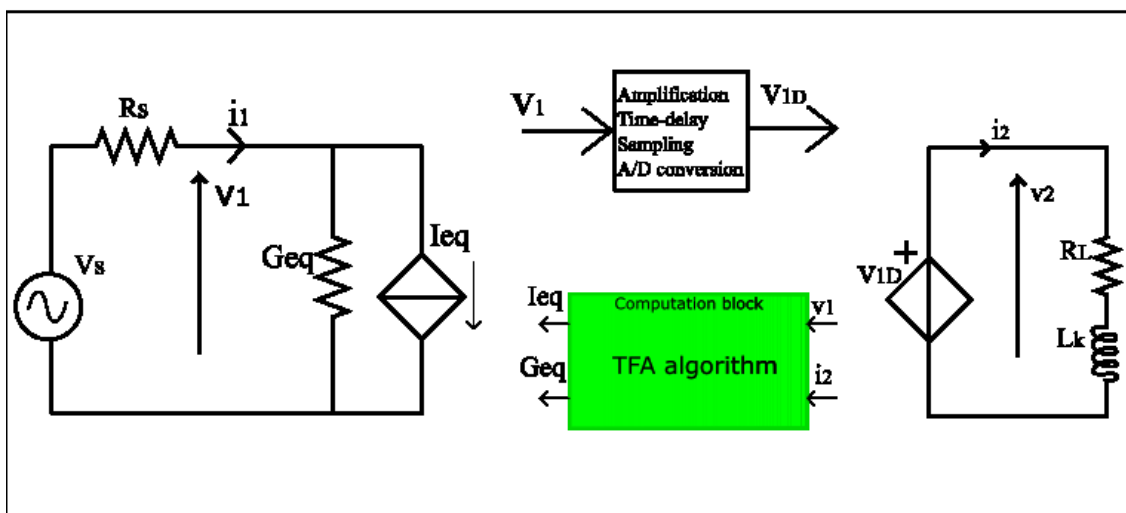


Figure 3.1.7: TFA-IV interface topology

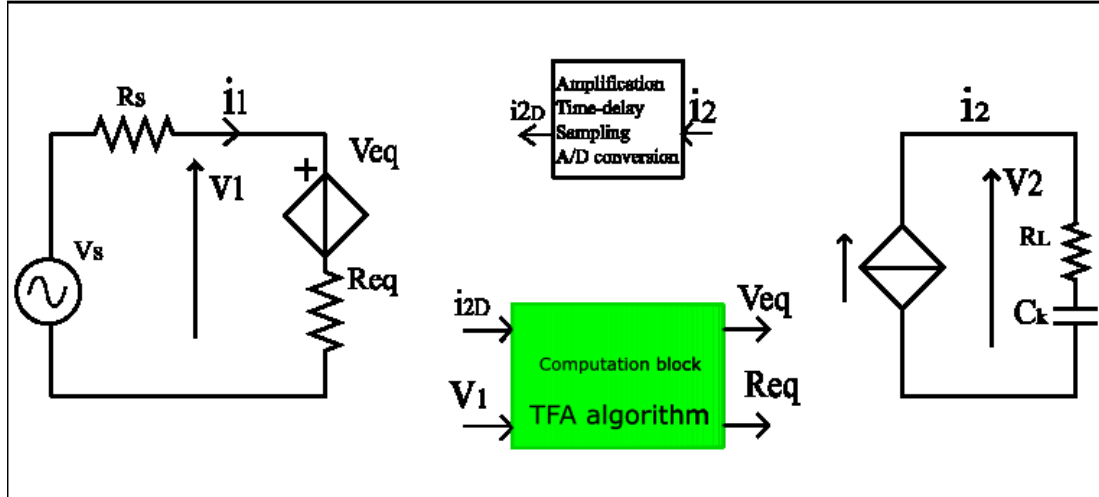


Figure 3.1.8: TFA-VI interface topology

The equations to derive the algorithm will be here introduced, considering an RL-type HuT that has a generic derivative equation:

$$\frac{di_2}{dt} = ai_2 + bv_1 \quad (3.1)$$

Taking the trapezoidal rule to approximate the integral, equation (3.1) can be derived in discrete-time:

$$\frac{i_2(k) - i_2(k-1)}{T_s} = a \frac{[i_2(k) + i_2(k-1)]}{2} + b \frac{[v_1(k) + v_1(k-1)]}{2} \quad (3.2)$$

If the simulation time-step T_s is short enough to neglect changes in voltage v_1 during one time-step so that $v_1(k) = v_1(k-1)$, (3.2) can be rewritten as:

$$i_2(k) = \alpha \cdot v_1(k-1) + \beta \cdot i_2(k-1) \quad (3.3)$$

where $\alpha = \frac{bT_s}{1 - \frac{aT_s}{2}}$ and $\beta = \frac{1 + \frac{aT_s}{2}}{1 - \frac{aT_s}{2}}$.

Therefore, (3.3) provides the values of the interface elements:

$$\begin{aligned} G_{eq}(k) &= \alpha \\ I_{eq}(k) &= \beta \cdot i_2(k-1) \end{aligned} \quad (3.4)$$

The algorithm allows then calculation of $i_2(k)$ using circuit information of the previous time-step, but the problem is determining parameters α and β , which are based on variable simulation parameters a and b .

Therefore, a proposed approach is calculation of α and β using the results of the simulation itself and updating every time-step. In other words, tracing two time-steps back equation (3.3), we can get the system necessary to find α and β :

$$\begin{bmatrix} \alpha \\ \beta \end{bmatrix} = \begin{bmatrix} v_1(k-2) & i_2(k-2) \\ v_1(k-3) & i_2(k-3) \end{bmatrix}^{-1} \begin{bmatrix} i_2(k-1) \\ i_2(k-2) \end{bmatrix} = A^{-1} \cdot \begin{bmatrix} i_2(k-1) \\ i_2(k-2) \end{bmatrix} \quad (3.5)$$

Since all the currents and voltages in (3.5) can be either measured from the HuT or determined from the simulation, system (3.5) can be solved.

The dual version of the interface can be derived, following the dual steps, for an RC-type load.

PHIL simulation using TFA interface can be implemented in a pure software environment using MATLAB/Simulink for the purpose of analysis. Considering an IV-type topology, the theory of this method requires a variable conductance on the VSS. However, initial tests have shown how using a resistive element whose value changes over the simulation, can make the simulation inaccurate and unstable, due to numerical issues.

Instead, as proposed in [11], the computed quantities using the TFA algorithm are directly used in their assembled form, shown in eq. (3.3), to control a current source. In this way, it is possible to generate more robust results for the simulation. Using the same original circuit (Figure 3.1.1) used in the previous section for ITM interface, and the same parameters that made the simulation with ITM stable (Table 1) results of simulation compared to original circuit are reported in Figure 3.1.9. In this case as well, a time delay of $\Delta T = 250 \mu s$ and a sampling rate $5 \cdot T_s$ have been selected, whereas an ideal unity gain is assumed for amplification.

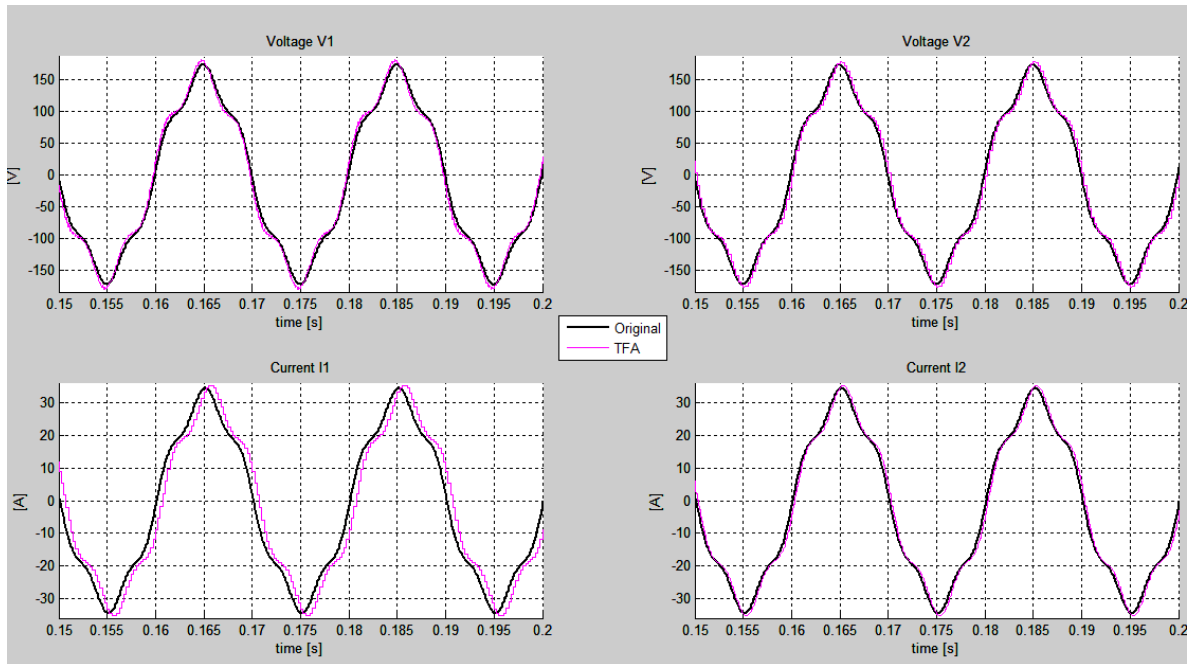


Figure 3.1.9: Simulation results of a PHIL simulation using TFA-IV interface with a small time-delay

If instead the interface delay for simulation is selected to be $\Delta T = 15 \text{ ms}$, the algorithm works just for around 50 ms of simulation with inaccurate results, as reported in Figure 3.1.10, where after numerical problems arise in inverting matrix A , interrupting the calculation.

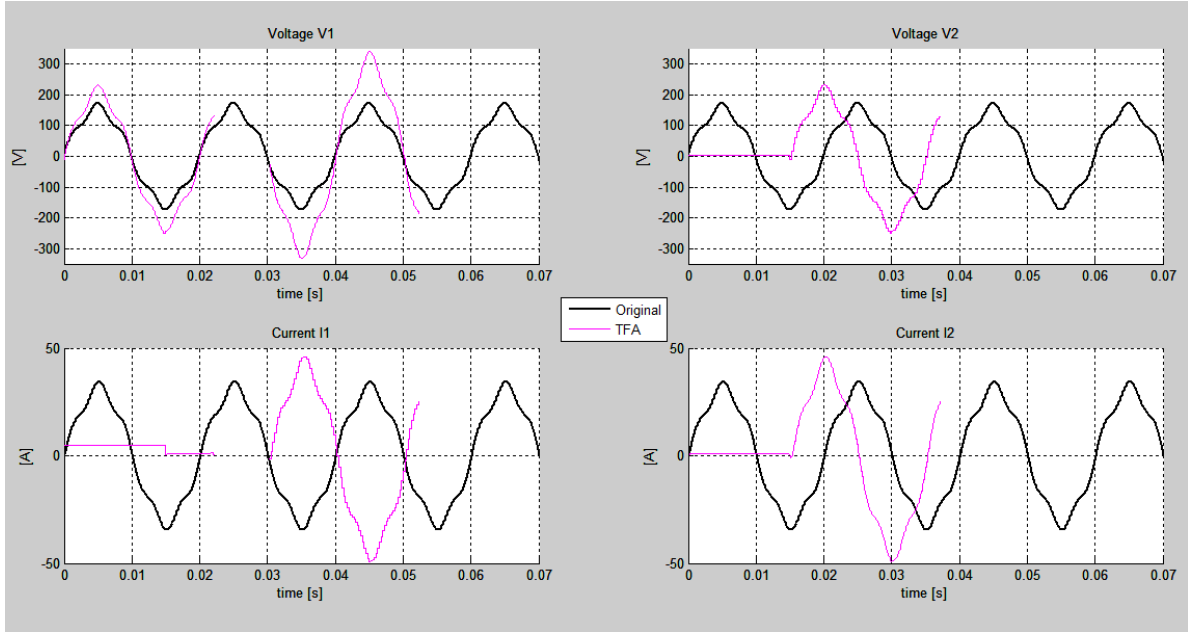


Figure 3.1.10: Simulation results of a PHIL simulation using TFA-IV interface with a large time-delay

A common issue of this method is indeed inverting the matrix A , which especially in DC steady-state (i.e. quantities do not change rapidly over the simulation time, not to mention over one time-step) and when simulation time-step is very small, can become singular. Moreover, other problems inherent for TFA algorithm are:

- Limitations with non-linear systems, due to the algorithm predictive nature: it is harder to compute state variables with systems that have rapid changes
- Need to change the interface topology for different types of loads
- Values of $v_1(k)$ and $i_2(k)$ for eq. (3.5) must be initialized for the first time-steps of simulation, and a wrong choice can lead to numerical issues or slow convergence

In [31], a solution to the first issue is introduced, based on keeping previous values once that steady state is reached, and adding a further controlled source on VSS side to compensate errors caused by numerical issues.

3.2 Bilateral teleoperation methods

Due to its wide range of applications, teleoperation has a numerous control strategies that have been studied and tested for a long time. The main issues in teleoperation methods are represented by the presence of time-delay in the communication channel between the human operator and the robot, which jeopardizes the stability of the system and might also compromise the transparency of the operation. These issues have been addressed in [21], using a passivity-based theory, which will be here summarized.

3.2.1 Passivity formalism

The idea behind this theory is to implement a mathematical system that reproduces a physical system and thus is passive. The power P entering a system is defined as the scalar product between the input vector x and the output vector y of the system itself. Moreover, an energy

storage function E , which has a low boundary, and a non-negative power dissipation function P_{diss} are defined. According to these definitions, a system is passive if it follows:

$$P = \mathbf{x}^T \mathbf{y} = \frac{dE}{dt} + P_{diss} \quad (3.6)$$

This means that power is either stored or dissipated. In other words, the energy supplied by the system until time t is limited to the initially stored energy, which is negative:

$$\int_0^t P d\tau = \int_0^t (\mathbf{x}^T \mathbf{y}) d\tau = E(t) - E(0) + \int_0^t P_{diss} d\tau \geq -E(0) = \text{constant} \quad (3.7)$$

Using the control theory of non-linear systems to analyze stability, it can be proved that a passive system is stable.

Generally, any number of input and output variables can exist for the system, and they can always be brought to single vectors of inputs and outputs. Nevertheless, it is easier to consider a 2-ports system. So far, power was assumed positive if entering the system. When a 2-ports system is taken into account, it is convenient to assume a first-side port 1 that has positive power entering the system, and a second-side port 2 with positive power leaving the system. In this asset, the total power flow that regulates the stored energy variation of (3.6), in a teleoperation system involving velocities $\dot{\mathbf{x}}$ and forces \mathbf{F} , can be written as:

$$P = \dot{\mathbf{x}}_1^T \mathbf{F}_1 - \dot{\mathbf{x}}_2^T \mathbf{F}_2 \quad (3.8)$$

3.2.2 Wave transformation

The theory of wave transformation is the next step of this formulation. The basic notion is to separate the total power flow of the system into two parts, power input and output, which then are related to the physical concept of input and output waves. Assuming the 2-port element with a first-side port 1 and a second-side 2, the total power flow is:

$$P = \dot{\mathbf{x}}_1^T \mathbf{F}_1 - \dot{\mathbf{x}}_2^T \mathbf{F}_2 = \frac{1}{2} \mathbf{u}_1^T \mathbf{u}_1 - \frac{1}{2} \mathbf{w}_1^T \mathbf{w}_1 + \frac{1}{2} \mathbf{u}_2^T \mathbf{u}_2 - \frac{1}{2} \mathbf{w}_2^T \mathbf{w}_2 \quad (3.9)$$

In this formalism, the vectors \mathbf{u}_1 and \mathbf{u}_2 are the input waves of the system described in wave variables, because they increase the power flow. Conversely, \mathbf{w}_1 and \mathbf{w}_2 are the output waves. Equation (3.9) describes, implicitly, a transformation of variables from physical quantities (velocities $\dot{\mathbf{x}}$ and forces \mathbf{F}) into wave variables \mathbf{u} and \mathbf{w} . Therefore:

$$\begin{aligned} \mathbf{u}_1 &= \frac{1}{\sqrt{2b}} (\mathbf{F}_1 + b\dot{\mathbf{x}}_1), \quad \mathbf{u}_2 = \frac{1}{\sqrt{2b}} (\mathbf{F}_2 - b\dot{\mathbf{x}}_2) \\ \mathbf{w}_1 &= \frac{1}{\sqrt{2b}} (\mathbf{F}_1 - b\dot{\mathbf{x}}_1), \quad \mathbf{w}_2 = \frac{1}{\sqrt{2b}} (\mathbf{F}_2 + b\dot{\mathbf{x}}_2) \end{aligned} \quad (3.10)$$

The parameter b must be strictly positive and, theoretically, it can be chosen arbitrarily. However, it defines a characteristic impedance between wave variables and, consequently, it

affects the system behavior: a proper choice of this wave impedance is thus critical for a transparent operation.

The transformation (3.10) can be inverted to provide power variables as a function of the wave variables:

$$\begin{aligned} F_1 &= \sqrt{\frac{b}{2}}(u_1 + w_1), \quad F_2 = \sqrt{\frac{b}{2}}(v_2 + w_2) \\ \dot{x}_1 &= \frac{1}{\sqrt{2b}}(v_1 - w_1), \quad \dot{x}_2 = -\frac{1}{\sqrt{2b}}(v_2 - w_2) \end{aligned} \quad (3.11)$$

An important remark about these equations is that every port of the system is uniquely defined by one wave variable and one power variable. Thus, a system defined in wave variables can be connected to systems that gives either flow or effort references. In particular, it is possible to choose a velocity reference at port 1 while specifying a force reference at the other port. In this causality, the transformation can be graphically explained by Figure 3.2.1.

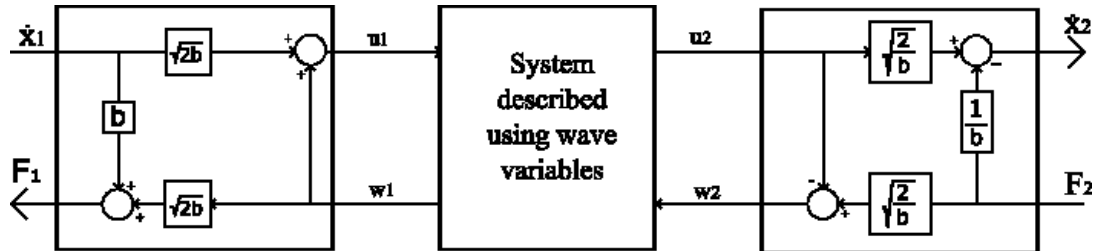


Figure 3.2.1: Wave transformation using \dot{x}_1 and F_2 as inputs

Wave transformation is related to passivity with the following statement: a system is passive if the energy brought by the output waves is limited to the energy received through the input waves:

$$\int_0^t \frac{1}{2} \mathbf{w}^T \mathbf{w} d\tau \leq \int_0^t \frac{1}{2} \mathbf{u}^T \mathbf{u} d\tau \quad (3.12)$$

This condition is satisfied when output waves \mathbf{w} amplitude is bounded by the amplitude of the input waves \mathbf{u} , which can possibly be delayed. Thus, time-delays can be included into systems described by wave variables with preserving the stability. The mathematical proof behind this method is connected to control theory small gain theorem, which states that a closed-loop system is stable if the H-infinity norm of the open-loop system is limited to unity. A system expressed in wave variables satisfies this theorem and it is thus stable [21].

Usually, introducing even small time-delays can lead to instabilities in feedback systems. It is possible to separate the communication channel from the remaining subsystems, and it is enough to use a passive communication to guarantee the stability of the whole system. Keeping the same topology of control mentioned so far (i.e. sending a velocity reference from system 1 to system 2, from where a force feedback returns), the normal communication set-up with time-delays would be:

$$\begin{aligned}\dot{x}_2(t) &= \dot{x}_1(t - \Delta T) \\ F_1(t) &= F_2(t - \Delta T)\end{aligned}\tag{3.13}$$

where ΔT is the time-delay. Analysing the power flow of the system with this standard communication, the conclusion would be that the communication is passive as long as the power dissipation of (3.6) is positive. However, certain values of the input variables can lead to negative dissipation and, thus, instability.

A traditional way to stabilize such communication used to be making the system more damped. Therefore, dissipating element would be placed next to communication, ensuring passivity but changing the dynamics and the operation of the system. The wave scattering approach, instead, was introduced in [32] and it is based on imitating physical systems with wave phenomena, as mentioned earlier in this chapter. The method allows constructing a communication procedure based on a lossless electric transmission line, where time-delays are stably present in physical lines, thus preserving stability regardless of the time delay. Therefore, exchanging wave variables instead of power variables, the analysis of the power flow shows [21] how passive communication is achieved in spite of the time delay:

$$\begin{aligned}w_1(t) &= w_2(t - \Delta T) \\ u_2(t) &= u_1(t - \Delta T)\end{aligned}\tag{3.14}$$

Therefore, this method provided in literature allows to have a passive and stable communication for ideally any time-delay.

3.2.3 Main issues of the method

Since it is based on an imitation of natural wave phenomena, wave transformation interface has some drawbacks deriving from wave concept. In physical systems, waves are reflected at points of the wave transporter where the impedance changes. Similarly, in a wave transformation scheme, reflections might happens in the local and remote port. In this context, such reflections may jeopardize the content of exchanged information in the communication, thus decreasing transparency. What is more, they could show oscillatory behavior that, if it is not damped, could lead to vibrations of the same amplitude of the exchanged signals, compromising stability of the operation.

Therefore, matching the wave impedance of the interface to the real impedance of the remaining system is an actual issue that can degrade the results of the teleoperation itself. The most intuitive solution would be to match the wave impedance to the system's impedance, but that is not always possible. For instance, an estimation of the system impedance could be not precise enough or, more likely, that impedance changes a lot and rapidly during the operation of the system. Thus, if that approach cannot be adopted, it is possible to add matched terminations to the wave transmission, as shown in Figure 3.2.2. They are basically dissipating elements with impedance of the same value of the wave impedance: and thus, they eliminate the reflections. The problem with this approach is that such terminations modify the response of the system, meaning that signals in communication are scaled and, moreover, relative position between the operator controller and robot controller is drifted.

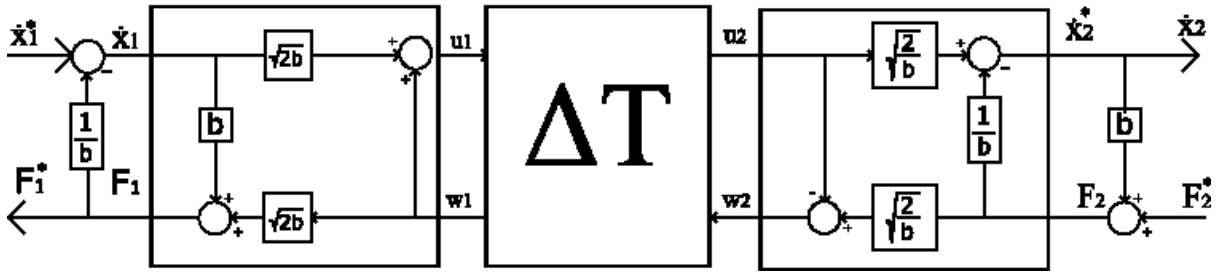


Figure 3.2.2: Wave transmission with matched terminations

Choosing a proper value of b according to the system characteristics is not the only issue about designing a wave transformation interface. In fact, as mentioned in [33], “*the parameter b should be tuned according to the delay*”. This means that if a teleoperation interface is implemented through a communication channel with a time-varying delay during the operation, the chosen value of b could compromise transparency of the system. This problem is connected to the violation of passivity condition. Namely, passivity of communication is not respected when a wrong value of b is set for a certain time-delay. Therefore, this problem is addressed in literature implementing passivity control methods, like the ones described in chapter 2.

For this reason, implementing a teleoperation system with this particular approach over the Internet, where time-delay is variable in an unpredictable way, seems not feasible. This has been addressed in [34], where the scattering transformation equations have been modified to include a time-varying delay, after having proved that stability of teleoperation is not guaranteed with a variable delay, since communication is not generally always passive. The approach used in this research was to add a time-varying gain, tuned according to the rate of change of the delay during the operation. Then, the tracking of the delay is done adding a further feed-forward path in the interface, between the operator side and the slave side. This proof eliminates, theoretically, the time-varying terms that make the communication channel not passive in the power flow balance, but still many problems remain to be solved, like precision of the tracking estimation and rates of change of time-delay larger than unity.

Finally, a further issue of wave variable control is represented by the fact that the remote environment controlled by the operator might have an unknown behavior. In other words, if the controller of the robot is implemented in discrete-time and the state of the environment is computed online, an algebraic loop arises when it is not possible to calculate the state in advance. This has been addressed in [35] with the following method. Reordering the second equation in (3.10) to get the velocity command that system 2 obtains from the wave signal u_2 :

$$\dot{x}_2(t) = \sqrt{\frac{2}{b}} u_2(t) + \frac{-F_2(t)}{b} \quad (3.15)$$

In discrete time, (3.15) is:

$$\dot{x}_2(k) = \sqrt{\frac{2}{b}} u_2(k) + \frac{-F_2(k)}{b} \quad (3.16)$$

where k represents the current time-step of the remote environment simulation. The problem is that in (3.16), the environment force F_2 depends on the velocity reference \dot{x}_2 :

$$F_2(k) = h_{EN}[\dot{x}_2(k)] \quad (3.17)$$

where h_{EN} is the transfer function of the environment. Therefore, the right side of (3.16) depends on the left side, creating an algebraic loop. If the solution of the environment is not fast enough, the algebraic loop can be unwrapped introducing a one time-step computational delay, as shown in Figure 3.2.3:

$$\dot{x}_2(k) = \sqrt{\frac{2}{b}} u_2(k) + \frac{-F_2(k-1)}{b} \quad (3.18)$$

Unfortunately, the introduction of that one time-step delay dramatically decreases the stability of the operation under wave transformation interface. Namely, the issue related to the violation of the passivity condition due to a virtually added energy to the communication by the computational delay.

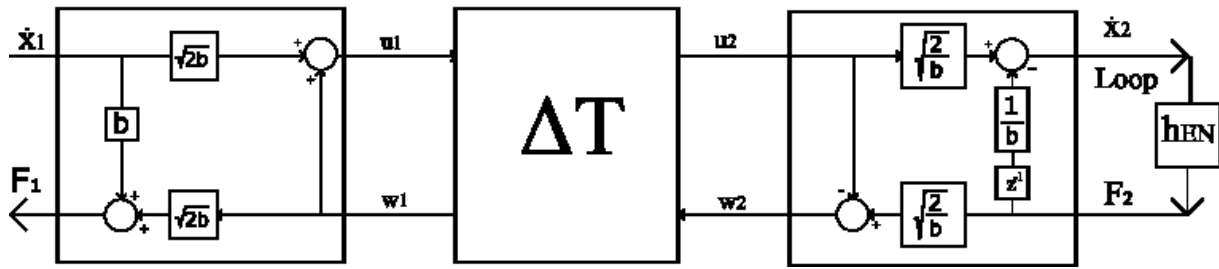


Figure 3.2.3: Algebraic loop arising at the connection between wave transformation and environment

The issue is solved developing a time domain passivity control that computes the energy generated by the computational delay using:

$$\Delta E_{delay}(k) = \sum_{k=0}^t \frac{-F_2^2(k) + F_2(k)F_2(k-1)}{b} \quad (3.19)$$

where t is the current simulation time-step. Then, a compensation algorithm that acts when $\Delta E_{delay} < 0$ is implemented, decreasing the returning wave variable w_2 so that ΔE_{delay} becomes zero:

$$w_{2new}(k) = sgn(w_2(k)) \sqrt{w_2^2(k) - 2\Delta E_{delay}(k)} \quad (3.20)$$

This allows to maintain stability of the operation despite the introduction of a computational time-delay that unwraps the algebraic loop.

3.3 Representation of interface quantities

Electric systems are known to be represented through several domains, according to the type of system and, especially, to the purpose for which they are analyzed. When it comes to power systems simulation, particularly, complexity and size of the problems become larger, since they have a wide range of diverse elements operating at various levels of power and frequency. Consequently, transients can have a timeframe from nanoseconds to hours. Usual simulation tools tend to focus on a specific range of dynamics, but lately it has become important to develop new approaches capable of simulating the wide variety of timescales.

This problem has been addressed in [36], a thesis focused on developing a new simulation technique based on dynamic phasors, in order to cover the entire spectrum of frequencies characterizing power system dynamics. Here follows a short explanation of the basics of dynamic phasors, highlighting their advantages and drawbacks as well. Later in this section, the concept of dynamic phasors will be applied to co-simulation interface algorithms, referring to a previous work that has shown how they can improve simulation fidelity, even though they are only used as communication variables while the system is simulated in time domain.

3.3.1 Dynamic phasors theory

Phasors represent sinusoidal quantities in steady state as complex numbers, at a certain frequency. Dynamic phasors were first introduced simply as phasors whose magnitude and phase can vary over time, to include further dynamics of power systems into a simulation by extending the bandwidth of frequencies. Nevertheless, using this approach still limits the analysis around the base frequency of the power system, but the use of power electronics devices or simply the DQ0 reference for machines, give rise to other harmonics in the system. The generalized state space averaging method, introduced in the field of power electronics, allows incorporating the behavior of higher order harmonics.

The main idea is assuming that “*all quantities in a system model may be represented by a Fourier series with time-varying coefficients*” [36]. Analyzing the method, it results that those coefficients are dynamic phasors themselves, defined for the fundamental frequency and all of its harmonics, allowing for simulation of the whole range of dynamics inherent in a power system.

If such frequency contents $\tilde{\mathbf{X}}_k$ of transients are around $k\omega_0$, with ω_0 being the fundamental frequency, the global spectrum is a combination of the spectra around $k\omega_0$ [37]:

$$\mathbf{X}(j\omega) = \sum_{k=-\infty}^{+\infty} \tilde{\mathbf{X}}_k(j\omega) \quad (3.21)$$

where the spectral content $\tilde{\mathbf{X}}_k(j\omega)$ is the frequency shifted version of the baseband signal $\mathbf{X}_k(j\omega)$, i.e. $\tilde{\mathbf{X}}_k(j\omega) = \mathbf{X}_k(j\omega - jk\omega_0)$. Therefore:

$$\mathbf{X}(j\omega) = \sum_{k=-\infty}^{+\infty} \mathbf{X}_k(j\omega - jk\omega_0) \quad (3.22)$$

Using the inverse transformation from frequency to time domain for (3.22):

$$x(t) = \sum_{k=-\infty}^{+\infty} X_k(t) e^{jk\omega_0 t} \quad (3.23)$$

where $X_k(t)$ is the analytical baseband signal.

This method can be considered as an adjusted form of Fourier series with time-dependent coefficients. For periodic signals with period T_0 , the complete Fourier series of $x(t)$ would be:

$$x(t - T_0) = \sum_{k=-\infty}^{\infty} X_k(t) e^{jk\omega_0(t-T_0)} \quad (3.24)$$

where $\omega_0 = 2\pi / T_0$ and $X_k(t)$ is the k^{th} Fourier coefficient. (3.24) can be also seen as an orthogonal signal expansions of $x(t)$ with orthonormal basis $e^{jk\omega_0(t-T_0)}$. Therefore, the k^{th} Fourier coefficient can be computed using the following inner product:

$$X_k(t) = \langle x(t), e^{jk\omega_0(t-T_0)} \rangle = \langle x(t) \rangle_k \quad (3.25)$$

Which, if $\tau = t - T_0$, is given by:

$$\langle x \rangle_k(t) = \frac{1}{T_0} \int_{t-T_0}^t x(\tau) e^{-jk\omega_0 \tau} d\tau \quad (3.26)$$

From (3.26) one can see how periodic functions, with period T_0 , have the same time-dependent coefficients $\langle x \rangle_k(t)$ as $x(t)$. Those coefficients are dynamic phasors, defined for fundamental frequency and its harmonics. What is more, this formula shows the idea behind this method: the series catches a part of $x(t)$ by using a time window of length T_0 , and dynamic phasors are computed across this time window. Then, the window moves along the waveform, calculating dynamic phasors for each point in time. [36]

In practical applications, (3.24) is truncated to a certain number of harmonics K , so that all significant ones are considered in the system model, according to the desired level of detail given by this approximation.

This process is suitable for applications in which waveforms are known for every point. Nevertheless, when it comes to simulations, waveforms of a system need to be generated by using information belonging to previous states of the systems. Therefore, it is more meaningful to consider (3.26) as the definition of the dynamic phasors operator, $\langle \cdot \rangle_k$, which can be applied to time-domain equations. Considering a set of non-linear state equation, and applying the dynamic phasors operator:

$$\left\langle \frac{dx}{dt} \right\rangle_k = \langle \mathbf{f}(t, \mathbf{x}, \mathbf{u}) \rangle_k \quad (3.27)$$

The derivative can be evaluated using the dynamic phasors differentiation property, given by:

$$\left\langle \frac{dx}{dt} \right\rangle_k = \frac{d\langle x \rangle_k}{dt} + jk\omega_0 \langle x \rangle_k \quad (3.28)$$

Since no generic form of the right-hand side of (3.27) exists, it has to be evaluated for every individual system. Moreover, if the system is non-linear, it is not possible to get a closed-form expression for the right-hand side, except for polynomial nonlinearities, where convolution property can be applied. Generally, an approximation is necessary when using dynamic phasors for simulation of non-linear systems.

The final form of (3.23) can be thus obtained by using (3.24), which yields to:

$$\frac{d\langle x \rangle_k}{dt} = -jk\omega_0 \langle x \rangle_k + \langle \mathbf{f}(t, \mathbf{x}, \mathbf{u}) \rangle_k \quad (3.29)$$

Besides the main advantage of providing a larger bandwidth in the frequency domain, compared to standard phasors approach, the use of dynamic phasors offers other benefits. [37]

Dynamic phasors are narrow banded signals, so they may be numerically calculated more efficiently. Moreover, in presence of power electronics devices with periodic switching, this approach approximates a periodically switched system with a continuous system, reducing the computational burden and allowing more detailed studies of the sensitivity of the system itself, in order to improve the design of controllers schemes. On the other hand, a major drawback of the dynamic phasors method is that the number of variables and equations increases when compared to time-domain, which can lead to inefficiency of the simulation. However, this loss in efficiency is often compensated by the one gained due to slower variations of Fourier coefficients than instantaneous values under certain conditions [37].

3.3.2 Time-frequency interface quantities for co-simulation

The possibility to use dynamic phasors (DP) as interface variables in a co-simulation set-up has been explored in [38], where the basic ITM interface is further modified by using DP as means of communication between two real-time simulators (Figure 3.3.1).

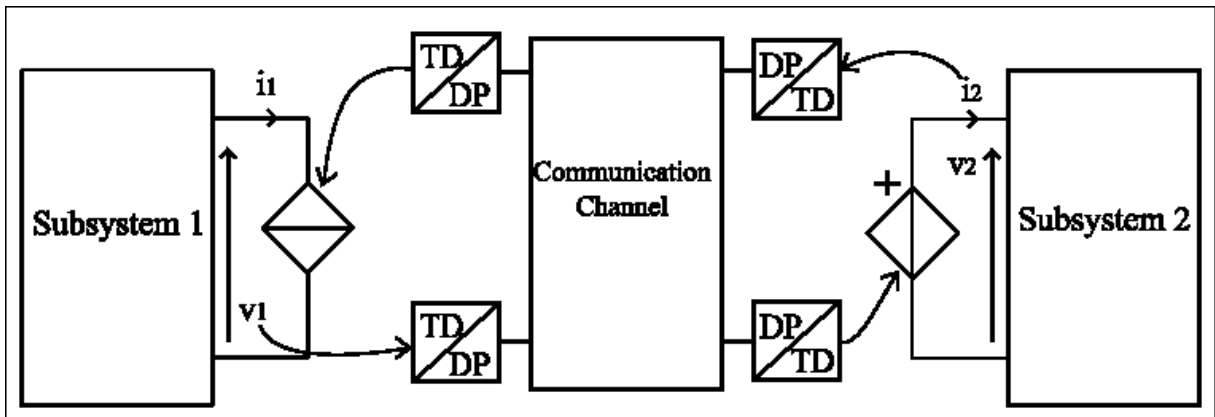


Figure 3.3.1: Co-simulation interface based on ITM and using DP

The discrete-time form of the dynamic phasors operator defined in (3.26) is applied to interface quantities of the two decoupled subsystems before being sent into the communication channel,

as Figure 3.3.1 shows. However, the simulators perform simulations in time domain (TD), whereas DP are used only to exchange information.

In that work, several electric systems are simulated with both deterministic and time-varying delay, the latter one through a geographically distributed co-simulation over the Internet. The main objective was to determine improvements obtained by using DP as interface quantities rather than TD values. In that case, both simulation have been run using OPAL-RT simulators. Results of that analysis proved two main points:

- The negative damping effect caused by time-delay in the interface is partially eliminated by using DP, i.e. stability of the system is guaranteed for higher interface delay values than the case in which TD values are exchanged
- Using DP improves simulation accuracy in steady-state, both with deterministic and real time-delay over the internet. This result has been evaluated using a 2-norm metric, and obtained based on a simple AC circuit and on a more complex non-linear system.

As an example, considering the same simulation scenario implemented for the ITM interface with a large time-delay $\Delta T = 15$ ms, which produced inaccurate results (Figure 3.1.6), it is possible to compare results using the ITM interface modified with dynamic phasors for interface quantities. Basically, variables v_1 and i_2 are transformed into a set of complex numbers representing the harmonic orders that are considered for the waveform approximation. In this case, we consider the first 5 harmonics including the DC component. Results of this simulation are shown in Figure 3.3.2.

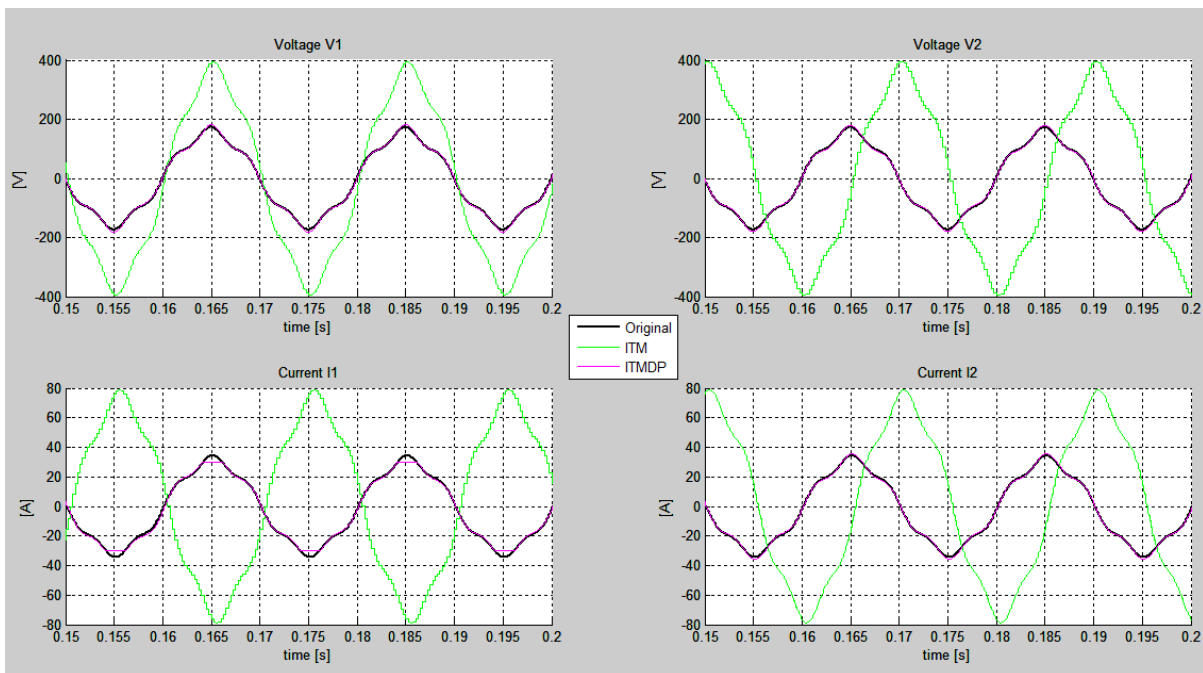


Figure 3.3.2: Simulation result using ITM-IV interface with a large time-delay, using DP to exchange information over the communication

As it can be seen, accuracy of simulation is much higher using dynamic phasors, although this is just a simple example.

Therefore, this previous achievement encourages to further explore the possible improvements deriving from implementing a dynamic phasor-based interface algorithm for geographically distributed co-simulations.

4. Co-simulation interface algorithms

The aim of this chapter is to adapt the two interfaces that have been introduced in chapter 2 for co-simulation of power systems. This process has been done in different ways for the two IA:

- 1) For the TFA interface, introduced in literature as an interface for PHIL, the topology has been modified to consider the fact that no physical device is present in co-simulation, but the two subsystems are completely simulated. Therefore, the computation block is present on both sides of the decoupled system and not only on the HuT side.
- 2) For the WT interface, used in telerobotics, it was necessary to change variables from mechanical to electrical systems.

Later, the two interfaces have been furtherly modified using DP as means to exchange information from one simulator to the other. Again, different precautions were necessary for the two interfaces, as it will be shown later in this chapter.

Moreover, the new interfaces will be implemented, off-line, using simple circuits to test their feasibility and to show their main advantages and drawbacks.

4.1 Co-simulation interface algorithm based on Time-variant First-order Approximation

The TFA interface algorithm illustrated in the previous chapter refers to a PHIL simulation set-up. That means that a VSS is connected to a HuT. When it comes to co-simulation, instead, two simulators are linked: it makes sense, thus, to modify the interface implementing the prediction algorithm on both sides of the decoupled system. Considering the topology shown in fig. 3.4, this approach means that not only the computed current is used to control the current source, but also another computation block is used to calculate a voltage based on previous states of the system in order to control the voltage source, as shown in Figure 4.1.1:

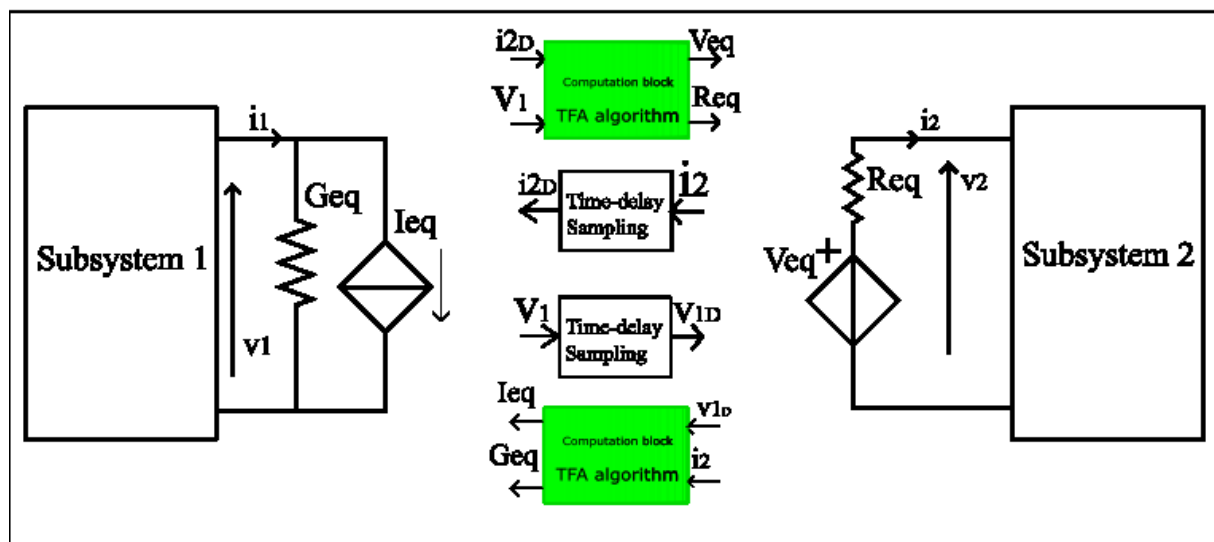


Figure 4.1.1: Modified TFA interface algorithm implemented on both sides of decoupled system for co-simulation

Therefore, considering a given interface delay ΔT , let us define a discrete quantity x that is transferred through the communication channel in the following fashion:

$$x(k - \Delta T) = x_D \quad (4.1)$$

where the subscript D indicates the delay. This simple definition allows for an easier description of the modified TFA algorithm for co-simulation. Like already stated in chapter 3, different topologies can characterize the same interface algorithm. This means that some IAs can be implemented either in voltage-type or in current-type, depending on the relative position of controlled voltage and current sources in the decoupled system.

Thus, let us consider a voltage-type scheme, as shown in fig. 4.1, starting by stating that the algorithm could totally be implemented in the dual way using the same equations, as long as the correct variables are chosen.

4.1.1 Description of the modified algorithm in time-domain

At time step k , simulated voltage $v_1(k)$ is sent from SS1 through the communication channel, where it is sampled with a certain sampling rate and it is received in SS2 as $v_{1D}(k)$. In SS2, the TFA algorithm is implemented in a computation block that calculates, for every time step, the feedback quantities used to control SS1 interface using the eq. (3.3), slightly modified here to include time-delay reference:

$$i_{2C}(k) = \alpha \cdot v_{1D}(k - 1) + \beta \cdot i_2(k - 1) = Geq \cdot v_{1D}(k - 1) + Ieq \quad (4.2)$$

where the subscript C indicates a quantity computed using the algorithm. Then, $i_{2C}(k)$ is sent back, delayed as $i_{2CD}(k)$ to SS1 to control the variable conductance and the controlled current source. The parameters α and β are computed using the same method illustrated in subsection 3.1.2.

In parallel, simulated current $i_2(k)$ is sent from SS2, sampled and delayed into $i_{2D}(k)$ in SS1 where another computation block calculates the quantities necessary to control SS2 using the following formula:

$$v_{1C}(k) = \gamma \cdot i_{2D}(k - 1) + \delta \cdot v_1(k - 1) = Req \cdot i_{2D}(k - 1) + Veq \quad (4.3)$$

Again, $v_{1C}(k)$ is sent to SS2 via the communication channel to command the controlled voltage source and the variable resistance. Parameters γ and δ are calculated, for every time-step of simulation, using the already mentioned method in a dual way.

Applying this algorithm to both sides of the decoupled system is more appropriate for co-simulation because it is a simulator-to-simulator set-up. The suitability of this modified interface has been tested using the same original circuit that is the simple voltage divider used in the previous chapter. The test has been executed using Simulink, selecting parameters of Table 1 with a small interface delay $\Delta T = 250 \mu s$ and a sampling rate five times the simulation time steps. The results are shown in Figure 4.1.2 with a zoom on half-waveform to highlight

differences in accuracy compared to the simulated original system and to a simulation done using the original TFA method.

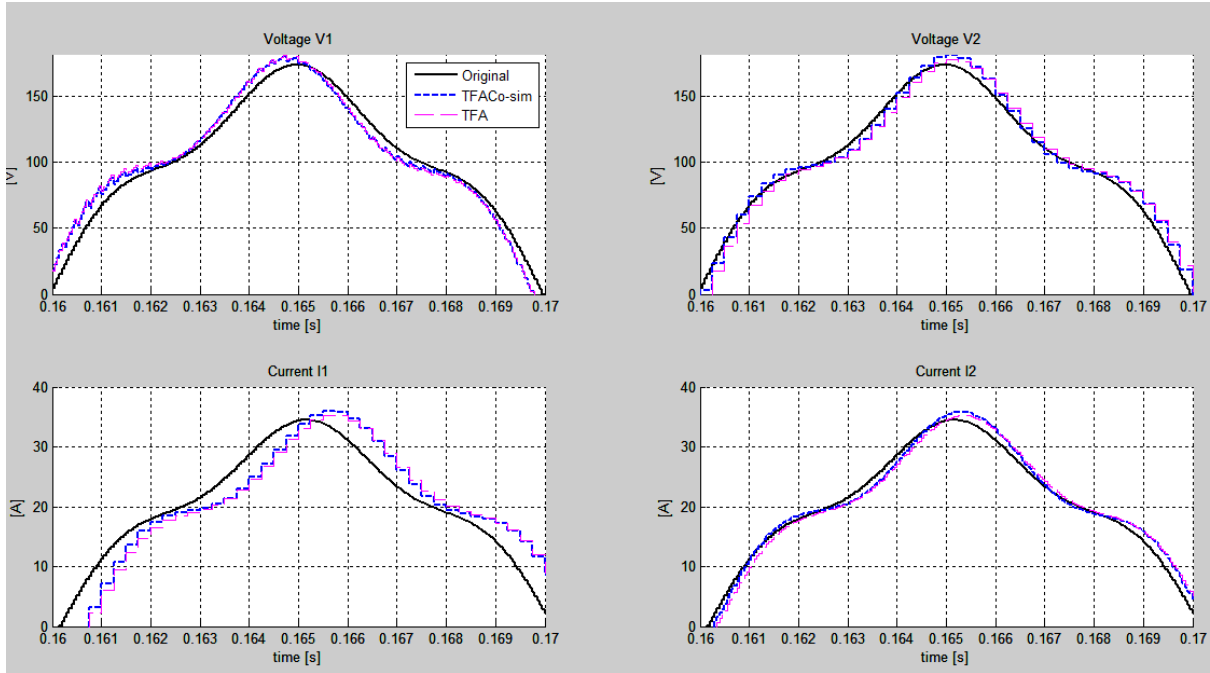


Figure 4.1.2: Simulation result of a simple voltage divider circuit using original TFA and modified TFA interfaces.

4.1.2 Modification of the algorithm using dynamic phasors

Besides the implementation on both sides of the decoupled system, the TFA algorithm is basically unchanged. Therefore, advantages and drawbacks present in literature [11] are expected to be preserved as well. The main limitation of this approach is the approximation required for the system to be a first-order element: this means that nonlinearities and related consequences, such as higher harmonics, can lead to an inaccurate and even unstable simulation. What is more, the implementation in time-domain, as mentioned in 3.3.2, is susceptible to large delay in communication, which compromises results of simulation, and to the inevitable sampling, that degrades furtherly the accuracy.

Therefore, implementing the algorithm using dynamic phasors as interface quantities is likely to solve those issues. Using the formalism introduced in section 3.3, and keeping the same example of Figure 4.1.1, the DP operator is applied to the exchanged variables v_1 and i_2 before they are sent into the communication channel. The result of the DP operator, depend on the number of harmonics H (including the DC component, $h = 0$) selected to approximate the original waveform. The result is H couples magnitude-phase or, alternatively, a complex number representing the h^{th} harmonic order of the time-varying variables.

Since the TFA method contains an algorithm that computes algebraically, for every time step, feedback quantities on the basis of previous states of the system, the complex number form of dynamic phasors is the only one suitable to execute the required calculations, i.e. inverting matrix A of eq. (3.5) to obtain parameters α and β at every time-step of simulation. With this assumption, let us see how the TFA algorithm described in 3.1.2 can be modified to DP domain. For simplicity, again, only the voltage-side algorithm will be derived, because it is possible to derive the current-side in a dual way.

The dynamic phasors differentiation property (3.28) is applied to eq. (3.1):

$$\frac{d\langle i_2 \rangle_h}{dt} + jh\omega_0 \langle i_2 \rangle_h = a \langle i_2 \rangle_h + b \langle v_1 \rangle_h \quad (4.4)$$

Taking again Trapezoidal approximation and reordering the terms, a formally identical expression of the algorithm in discrete time, for every harmonic h , is obtained:

$$\langle i_2 \rangle_h(k) = \alpha \cdot \langle v_1 \rangle_h(k-1) + \beta \cdot \langle i_2 \rangle_h(k-1) \quad (4.5)$$

However, in this case, parameters α and β are complex numbers with the following expressions:

$$\alpha = \frac{bTs}{1 + \frac{jh\omega_0 - a}{2}Ts} \quad (4.6)$$

$$\beta = \frac{1 - \frac{jh\omega_0 - a}{2}Ts}{1 + \frac{jh\omega_0 - a}{2}Ts}$$

Thus, the TFA computation block, using dynamic phasors, contains actually H computation block that calculate, for every time-step, $\langle i_2 \rangle_h(k)$ and, on the other side, $\langle v_1 \rangle_h(k)$ for every harmonic order. Then, such quantities are transformed back into time-domain before being used as references for controlled sources in the two decoupled subsystems. Besides these transformations, the algorithm described in the previous subsection is unchanged.

It has been mentioned in chapter 3, that TFA algorithm shows numerical problems in DC steady state, because matrix A becomes singular when exchanged quantities v_1 and i_2 do not change over a single simulation time. As a matter of fact, using dynamic phasors in calculation means using continuous quantities in steady state, represented by real and imaginary parts. Therefore, numerical issues are expected to arise during simulation using dynamic phasors: a partial solution to this problem will be described for TFA interface with DP.

4.1.3 Issues of the interface

About the interfaces based on TFA method, the original description of the algorithm [31] consists of adding a controlled source and a variable resistor on the decoupled subsystem terminations, as shown in Figure 4.1.1. Early tests of the interface for co-simulation confirm that controlling a variable resistor in parallel to a controlled current source creates numerical issues in the algorithm, as mentioned in the previous chapter. In this thesis the approach that Wei Ren used in his dissertation [11], that is using as feedback quantity the whole current to control only a current source (or voltage, on the dual side) instead of changing the resistor and the source separately. Therefore, basically the topology of the method is the same as the ITM topology, but computed variables are used to control the sources instead of the ones measured from the other subsystem. Moreover, it is important to initialize properly the exchanged variables $i_2(k)$ and $v_1(k)$ for the first 3 time-steps of simulation, in order to allow the algorithm to converge quickly.

Regarding the implementation of TFA with dynamic phasors, as mentioned in 4.1.2, other issues arise, because of the singularity of the matrix when steady state is reached. To implement the interface, the following procedure has been adopted:

- The TFA algorithm computes, for every time-step of simulation, parameters of the system approximating them to a first-order system. In eq. (3.1), those parameters are called a and b , representing equivalent resistance and inductance of the circuit. In order to allow the algorithm described in DP domain to start, a and b need to be initialized for a certain number of time-steps. Therefore, eq. (4.2) and (4.3) are used, at the beginning of the simulation, making the terms α and β explicit and calculating i_{2c} and v_{1c} based on the single previous time-step only. For instance, for i_{2c} :

$$\langle i_2 \rangle_h(k) = \frac{bT_s}{1 + \frac{j h \omega_0 - a}{2} T_s} \cdot \langle v_1 \rangle_h(k-1) + \frac{1 - \frac{j h \omega_0 - a}{2} T_s}{1 + \frac{j h \omega_0 - a}{2} T_s} \cdot \langle i_2 \rangle_h(k-1) \quad (4.12)$$

- Then, after a certain time, the computation block is switched to the normal algorithm, calculating α and β based on solving the linear system represented by matrix A . Again, in order to avoid divisions by zero, the algorithm must be stopped before the determinant of matrix A becomes too small, maintaining the previous computed value.

Unfortunately, this process makes the algorithm very complicated to implement, since many elements need to be initialized, i.e. parameters of the circuit and, then, tolerance of matrix A determinant. Because of this, numerical issues are likely to arise anyway, especially for simulations containing several transients. In order to check whether the algorithm is correctly implemented a simple test has been executed on the simple voltage divider circuit. The results, shown in Figure 4.1.3, were unsatisfying: the numerical issues characterizing the TFA method are not solved. Further methods to overcome this problem should be developed. However, during the work on this thesis, all the executed tests using the TFA interface with DP have given unstable and inaccurate results because of numerical problems: for this reason, they will not be reported.

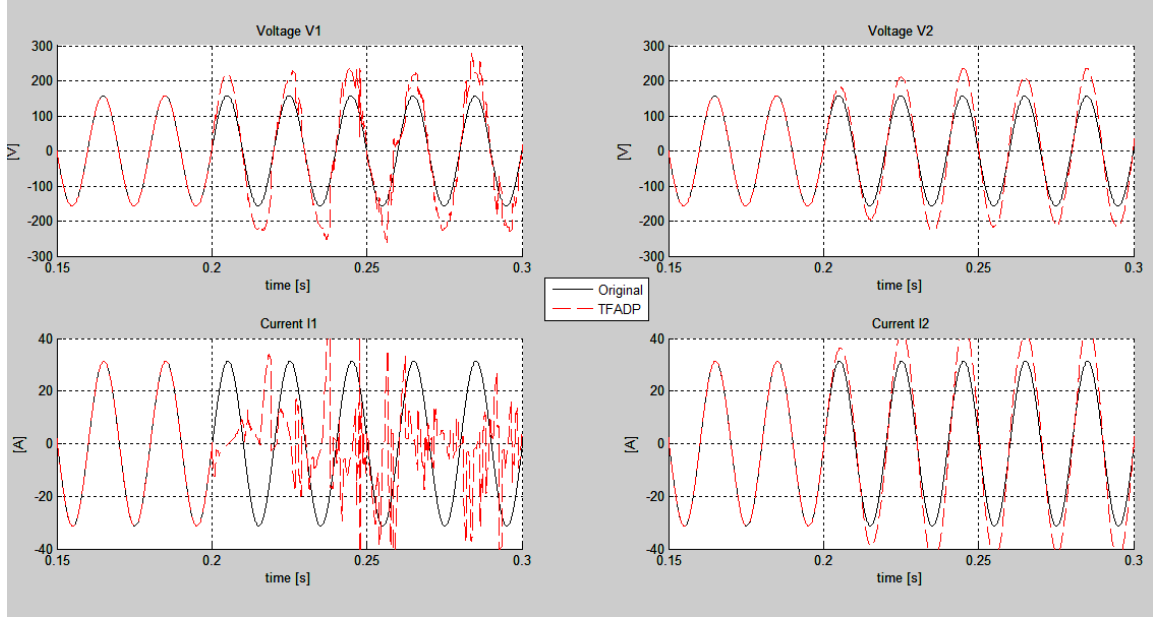


Figure 4.1.3: Results of simulation of the simple voltage divider circuit using the modified TFA interface using DP, initialized for the first 0.2 s of simulation

4.2 Co-simulation interface algorithm based on Wave Transformation

4.2.1 Adaption of the interface to electrical systems

Wave transformation method, introduced as a bilateral teleoperation strategy, was introduced in chapter 3 using a 2-ports system. Thus, two physical quantities of one subsystem were transformed into wave variables and sent to the remote subsystem, where they were transformed back into physical variables. As the theoretical background has shown, those quantities are usually chosen to be a couple whose product is a power, in order to represent the system power flow and to maintain the passivity condition.

For a teleoperation system, the most convenient choice is to assume the flow quantity as velocity and the effort as force. When it comes to electrical system, the most obvious choice is to choose current as the flow quantity and voltage as the forcing variable. Therefore, considering again a 2-ports decoupled system, eq. (3.9) can be rewritten for electrical system as:

$$P = i_1 v_1 - i_2^T v_2 = \frac{1}{2} u_1^T u_1 - \frac{1}{2} w_1^T w_1 + \frac{1}{2} u_2^T u_2 - \frac{1}{2} w_2^T w_2 \quad (4.7)$$

Repeating the same operations done in paragraph 3.2.2, it is possible to derive the equations describing the wave variables as function of the physical quantities:

$$\begin{aligned} u_1 &= \frac{1}{\sqrt{2b}}(v_1 + bi_1), & u_2 &= \frac{1}{\sqrt{2b}}(v_2 - bi_2) \\ w_1 &= \frac{1}{\sqrt{2b}}(v_1 - bi_1), & w_2 &= \frac{1}{\sqrt{2b}}(v_2 + bi_2) \end{aligned} \quad (4.8)$$

Equations (4.7) can be inverted to obtain physical quantities in terms of wave variables:

$$\begin{aligned} v_1 &= \sqrt{\frac{b}{2}}(u_1 + w_1), \quad v_2 = \sqrt{\frac{b}{2}}(v_2 + w_2) \\ i_1 &= \frac{1}{\sqrt{2b}}(v_1 - w_1), \quad i_2 = -\frac{1}{\sqrt{2b}}(v_2 - w_2) \end{aligned} \quad (4.9)$$

As stated in the previous chapter, it is possible to have several combinations of wave transformation schemes, according to the way the wave transformation blocks are connected to the subsystems. Namely, either a voltage or a current command can be imposed from the two circuits and, in the same way, either a voltage or a current can be fed back from one circuit to another. Thus, four combinations are possible. However, in order to have possibility to compare results of various IA, in this thesis only two combinations will be taken into account, respecting the two basic ITM interface types shown in chapter 3.

Thus, if the first port current i_1 and the right-hand port voltage v_2 are given, the wave transformations are:

$$\begin{aligned} u_1 &= \sqrt{2b} \cdot i_1 + w_1, \quad u_2 = \sqrt{\frac{2}{b}} v_2 - w_2 \\ v_1 &= b \cdot i_1 + \sqrt{2b} \cdot w_1, \quad i_2 = -\frac{1}{b}(v_2 - \sqrt{2b} \cdot w_2) \end{aligned} \quad (4.10)$$

Considering already the time delay ΔT in communication, transformations (4.9) can be illustrated: the wave transformation current type interface (WT-VI) is shown in Figure 4.2.1:

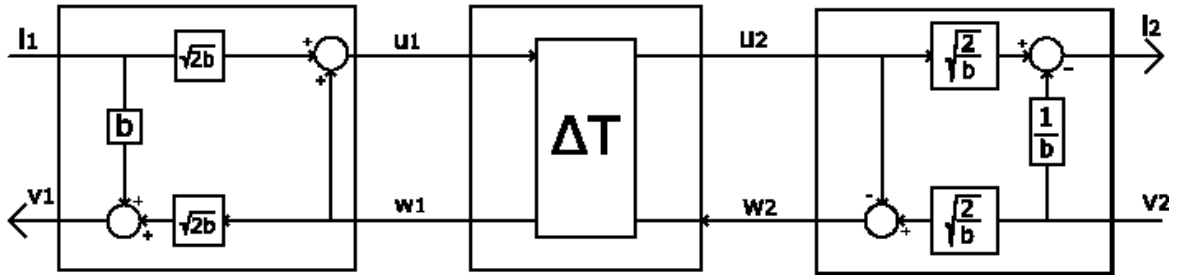


Figure 4.2.1: WT-VI interface

Dually, i.e. when the first port voltage v_1 and the second port current i_2 are controlled, the wave transformation voltage-type interface (WT-IV) is described by equations (4.10) and Figure 4.2.2:

$$\begin{aligned} u_1 &= \sqrt{\frac{2}{b}} v_1 - w_1, \quad u_2 = -\sqrt{2b} \cdot i_2 + w_2 \\ i_2 &= \frac{1}{b}(v_1 - \sqrt{2b} \cdot w_1), \quad v_2 = -b \cdot i_2 + \sqrt{2b} \cdot w_2 \end{aligned} \quad (4.11)$$

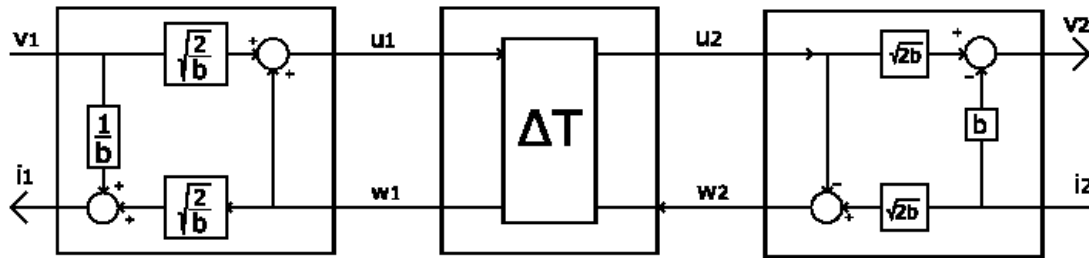


Figure 4.2.2: WT-IV interface

The major priority of teleoperation schemes is usually to maintain stability of the operation. Therefore, an expectation about wave transformation applied to co-simulation is supposed to be an improvement in the simulation stability. Thus, the two topologies just introduced should be used according to the decoupling point of the system: in other words, there can be cases when it is more convenient to send a voltage reference rather than a current one, and vice versa, regardless of the simulation stability.

To prove this property of the WT interfaces, the same simple example used in the previous chapter for the ITM interface will be here repeated. Recalling that, a simple voltage divider circuit had been simulated using an ITM-IV interface with parameters that made $Z_s > Z_L$, i.e. source impedance larger than load impedance. Under these conditions, the results of the simulation were unstable and the only possibility to get a stable result was to change topology of the interface algorithm, using an ITM-VI interface. When it comes to wave transformation interfaces, instead, a stable result is possible with any topology. In Figure 4.2.3, results of a simulation where the simple circuit has parameters that make ITM-IV interface unstable are shown. In this case, both WT-IV and WT-VI are used, and the simulation is stable anyway. For this test, wave impedance has been selected similar to load impedance: $b = 5\Omega \approx Z_L$.

This simple example clarifies what just stated about choosing properly topology for the simulation: in fact, the inductance on the right-side of the decoupled system cannot be located in series to a controlled current source, used in a VI-type interface. Thus, a high value resistance must be positioned in parallel to the current source, so further precautions need to be taken.

Nevertheless, although the stability of simulation with certain circuit parameters is not an issue as in ITM interface, meaning that region of stability of WT is larger than ITM, for more complicated systems, further attention must be taken when choosing the topology of the interface. As a matter of fact, an important property of bilateral teleoperation methods needs to be considered: one side of the decoupled system acts like the “operator” and the other one as the “environment”. Therefore, in voltage source-based systems (which are almost the totality of power systems), the voltage reference has to be positioned on the subsystem from where the power flow comes.

In other words, if the decoupled system has a power flow that goes from the right side to the left one, a VI-type scheme has to be implemented for co-simulation. Otherwise, an IV-type scheme is necessary.

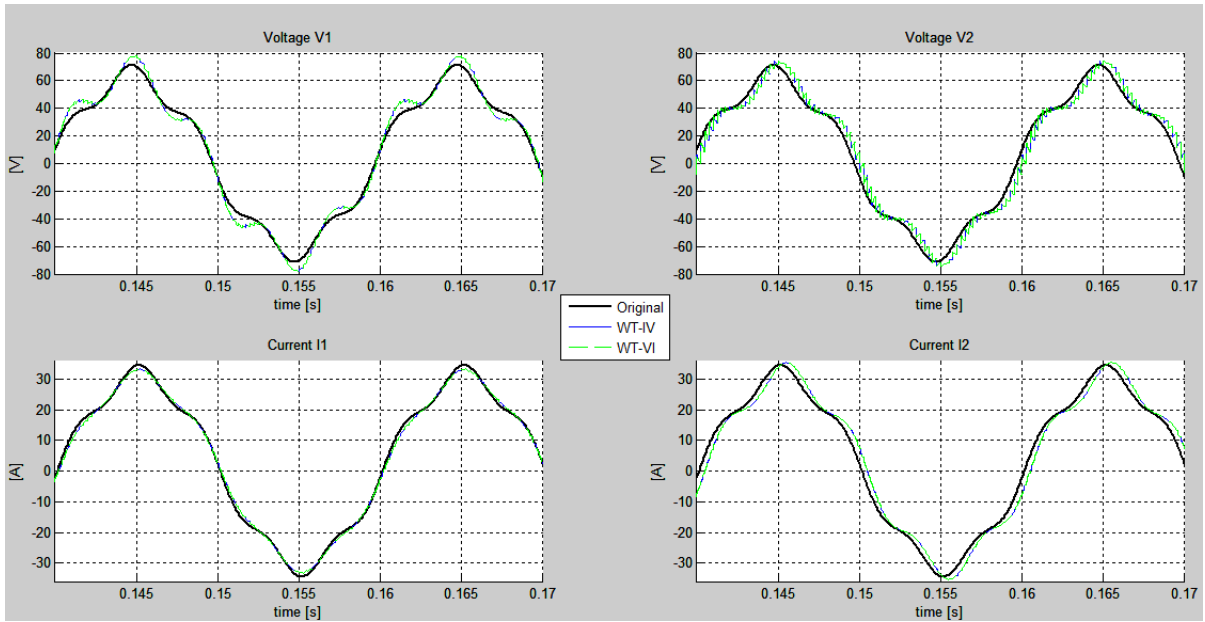


Figure 4.2.3: Results of simulation using both WT-IV type and WT-VI interfaces, showing equal stability in both cases with parameters of the circuit that make ITM interface unstable

4.2.2 Modification of the method using dynamic phasors

Recalling the same issues regarding implementation using instantaneous values in communication, wave transformation theory guarantees a stable simulation with ideally any constant time delay. However, in chapter 3 it has been mentioned how large and variable time-delay can compromise passivity of the operation and, thus, stability itself.

Moreover, the scattering theory has been formulated for linear systems. Therefore, nonlinearities in the simulation model can cause instability and inaccuracy. To address these issues, again, it would be suitable to implement the WT interface using dynamic phasors rather than instantaneous values in communication.

In this case, the equations of the method are not modified. The approach used is to apply the dynamic phasors operator directly to the wave variables u and w , after they have been transformed from physical quantities, but before they are sent to the communication channel. Thus, H couples magnitude-phase representing the wave variables for every selected harmonic order, are sent instead of instantaneous values. Then, before wave variables are transformed back into physical quantities, they are reconstructed in time-domain. This process is displayed in Figure 4.2.4 for an IV-type interface.

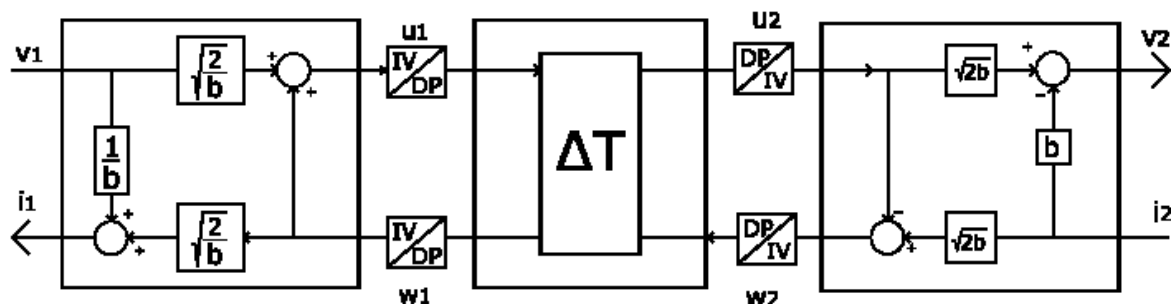


Figure 4.2.4: WT-IV interface using DP as interface quantities

The main benefits coming from this modification of the interface are a major resiliency to large values of interface-delays and, generally, to not-ideal behaviors of the communication, such as sampling, packet loss over the Internet, etc. Moreover, besides the reason that led to implementing a transformation into dynamic phasors in the first place, tests of the interface have shown that using DP improves some issues of the interface itself.

Namely, a wave impedance must be selected to perform the wave transformation. According to what stated in the previous chapters, that impedance should be tuned similarly to the impedance of the circuit in the decoupling point, in order to avoid wave reflections. Therefore, an estimation of the impedance must be done on the integrated circuit before degrading the simulation.

What just stated is valid for low values of interface time-delay. In fact, wave impedance should be tuned according to the delay as well, meaning that it should be larger if the time-delay increases. In other words, if the time-delay varies during the simulation, as it happens in communication over the Internet, the wave impedance should vary along the delay. Unfortunately, such an implementation is hardly feasible, because estimation of the delay over the Internet is difficult to get and the wave transformation requires further modifications to be implemented with a variable wave impedance.

To illustrate the issue with a large and variable delay, a simulation is executed for the simple voltage divider circuit. In Figure 4.2.5, the simulation is executed using the WT-IV interface in time-domain with a variable time delay $\Delta T(t)$ of average value $\Delta T = 15$ ms. As it can be seen, on the right side of the decoupled system, waveforms are subject to a huge phase shift if compared to waveforms of the simulated original circuit, and accuracy of current on the left side is poor as well.

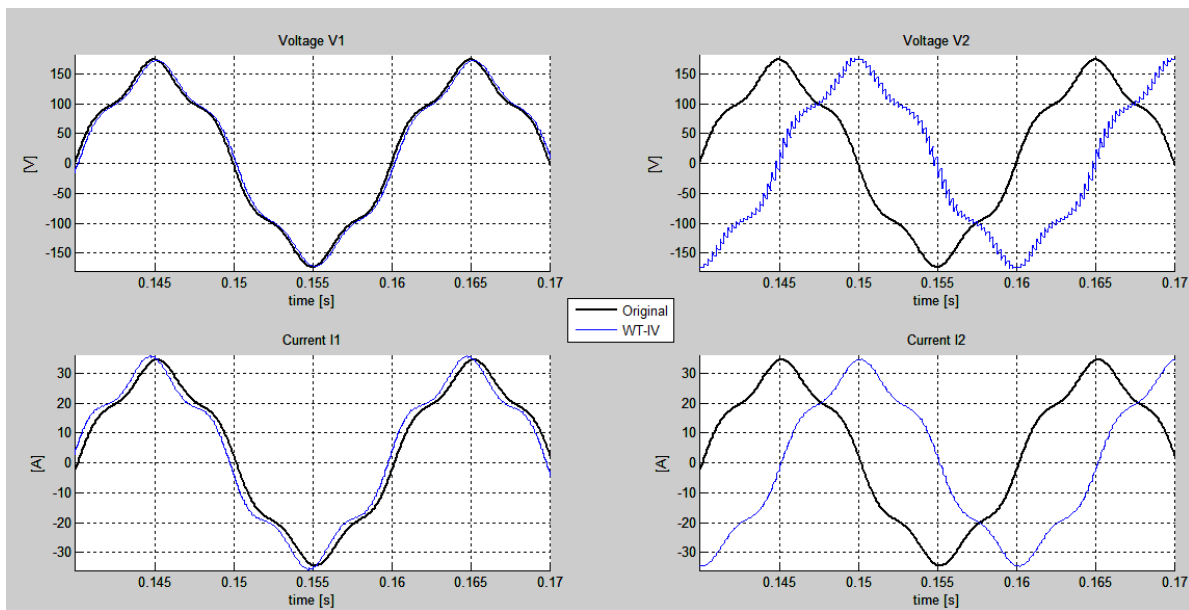


Figure 4.2.5: Results of simulation of the simple voltage divider circuit using the WT-IV interface in time-domain with a large variable interface delay in communication

If the same simulation is executed using the WT-IV interface when DP are used to exchange information, the result of simulation is illustrated in Figure 4.2.6. As it appears, accuracy of the simulation increases remarkably using dynamic phasors, since the phase shift disappears, in spite of the large interface-delay.

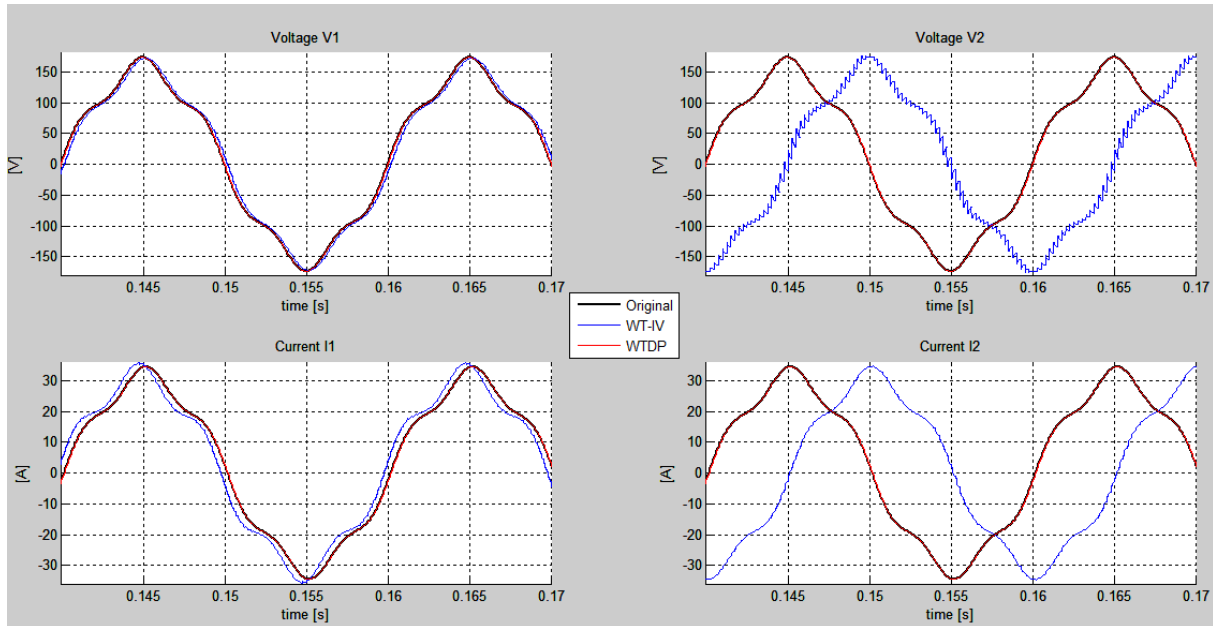


Figure 4.2.6: Results of simulation of the simple voltage divider circuit using the WT-IV interface with dynamic phasors, with a large variable interface delay in communication

Therefore, using dynamic phasors with wave transformation-based interfaces has the double effect on simulation accuracy improvement and stability against high values of interface delay and, at the same time, improves the interface itself.

4.2.1 Algebraic loop in the wave transformation-based interfaces

As already mentioned in the previous chapter, in standard wave transformation method an algebraic loop could arise on the remote side of the teleoperation system. In a co-simulation set-up, instead, an algebraic loop might arise on both sides of the decoupled system, since there are systems that need to be solved, for every time-step, in order to obtain the values of the exchanged variables. This problem is more challenging when the simulation model is more complex.

However, this issue can be solved adding a single time-step delay on the feedback paths of both wave transformation blocks, as shown in Figure 3.2.3 for one side only. When this delay is added, wave impedance must be tuned with a certain factor of safety (empirical tests have shown that 2-3 times the system impedance in the decoupling point allows performing high-fidelity simulation results) since virtual energy is furtherly added in the communication.

As a matter of fact, in order to solve this last problem, an alternative method to guarantee stability of simulation when the single time-step delay is added, an energy compensation algorithm can be implemented, as already explained in 3.2.3. However, this problem represents an obstacle only when complexity of the model of the system to simulate increases. Thus, it will be furtherly addressed later in the next chapters.

4.3 Implementation of the interfaces

The aim of this section is to show an off-line implementation of the above described interfaces, highlighting which precautions need to be taken into account in practical applications. Actually, some issues arise when it comes to applying such methods to models that represent real power systems. For this reason, this section is meant to illustrate simple steady state cases in time

domain first, in order to test the interfaces. Later, the modified interfaces using dynamic phasors will be tested, showing how the issues deriving from using instantaneous quantities can be overcome. Finally, a more realistic case will be considered, so that problematics of co-simulation of power system can be introduced.

In order to have a comparison to previous work, the TFA and the WT interfaces will be also compared to the ITM interface.

4.3.1 Models used for simulation

In the next subsections, two simple circuits will be considered, whose parameters will be selected differently for the various tests:

- A) simple single-phase circuit, shown in Figure 4.3.1.
- B) simple three-phase AC power system, shown in Figure 4.3.2.

The decoupling point selected for co-simulation is represented in the figures by a red line.

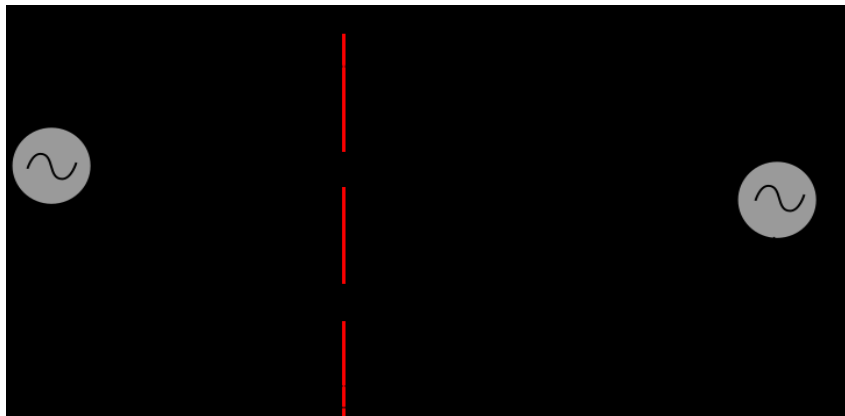


Figure 4.3.1: Simple circuit A

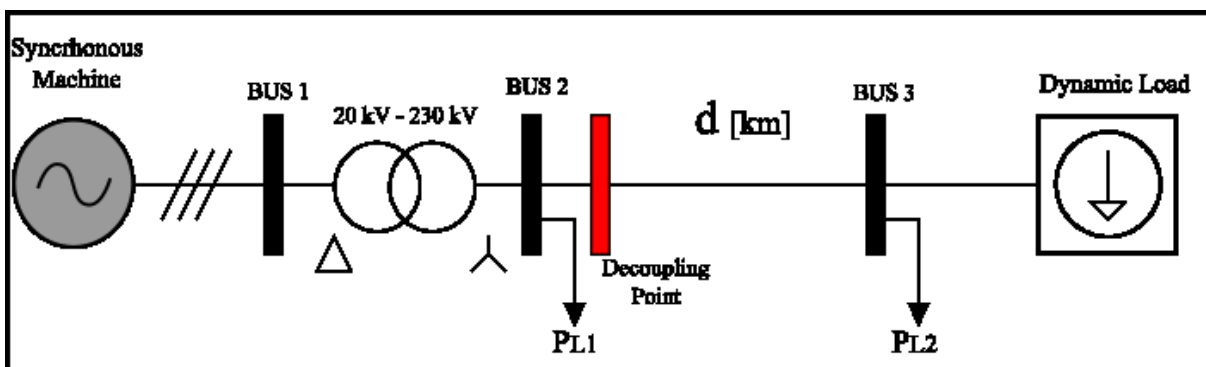


Figure 4.3.2: Single line diagram of simple power system B

Following the steps to examine the issues that mostly affect the standard ITM interface, the following tests will be executed:

- I) stability check with circuit parameters that make ITM interface unstable
- II) simulation performance with large and variable interface time-delay
- III) simulation performance using a DC voltage source

Meanwhile, issues and related solutions deriving from implementing the interfaces will be explained. All the tests in this section will be executed using MATLAB/Simulink discrete time

solver, with a fixed simulation time-step $T_s = 50 \mu\text{s}$. Moreover, only IV-type interfaces will be taken into account for simplicity.

Results of simulation, which are voltages and currents at the decoupling point of the co-simulation, will be compared to waveforms of the integrated circuits at the same points. From here on in this chapter, for all the interfaces under test, the tested quantities will have the names described by the diagram in Figure 4.3.3

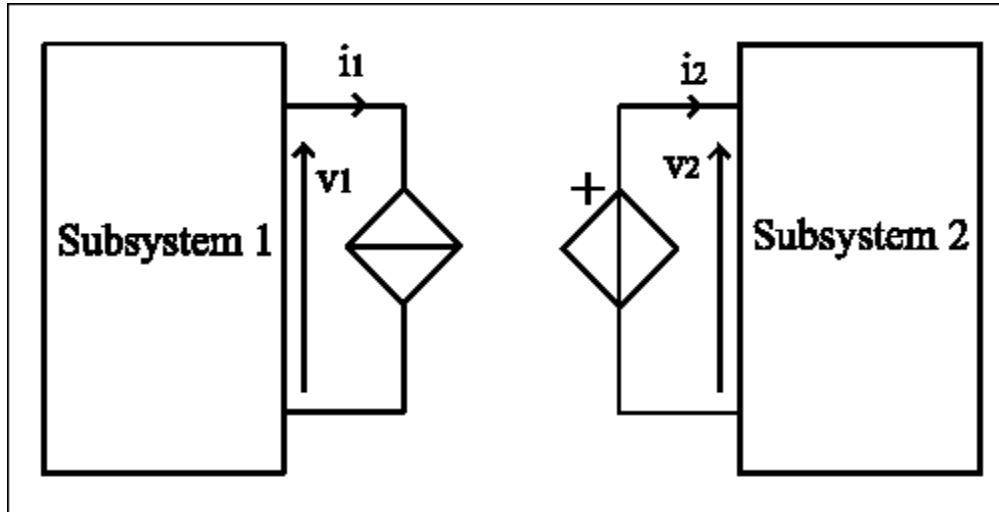


Figure 4.3.3: Definition of variables names for simulation results

4.3.2 Simulation case I: stability test using certain circuit parameters

Let us consider circuit A with parameters shown in Table 3 and circuit B with parameters shown in Table 4. In these circumstances, ITM-TD interface is not stable, meaning that waveforms diverge over the simulation time, so they will not be reported in order to show results of the remaining interfaces. A steady state simulation is executed to check whether ITM-DP, WT and TFA are stable. A small artificial time-delay of $\Delta T = 5 \cdot T_s = 0.25 \text{ ms}$ and a sampling rate $k = 5$ will be used.

Vs1 (rms)	155.56 V	Source 2 phase	$\pi/6 \text{ rad}$	L₁	8 mH	R₂	15 Ω
Source 1 phase	0 rad	Rs₁	30 Ω	Rf	5 Ω	L₂	1 mH
Vs2 (rms)	70.71 V	R₁	80 Ω	Lf	5 mH	Rs₂	1 Ω

Table 3: Values of circuit A used in simulation case I

PL1	500 MW	d	80 km
PL2	800 MW	f₀	50 Hz

Table 4: Values of simple power system B for simulation case I

Measurements of circuit impedance at the decoupling point using the impedance measurement block from SimPowerSystems Simulink library have shown: for circuit A, $b_A = 5 \Omega$. For circuit B, instead, $b_B = 25 \Omega$.

The simulation is executed using ITM with DP, TFA in TD, WT in TD and WT with DP. For circuit A, results of simulation show that all the interfaces, except the ones based on wave transformation, are not stable. For the transformation into dynamic phasors, in particular, the first 5 harmonics, including the DC component, have been considered. Since it might happen

that Fourier transform block act as a filter on the quantities, mining to stability of the simulation if an excessive number of harmonics is selected, for ITM interface the test has been repeated using the first 3 harmonics and then just the DC and the fundamental harmonic. Also in this last cases, the results show instability. For the WT interfaces, results are reported in Figure 4.3.4:

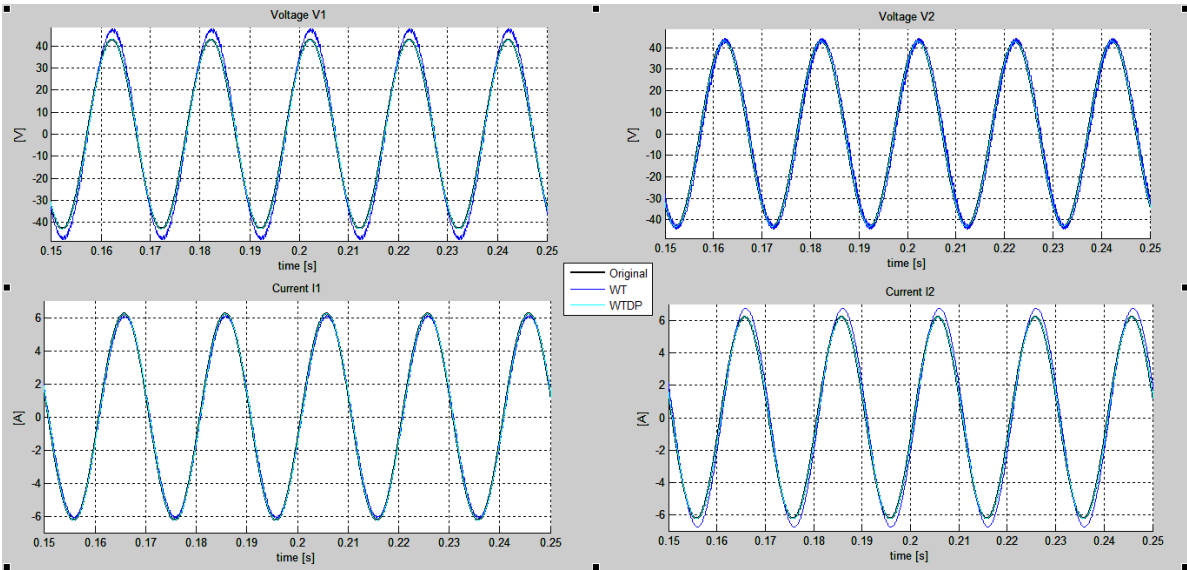


Figure 4.3.4: Results of simulation of circuit A showing stability of wave transformation interfaces

Repeating the same test using circuit B, ITM interface is unstable using dynamic phasors as well. Wave transformation, in time-domain and with dynamic phasors, and TFA interface, instead, perform a stable simulation, as shown in Figure 4.3.5:

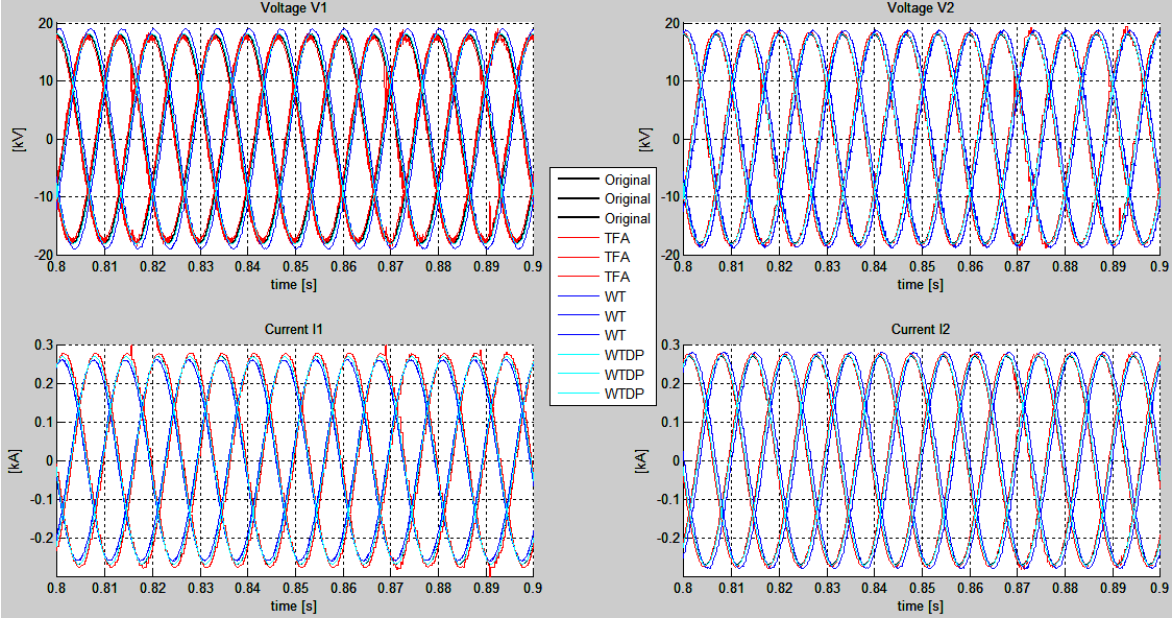


Figure 4.3.5: Results of simulation of circuit B showing stability of WT and TFA interfaces

As it appears to be, numerical issues using TFA interface occur: in certain time-steps of simulation waveforms generated show some spikes, due to matrix inversion that, in those instants, might have been with a very low determinant value.

4.3.3 Simulation case II: performance with large and variable interface time-delay

In order to verify how time-delay affects the performance of the interfaces, this scenario will consider an artificial interface delay that changes over the simulation time, having the values shown in Figure 4.3.6. A steady state case will be simulated; parameters of the circuits are now the ones provided in Table 5 and Table 6, which allow all the interfaces to generate a stable simulation. Parameters that are not specified have the same values of tables 1 and 2.

		L₁	8 mH	R₂	30 Ω
R_{s1}	2 Ω	R_f	10 Ω	L₂	1 mH
R₁	60 Ω	L_f	5 mH	R_{s2}	2 Ω

Table 5: Parameters of circuit A for simulation cases II and III.

P_{L1}	900 MW	d	80 km
P_{L2}	500 MW	f₀	50 Hz

Table 6: Parameters of circuit B for simulation case II.

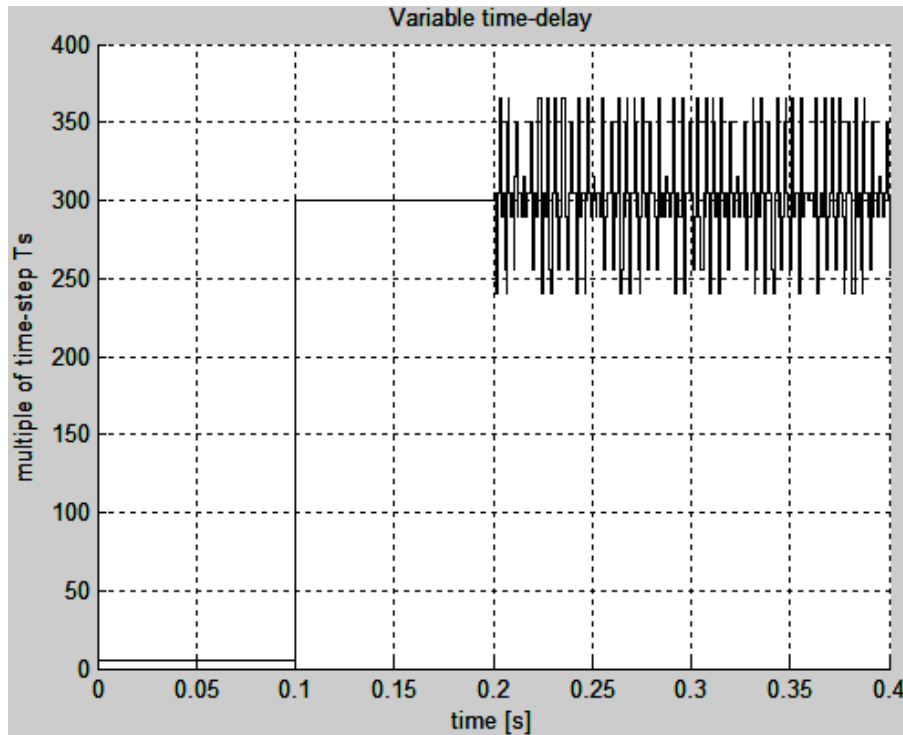


Figure 4.3.6: Artificial time-delay over simulation time. Initial value: 5·Ts. At t = 0.1 s delay increases to 300·Ts. At t = 0.2 s delay becomes variable

Regarding circuit A, for the interfaces that use dynamic phasors, 5 harmonics, including DC component, are selected. It is interesting to show results of simulation for interfaces that use

instantaneous values, shown in Figure 4.3.7, and those which use dynamic phasors, shown in Figure 4.3.9, separately:

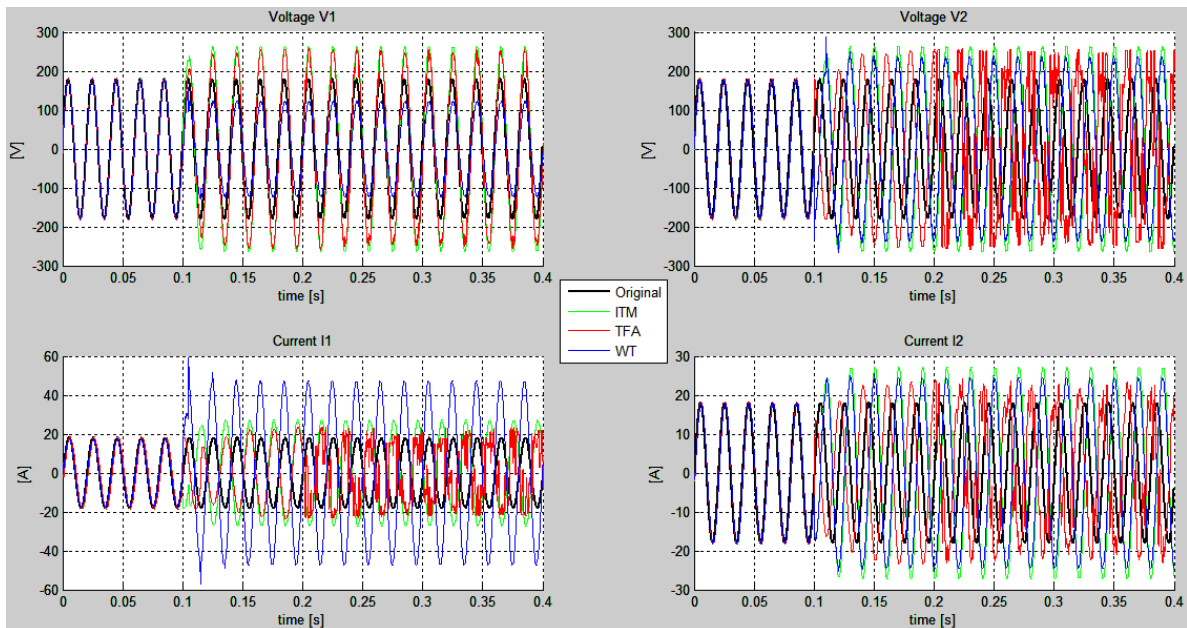


Figure 4.3.7: Results of simulation for circuit A using TD interfaces, with a variable time-delay over the simulation time

For low values of time-delay, the three interfaces show good performance. At time $t = 0.1$ s, time-delay goes up from 0.25 ms to 15 ms, which is an unrealistic increase but allows to consider what would happen in a communication over the Internet, for example. As Figure 4.3.7 proves, after an initial transient due to the dramatic change in the artificial delay, accuracy of the simulation gets worse.

In particular, for the WT interface, amplitude of the waveforms compared to the ones of the integrated circuit changes. What is more, a phase shift occurs between the original waveforms and the simulated ones. Then, at $t = 0.3$ s time-delay becomes variable: the mentioned amplitude difference and phase shift of the waveforms become variable as well. The decrease of accuracy is related to what already mentioned in the previous chapter about the requirement to tune the wave impedance of the interface. In fact, since b is chosen to be about the circuit impedance at the decoupling point (to avoid wave reflections) and, moreover, it has to be larger if time-delay is larger, it should change over the simulation according to the time delay. Regarding the phase shift, that is a consequence of the passivity condition: if the time-delay is larger, more energy is virtually added into the communication channel creating a phase-shift between the waveforms. In this condition, stability is not compromised if wave impedance is correctly tuned. As a matter of fact, Figure 4.3.8 shows what just stated: considering a fixed value of time-delay of $300T_s$ for the whole simulation and adjusting the wave impedance to about two times the previous value, accuracy of simulation is maintained, except for the phase shift.

ITM and TFA interfaces show worse performance with a large time-delay, since the delay is not compensated at all. Using TFA interface, in particular, accuracy of the simulation is very low, since the algorithm is not capable of computing correct results with so large time-delay values.

Using dynamic phasors to exchange information, issues of wave transformation and ITM interfaces can be solved: in fact, large and variable time-delay are compensated thanks to the continuous values of the DP exchanged over the communication. What is more, for WT

interface, there is no need to adjust the wave impedance according to time-delay. Repeating the same test, using the variable time-delay over the simulation time of Figure 4.3.6, results shown in Figure 4.3.9 are the ones generated using DP-based interfaces.

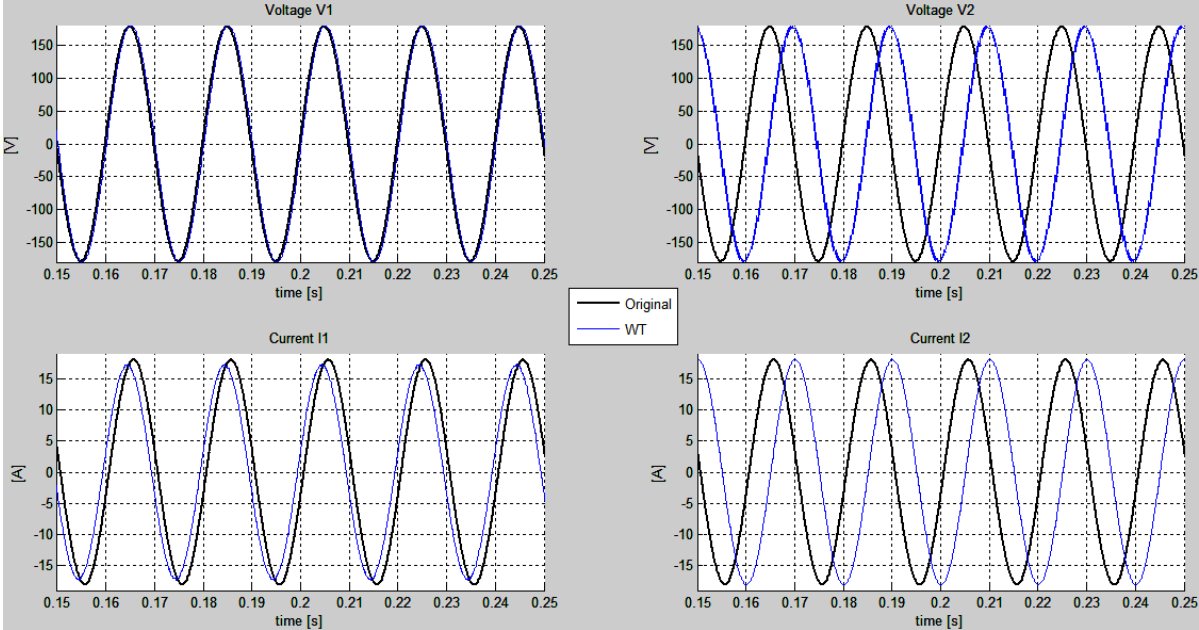


Figure 4.3.8: Simulation results of circuit A with WT interface considering only a large interface time-delay (15 ms) and an adjusted wave impedance ($b = 10 \Omega$)

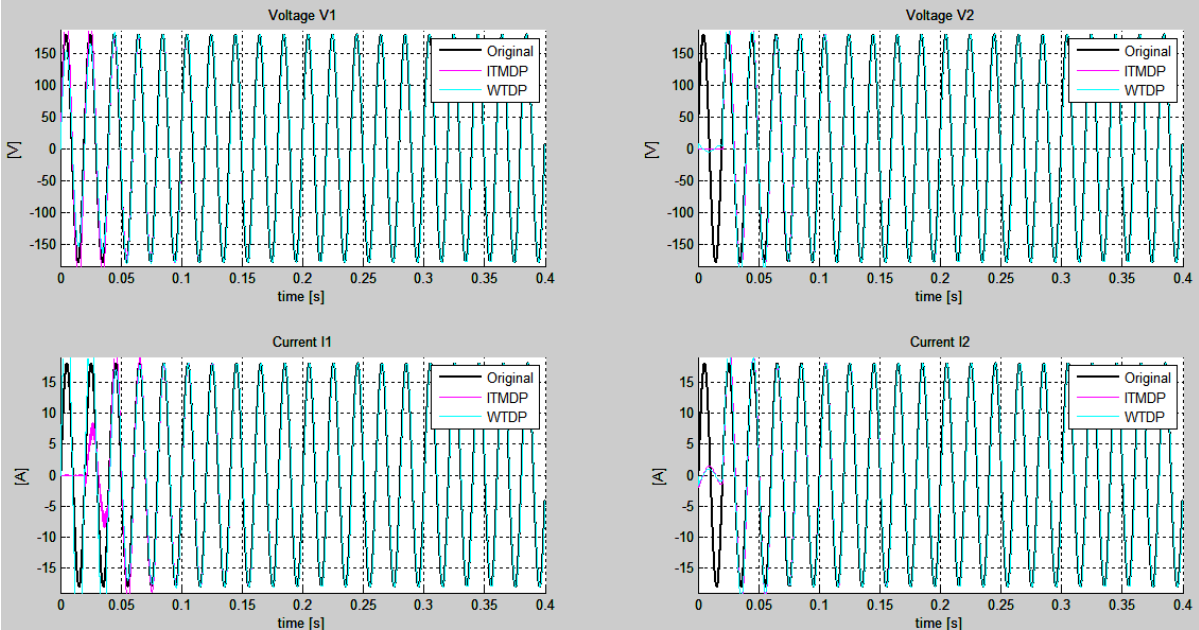


Figure 4.3.9: Results of simulation for circuit A using DP-based interfaces, with a variable time-delay over the simulation time

Therefore, using dynamic phasors, performance of the simulation is good and constant, regardless of the value of interface-delay as expected. An observation can be made for the beginning of the simulation: an initial time is required to reach the steady state, which is typical in co-simulation. In particular, from this simple example it is possible to see how WT interface is faster than ITM in this initial phase.

The same test can be repeated using circuit B. Again, it makes sense to show results for time-domain and dynamic phasors-based interfaces separately. Figure 4.3.10 shows waveforms generated when the interface does not include dynamic phasors: the decrease in performance is more significant for a power system. At $t = 0.25$ s, time-delay is increased to 15 ms: simulated waveforms using co-simulation interfaces are subject to change in amplitude and a phase shift, compared to the integrated circuit waveforms. At $t = 0.55$ s, interface delay become variable: instantaneous values exchanged over the communication channel are highly distorted and performance of simulation is compromised.

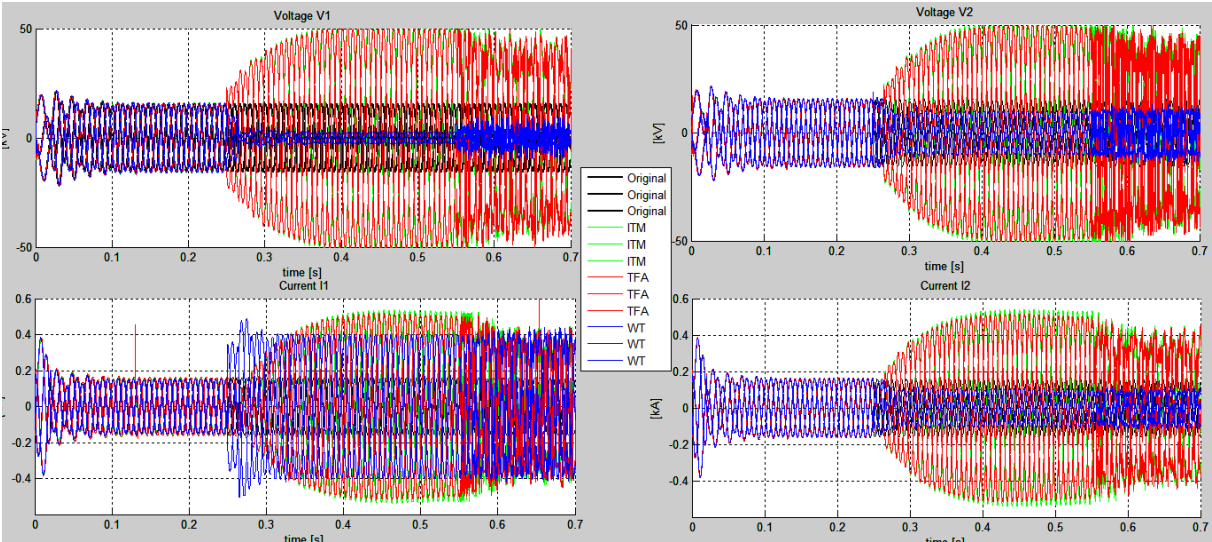


Figure 4.3.10: Results of simulation for circuit B using TD interfaces, with a variable time-delay over the simulation time

Using DP-based ITM and WT interfaces an observation can be done about ITM: for this circuit, although ITM in time-domain is stable, using DP the simulation becomes unstable. That does not mean that region of stability of ITM-DP interface is smaller, but it is different. Therefore, it might happen that using DP for communication compromises the simulation stability. In Figure 4.3.11, results of using wave transformation with dynamic phasors interface are shown, when only 3 harmonics including the DC component are used.

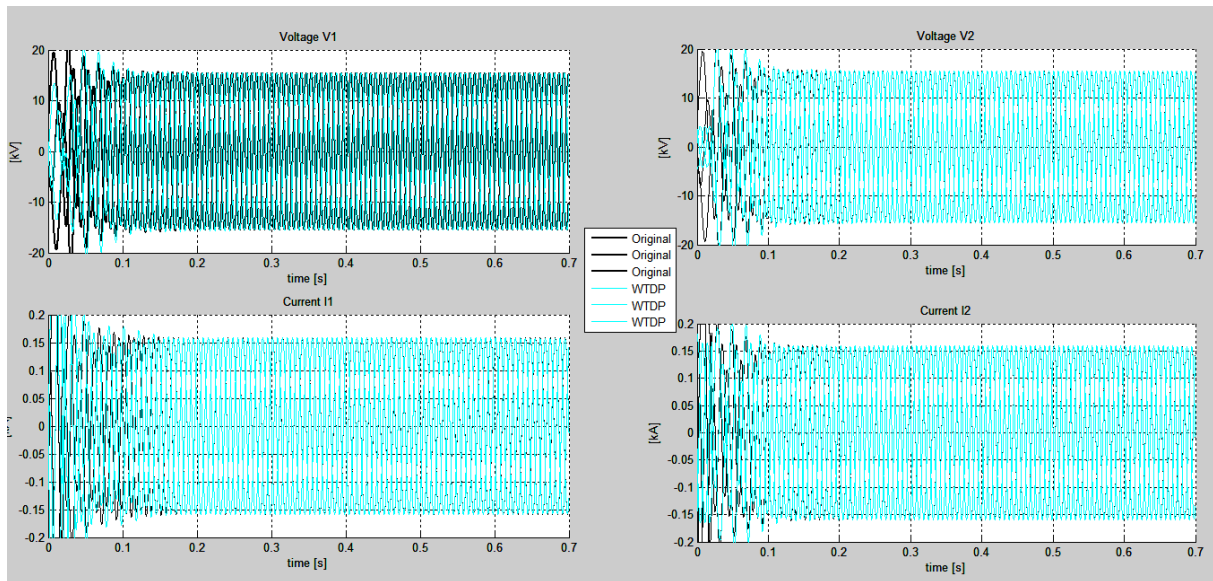


Figure 4.3.11: Results of simulation for circuit B using DP-based interfaces, with a variable time-delay over the simulation time

Also for this system, performance of simulation does not change over the simulation time, in spite of the variable time-delay, thanks to dynamic phasors properties.

4.3.4 Simulation case III: performance using DC voltage sources

In this scenario, only circuit A will be considered. Parameters of the circuit shown in table 3 will be used, but voltage sources V_{s1} and V_{s2} are now DC sources with some amplitude steps over the simulation time. A fixed interface time-delay $\Delta T = 15$ ms is considered, so that similar circumstances to geographically distributed co-simulation may be simulated. Results of simulation using all the interfaces (shown in Figure 4.3.12), consider both time-domain and DP-based communication channel, in order to make a comparison. The Fourier transformation for dynamic phasors, are truncated here to fundamental frequency of 50 Hz and DC component only, in order to consider oscillating transients over the amplitude steps.

Regarding the TFA interface, as mentioned in subsection 4.3.2, the algorithm stops when DC steady state is reached. Thus, a switching control on determinant of matrix A is implemented, in order to maintain previous values of calculated feedback variables when the circuit is in steady state.

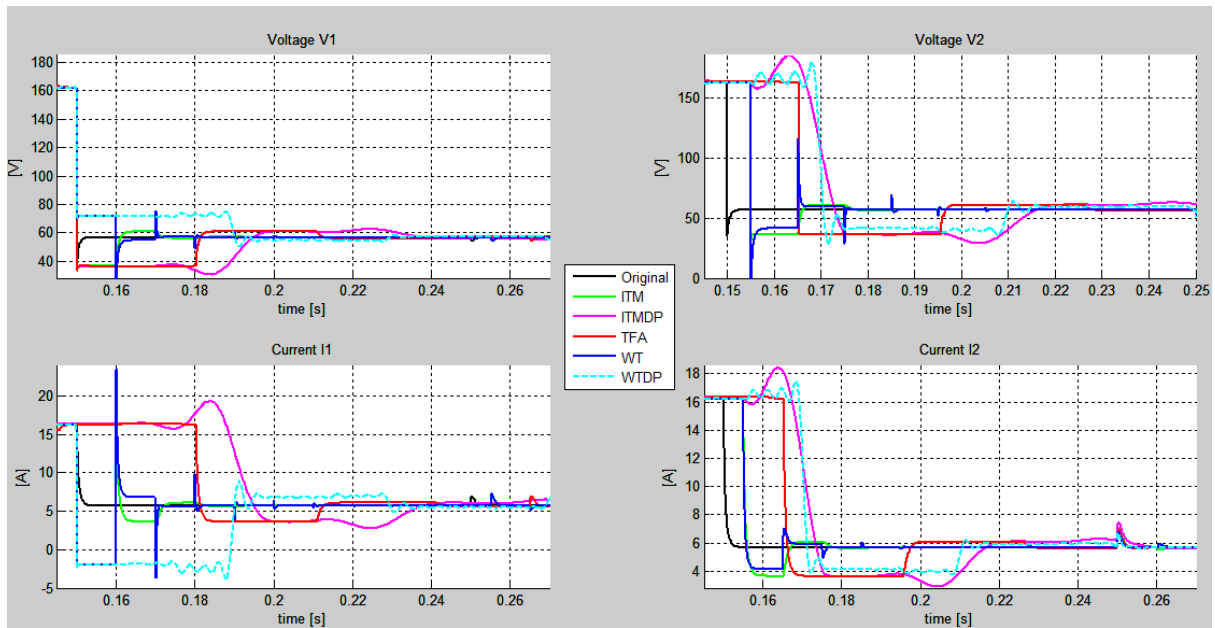


Figure 4.3.12: Results of simulation for circuit A using DC voltage source and a fixed time-delay $\Delta T = 15$ ms

Observation regarding this situation can be deduced considering a transient at $t = 0.15$ s, when voltage decreases from 160 V to 60 V. DP-based interfaces generate a long transient to adjust after a simple voltage amplitude variation, showing oscillating behavior as well. ITM interface allows reproducing the transients more accurately, compared to WT interface: this last one, generates spikes in waveforms, because of the wave transformations themselves that involve a change in variables physical behavior. In other words, wave variables are slower in transients and this behavior is more emphasized with DC quantities. TFA method results in a reproduction of the quantities of low accuracy; it in particular involves a very large phase shift and long transients to adjust after the variations.

Overall, ITM based interfaces show the best performances for this simple DC example.

5. Accuracy evaluation based on signal and energy residuals

The co-simulation interfaces introduced in the previous chapter have been tested, using simple examples to obtain a qualitative evaluation of simulation fidelity under certain circumstances. The analysis that it is going to be developed in this chapter, instead, is a quantitative evaluation of accuracy of the interfaces. In order to have such an evaluation, a metric has to be defined.

So far, all the variables simulated using the various IA have been compared to the waveforms generated simulating the original integrated circuits. This approach might be extended defining a metric based on absolute errors between the quantities simulated using the IA and the ones from the integrated circuit. Unfortunately, when it comes to co-simulation of power systems, this approach is not feasible. In fact, it is not possible to simulate the entire system; otherwise, there would be no need to decouple the circuit onto two simulators in the first place. Therefore, an approach based on energy residuals, proposed in [17] and [18], will be adopted. Basically, relative errors will be considered, since it has been proved in literature that the same evaluation of accuracy as with absolute errors can be obtained.

Thus, in this chapter, the adopted metric will be defined and, using the same examples from the previous chapter, the interfaces will be evaluated in an off-line simulation environment. Moreover, the results obtained with energy residuals will be compared to absolute errors results, in order to validate the approach. Results will be collected, when the systems are subjected to a series of transients. Moreover, in order to have two different co-simulation scenarios, both a low value of interface delay (similarly to what happens in locally distributed co-simulation) and a large and variable interface delay (likewise in geographically distributed co-simulation over the internet) will be selected for simulations.

5.1 Definition of metrics for co-simulation

Evaluating accuracy of an interface algorithm used for co-simulation of a decoupled system means to have a quantitative value of how results are close to results of the simulation of the whole system. Consequently, since an interface operates at the power terminals of the selected decoupling point, meaning that two variables are exchanged, with a certain topology, over the communication channel, it makes sense to evaluate the variables themselves. For power systems, those variables are voltages and currents.

In such a set-up, on each terminal, one variables acts as output of the decoupled subsystem and the other one is the input from the other subsystem. Considering the same topology used in the previous chapter (Figure 4.3.3), which is an IV-type scheme, v_1 and i_2 are the outputs of the two terminals, which are sent through the communication and arrive, as inputs, to the other one. Ideally, for a co-simulation to perfectly represent the original system, the following equations should be valid:

$$\begin{aligned}v_1 &= v_2 = v_o \\i_1 &= i_2 = i_o\end{aligned}\tag{5.1}$$

where the subscript “o” indicates the integrated original system. Naturally, due to the already mentioned interface delays, sampling and other issues regarding the communication, these relationships are never satisfied.

5.1.1 Absolute signal and power errors

Therefore, the most intuitive way to evaluate accuracy of a co-simulation would be to evaluate the absolute signal errors, i.e. to calculate:

$$\begin{aligned} v_{err1} &= v_1 - v_0, & v_{err2} &= v_2 - v_0 \\ i_{err1} &= i_1 - i_0, & i_{err2} &= i_2 - i_0 \end{aligned} \quad (5.2)$$

Nevertheless, this approach has a major drawback regarding units of measurement of the variables. In fact, it is not possible to compare a voltage error to a current error.

For this motivation, a more reasonable approach is considering the product between the variables defining one port or, in other words, the absolute power error:

$$P_{err1} = P_1 - P_0, \quad P_{err2} = P_2 - P_0 \quad (5.3)$$

where $P_k = v_k \cdot i_k$ for $k = 1, 2$ or 0

This approach allows comparing the accuracy of the simulation regardless of the considered quantities used to exchange information between the subsystems.

5.1.2 Relative signal errors: signal “residuals”

The idea proposed so far assumes that the behaviour of the integrated system is known and thus it is possible to use this information as a reference to determine the accuracy of the decoupled system. As suggested in [15] for Internet distributed PHIL simulations, which has similar issues to distributed co-simulation (see section 2.1), the main reason to implement a decoupled version of the system for simulation is that a complete model of the system cannot be simulated, either for lack of computational power of the simulator or for the need to interconnect hardware assets located in geographically distributed laboratories.

Therefore, an alternative way to evaluate *fidelity* of simulation is introduced in [15], based on the concept of coupling variables accuracy. It will be referred as signal residuals, since it represents the residual error introduced in co-simulation by the non-ideal behaviour of the communication. In other words, the relative error between the instantaneous values of the coupling variables at both ends of the decoupled system is considered. In terms of power system, considering again an IV-type interface algorithm scheme, this means defining both a relative voltage error e_v and relative current error e_i . So, as shown in fig. 5.1, for each subsystem the difference between the output variable of one subsystem and the corresponding input for the other subsystem are computed:

$$\begin{aligned} e_v &= v_1 - v_{1d} \\ e_i &= i_2 - i_{2d} \end{aligned} \quad (5.4)$$

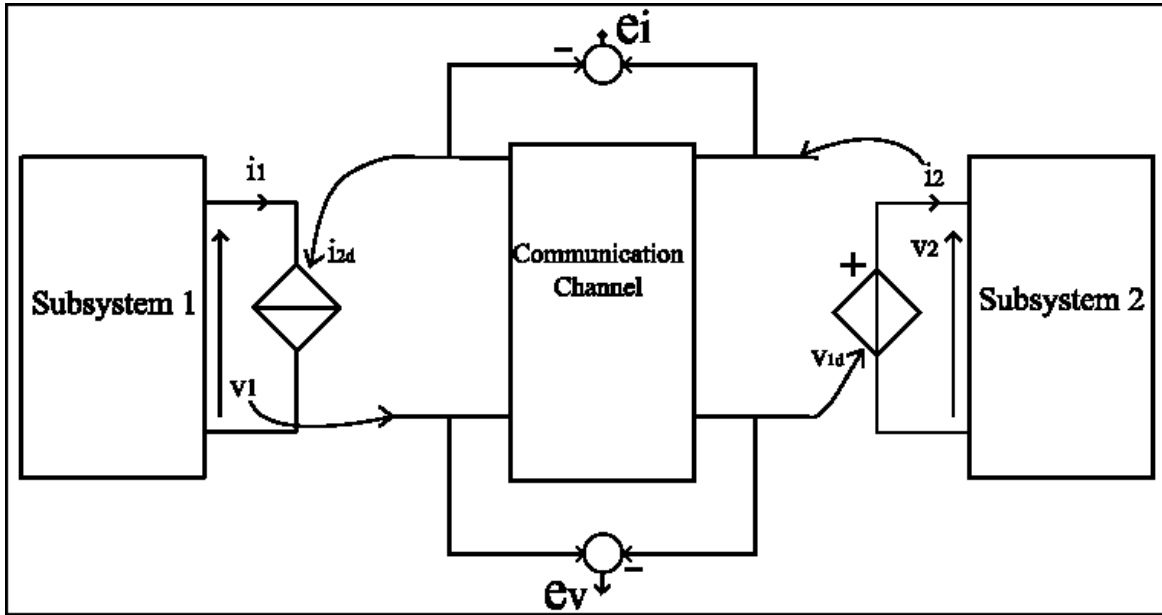


Figure 5.1.1: Explanation of defining relative errors between coupling variables for a co-simulation set-up

Eq. (5.4) needs to be adapted to different interface algorithms, according to which variables are actually outputs and inputs for each subsystem. As mentioned in the previous subsection for absolute signal errors, one disadvantage of using such a metric to evaluate accuracy is that voltage error cannot be compared to a current error. Furthermore, accuracy of an individual coupling variable does not imply accuracy of the other one. Thus, in order to overcome these issues, in [15] all coupling variable errors are aggregated into a single error metric, defined as:

$$E = \sqrt{\sum_{k=1}^n (w_k \|e_k\|)^2} \quad (5.5)$$

where n is the total number of coupling variables, and w_k is the weighting factor for a coupling variable k . Nevertheless, this aggregated error E is not a direct measure of the system accuracy, since its absolute value does not represent how good accuracy of the system is. For this reason, in the following (5.5) will not be used.

The approach described by eq. (5.4) will be used as one of the metrics for accuracy evaluation. Although the drawbacks above mentioned, when evaluating a co-simulation accuracy it is advantageous to have an overview about the behaviour of the single coupling variables, since it could be different from the global simulation performance.

5.1.3 Power and energy residuals

This approach, already mentioned in 2.4 and introduced in [18], is based on the bond graph theory, which describes the energy flows between subsystems as local energy continuity equations. Thus, the flow is balanced for each subsystem separately and then connected in order to satisfy the conservation of energy.

In a simulator-to-simulator set-up, the models of the two subsystems are solved with the local solvers of the two simulators, meaning that internal states evolve along the discrete communication time points t_k and t_{k+1} after having obtained inputs from each other. In general, the values of the input quantities are not known during two communication time-steps, thus they are usually kept constant during the time integration between t_k and t_{k+1} . Afterwards, outputs are calculated from the internal states and used again as inputs.

Let us consider a power flow between two simulators in a co-simulation setup. Using a power bond to exchange information means that one variable represents a flow and the other one an effort. It is interesting to notice that this approach, used in [18], recalls the bilateral teleoperation use of velocity and force as variables. Thus, using currents and voltages for power systems allows a straightforward calculation of the above mentioned power flow. The simulator that simulates subsystem 1 will transmit to the simulator in subsystem 2, through its power port k_1 a power given by:

$$P_{k_1}(t) = \tilde{i}_1(t)v_1(t) \quad (5.6a)$$

where the current represent the input and the voltage the output, respectively, for subsystem 1.

Similarly, the simulator for subsystem 2 will transmit through its power port k_2 :

$$P_{k_2}(t) = \tilde{v}_2(t)i_2(t) \quad (5.6b)$$

Hence, in general:

$$P_{k_1} - P_{k_2} \neq 0 \quad (5.7)$$

represents violation of conservation of energy. Such a violation is an inherent issue in a co-simulation, deriving from the fact that the simulators evolve their states independently from each other between communication time instances and that the communication itself is not ideal, but it is affected by time-delays, sampling and other issues if the co-simulation is performed over the Internet. This quantity can be directly used as a measure of how accurate the co-simulations results are at any given time, defining a *residual power*:

$$dP_k = P_{k_1} - P_{k_2} \quad (5.8)$$

A corresponding *residual energy* can be calculated, which represents how much energy is incorrectly added into the overall coupled system. Using the rectangle quadrature rule, residual energy can be approximated, without large errors, by:

$$dE_k \cong dP_k \cdot Ts \quad (5.9)$$

Such energy fluxes distort the dynamics of the system under test and in general decrease the accuracy of the co-simulation and challenge its stability. It is important to notice how much energy is virtually added to the global energy, intuitively explaining how results of a co-simulation can be inaccurate or diverging.

5.1.4 Error estimation based on power and energy residuals

As already stated, energy residuals give exactly the amount of energy that is incorrectly added to the total energy of the global coupled system. For this reason, they are well suited as versatile energy-based error estimators.

In order to have a global metric to evaluate the overall performance of a co-simulation, power residuals have to be integrated over the simulation time. It is possible to compare this result to the integration of absolute power errors (5.3), so that suitability of energy residuals as energy-conservation-based error estimators can be exemplified.

Thus, the absolute energy error, integrating in discrete time eq. (5.3) over the entire simulation time T , will be:

$$E_{err,k} = \sum_{i=0}^T |P_{err,k}(i)| \cdot Ts \quad (5.10)$$

for each power port k . Therefore, it is possible to define a global absolute energy error for both power ports by making an arithmetic average of (5.10):

$$\overline{E_{err}} = \frac{E_{err,1} + E_{err,2}}{2} \quad (5.11)$$

The total energy residual, virtually added during the simulation, will be instead:

$$E_k = \sum_{i=0}^T |P_k(i)| \cdot Ts \quad (5.12)$$

Hence, the residual power integrated in discrete-time.

5.2 Accuracy evaluation of the interface algorithms

The theoretical background necessary to define the adopted metric to evaluate accuracy of a co-simulation has been described in the previous section. Starting from there, a signal residual and an energy residual error have been proposed, explaining why using the second one is more suitable to estimate simulation fidelity.

Nevertheless, using energy residual as a metric could not be enough in certain circumstances. First of all, energy is a cumulative quantity. Hence, it does not provide information about instantaneous errors that might occur in specific moments of simulation, but only an overall evaluation of the whole performance. Moreover, as already explained in the previous section, accuracy of one coupling variable does not imply the same behaviour for the other one. Therefore, if for instance voltage residual error tended towards zero for a certain time of the simulation, power would tend towards zero consequently. However, at the same time, current residual error might have a different behaviour. Thus, information coming from power residual errors might not be enough to evaluate transients during a co-simulation, since single behaviour of each coupling variable could be different.

For this reason, in the following, the simulation fidelity for different IAs will be evaluated using:

- signal residuals
- power residuals
- energy residual stored during the simulation

As mentioned at the beginning of the chapter, two scenarios will be considered:

- I) steady state evaluation of interfaces accuracy.
- II) transient state evaluation of interfaces accuracy

For both scenarios, two different values of interface delay will be considered:

- Large variable value of interface delay $\Delta T(t)$ with average value $\Delta T = 15$ ms, in order to represent the case of a geographically distributed simulation over the Internet, even though packet loss will not be simulated.
- Low value of interface delay $\Delta T = 250$ μ s, in order to represent a locally distributed co-simulation

For this evaluation, the same circuits used in chapter 4 will be used, again with an IV-scheme topology, but, differently from what done before, the analysis will consider a series of transients characterising the evolution of the variables as well, in order to check the response of the interfaces to different conditions.

5.2.1 Implementation and suitability of the metrics

In order to clarify how the metrics will be used and to have a showcase of using relative residual errors instead of absolute errors, a simulation of the simple voltage divider circuit (Figure 3.1.1: Original circuit used to illustrate PHIL IA Figure 3.1.1) will be executed. The simulations in this chapter will take into account the ITM and WT interfaces both in TD and using DP, and the TFA interface implemented on both sides of the decoupled circuit. Thus, the same IAs will be considered in this subsection. Moreover, the circuit will evolve in AC steady state with a 5th harmonic 0.1 p.u. component. The interface delay for this example has been selected $\Delta T = 250$ μ s.

First, absolute errors will be considered. In detail, results of simulation consisting of voltages and currents, together with power measured during the simulation, at both ends of the decoupled circuit, will be used, off-line, to compute the all accuracy metrics proposed in the previous section. Waveforms resulting from the simulation using the various IAs are shown in Figure 5.2.1 .

The absolute signal errors, defined by eq. (5.2), are calculated subtracting values coming from simulating the original system not decoupled. Results of this approach are reported in Figure 5.2.2, where a short portion is zoomed to show details for each IA.

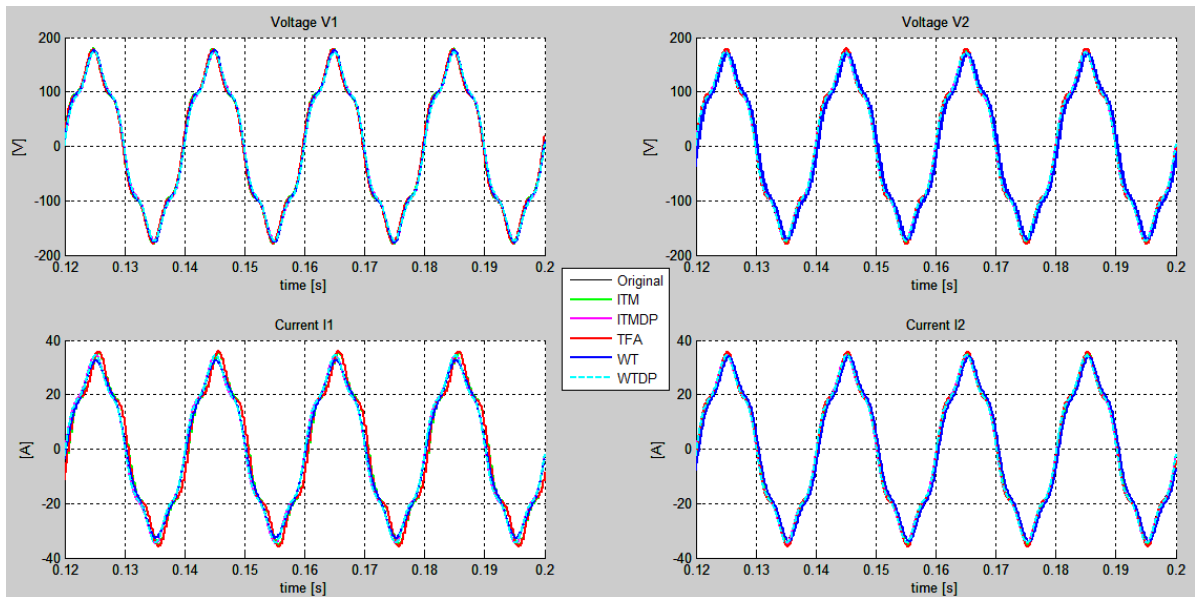


Figure 5.2.1: Simulation results for the simple voltage divider circuit using several IAs

It can be seen how time-domain-based interfaces present large and oscillating values of errors, although WT interface is more accurate on the subsystem 1, which represents the “operator” side of the system. On the other hand, DP-based interfaces are much more accurate, especially WT interface that has errors close to zero.

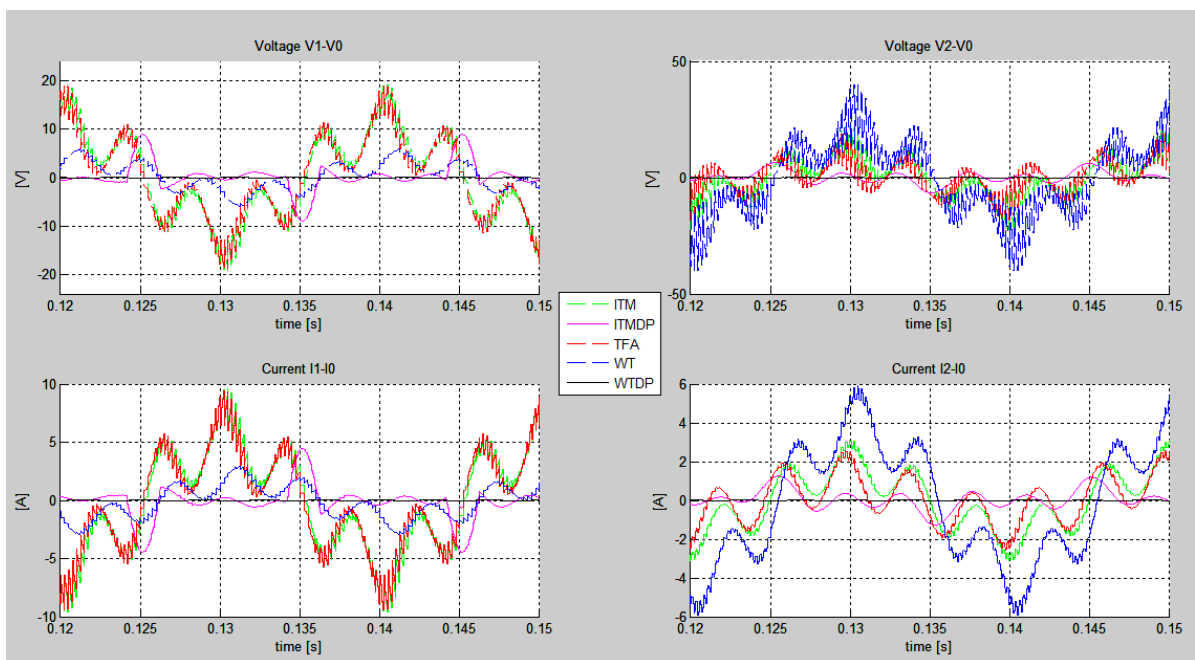


Figure 5.2.2: Absolute signal errors for the simple voltage divider circuit using several IAs.

Absolute signal errors allow seeing detailed accuracy for each coupling variable and for every power port of the decoupled system, but it is not possible to determine which interface is overall the most accurate, since errors in voltage and in current are not comparable.

In order to have a more global accuracy evaluation, absolute power errors need to be calculated, using formula (5.3). For this example, results of calculation are plotted in Figure 5.2.3.

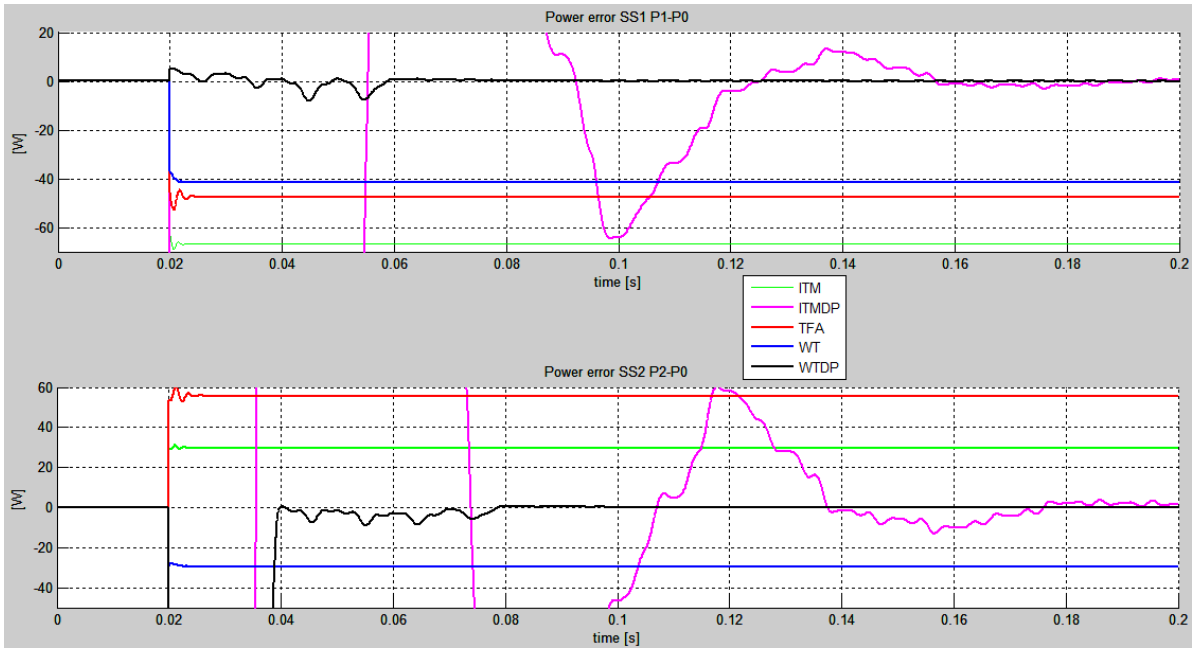


Figure 5.2.3: Absolute power errors for the simple voltage divider circuit using several IAs

Although the figures are zoomed to highlight details, it can be seen how DP-based interfaces show huge error spikes at the beginning of the simulation. Then, after some hundreds of milliseconds, WTDP interface allows having zero absolute power error in steady state. ITMDP interface is slower at reaching steady state error but its absolute power error tends towards zero as well. TD-based interfaces, instead, present steady state power errors different from zero for the whole simulation time.

As already mentioned, using absolute errors as evaluation metric allows having a direct comparison to a simulation that represents the integrated circuit. However, such an approach is not possible in co-simulation, since the system cannot be simulated with the same level of detail as a whole. Moving to the method that are referred to as signal residuals evaluation, the quantities defined in eq. (5.4) are calculated and plotted in Figure 5.2.4, which are substantially relative errors for the coupling variables.

From this analysis, the same conclusions regarding the various IAs can be deduced: ITM, WT and TFA interfaces in time-domain show large errors both in voltage and in current, even though the circuit is in steady state. The interfaces that use dynamic phasors in communication, instead, present small errors. In detail, ITM-DP interface shows oscillating errors anyway, whereas WT-DP interface has zero error in steady state.

According to the same logic expressed above, to have a wider evaluation of the simulation, power residuals can be taken into account, computed using eq. (5.8) and represented in Figure 5.2.5. Again, very large errors characterize the beginning of the simulation when using DP for the interfaces, although later these interfaces allow having very low power residuals in steady state. On the other hand, ITM and TFA in time-domain present a large constant power residual for the whole simulation time. WT interface in time-domain, instead, shows a power residual different from zero but much smaller than the other TD-based interfaces.

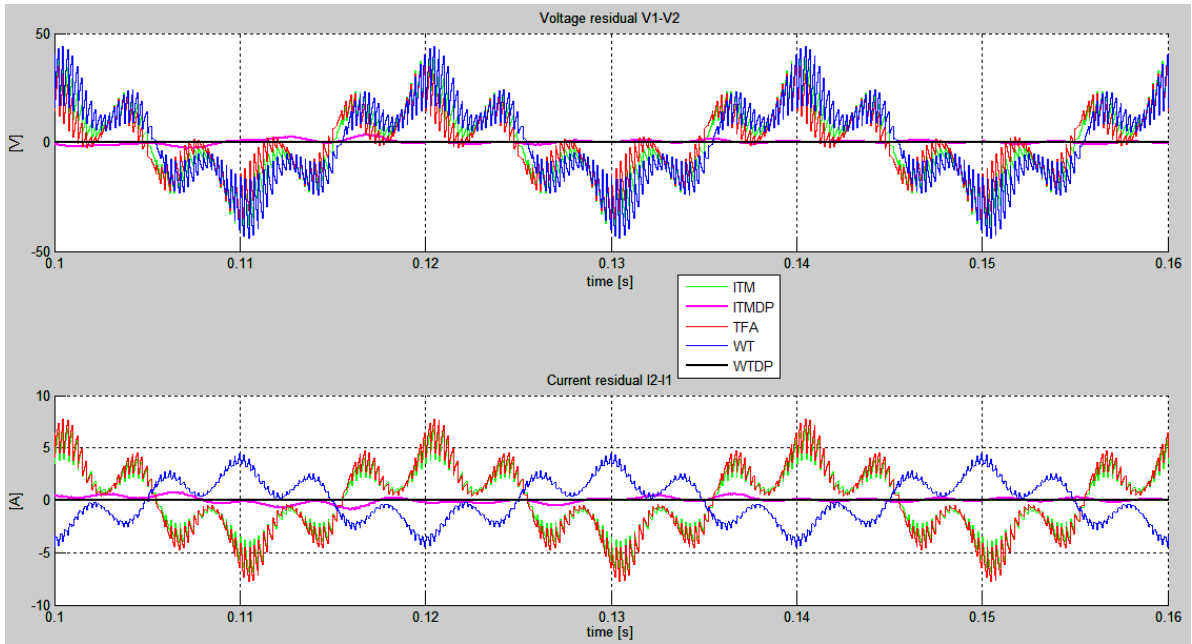


Figure 5.2.4: Signal residuals for the simple voltage divider circuit using several IAs

This evaluation is consistent with what observed using absolute power errors and it is useful to have an instantaneous evaluation of simulation accuracy for every time-step, particularly helpful when considering transients. To have a general evaluation of the whole simulation, power residuals can be integrated over the simulation time, using formula (5.12), obtaining residual energy for each interface algorithms. This result can be compared to the average energy error, defined by eq. (5.11), in order to show further equivalence of the two methods (Figure 5.2.6).

Although the curves are different, they present the same tendencies and allow concluding the same considerations about the various interface algorithms. WT and ITM interfaces using dynamic phasors have, for this circuit and this evolution of its states, the largest energy errors, due to the initial power errors spike. Nevertheless, reaching steady state energy errors are constant, since power errors tend towards zero. Furthermore, a proper initialization of the simulation parameters can fix this issue, avoiding the initial transients.

Interfaces that exchange information using instantaneous values, instead, have lower levels of energy errors, but curves are continuously growing, since power errors are constant and different from zero for the whole simulation. This observations are important because, besides the first instants of simulation, show how using dynamic phasors increases accuracy of a co-simulation in steady state.

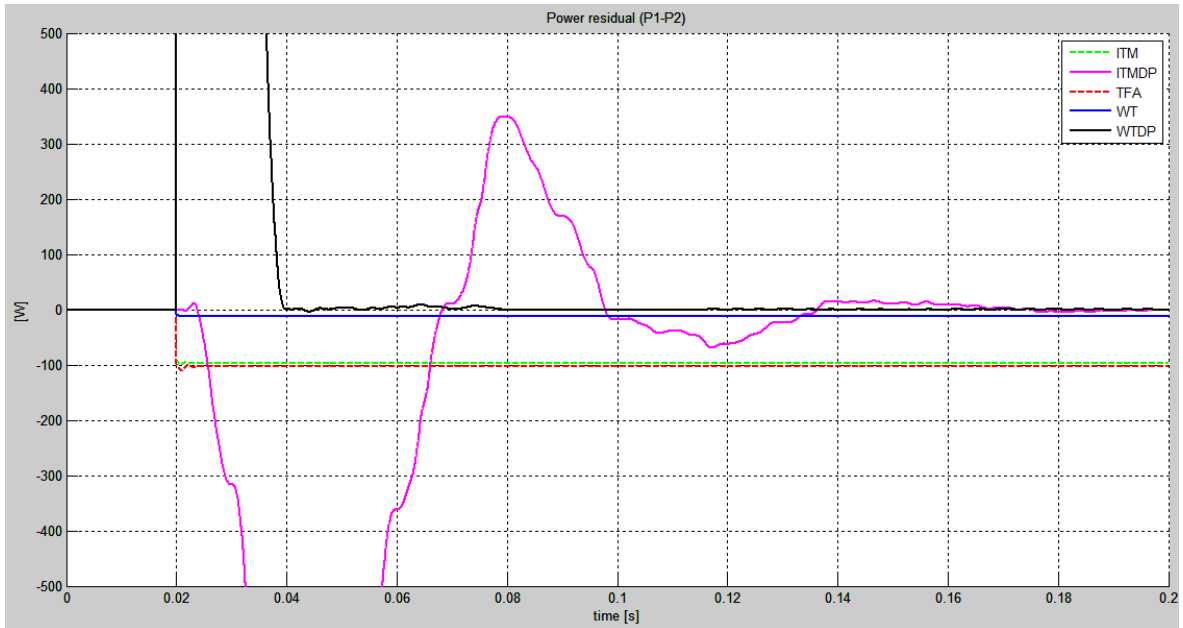


Figure 5.2.5: Power residuals for the simple voltage divider circuit using several IAs

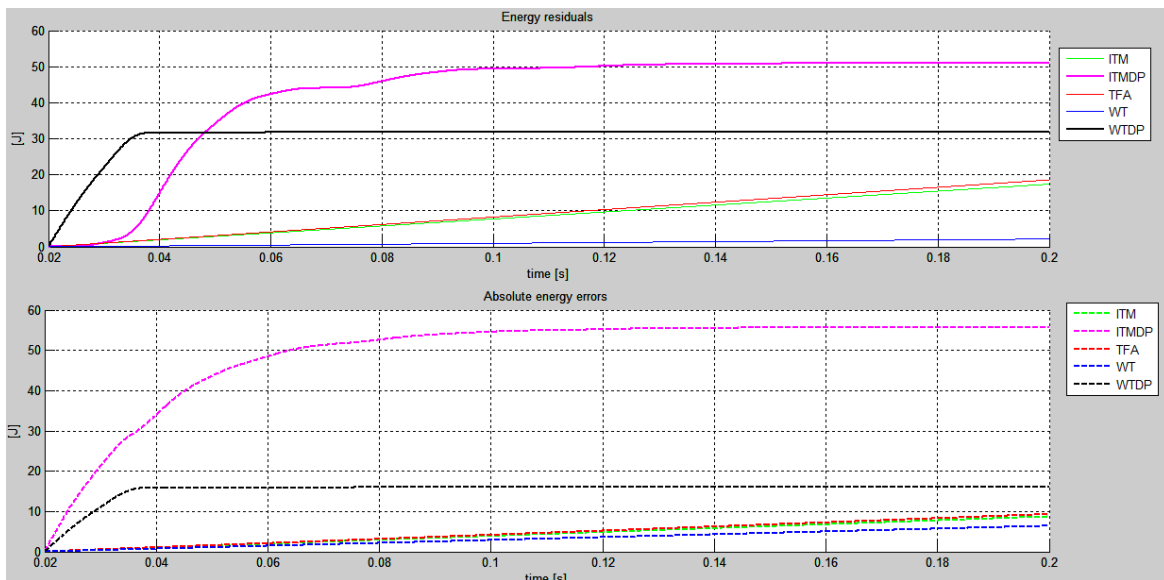


Figure 5.2.6: Energy residuals (top) and absolute energy errors (bottom) for the simple voltage divider circuit using several IAs

5.3 Steady-state accuracy evaluation of interface algorithms

Once that the metric has been theoretically defined and illustrated using a simple example in the previous sections, it is now possible to evaluate accuracy of interface algorithms using the same circuits used in the previous chapter.

They will be referred as circuit A for the simple single-phase circuit and circuit B for the simple three-phase power system. In order to have stable results, parameters shown in Table 5 and Table 6 have been selected for the circuits components.

In this section, the accuracy evaluation will be done when the circuits dynamics evolve in steady-state conditions, as well as it has been done in the previous chapter. For every circuit, the simulations will be executed considering a low value and a large value of interface-delay.

5.3.1 Evaluation using a simple single-phase circuit

The circuit evolves in AC steady state, when a 3rd harmonic, 0.1 p.u. component is injected in the voltage source V_{s1} . Plots showing signal residuals, power residuals and energy residuals will be reported (Figure 5.3.1, Figure 5.3.2 and Figure 5.3.3 respectively), for two different levels of interface delay, as explained earlier. The small time-delay is $\Delta T = 5 \cdot T_s = 250 \mu s$. The large time delay is $\Delta T(t)$ with average value $\Delta T = 300 \cdot T_s = 15 \text{ ms}$.

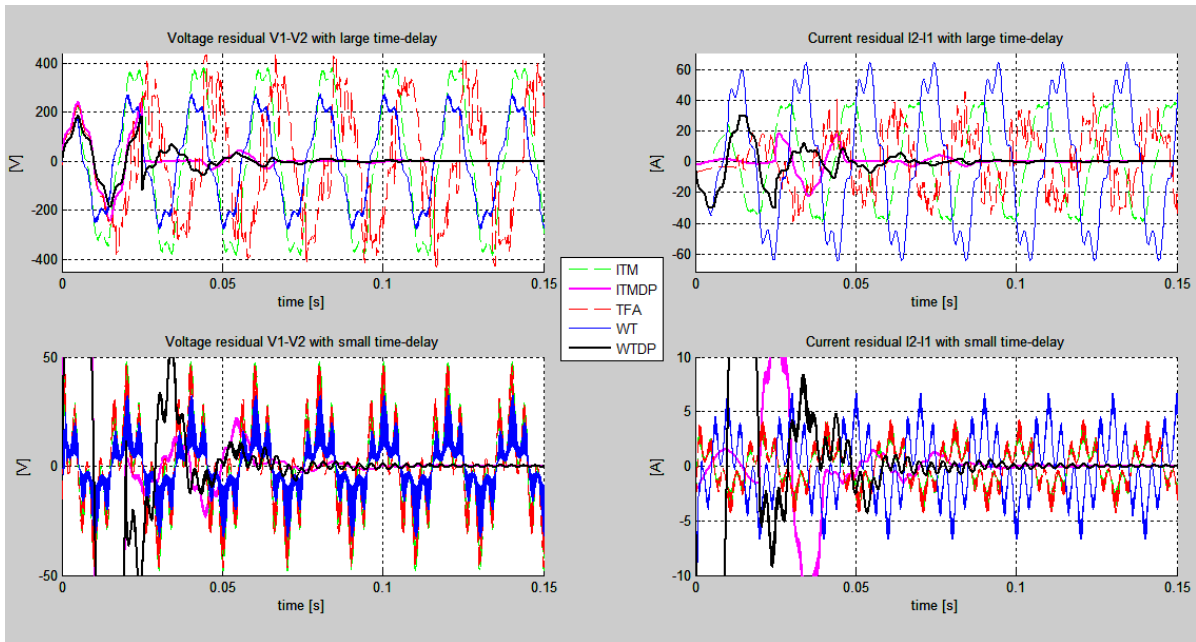


Figure 5.3.1: Signal residuals for circuit A in steady state, with two different levels of time-delay

Regarding signal residuals, the first milliseconds of simulation are characterized by large errors both in voltage and in current for DP-based interfaces. However, they both reach zero error in steady state, regardless of the interface-delay. For interfaces in time-domain, instead, large errors are present in steady state as well, with WT interface having slightly more accurate voltage simulation than ITM and TFA and low accuracy of reconstruction of currents (it is an IV-type scheme, thus a voltage reference is sent from subsystem 1). Nevertheless, from the figure it is possible to notice how with a large delay in communication, signal residuals are around 8 times the value they have with small delay. It has already been explained that exchanging information with instantaneous values causes poor accuracy with large delays.

Considering power residuals, the same conclusions can be derived. Using dynamic phasors assures the best accuracy in steady state, regardless of time-delay. ITM and TFA interfaces have the worst behavior, with large values of power residuals. WT interface, in time-domain, has a good trade-off with both levels of interface-delay, although it is definitely better with a small delay.

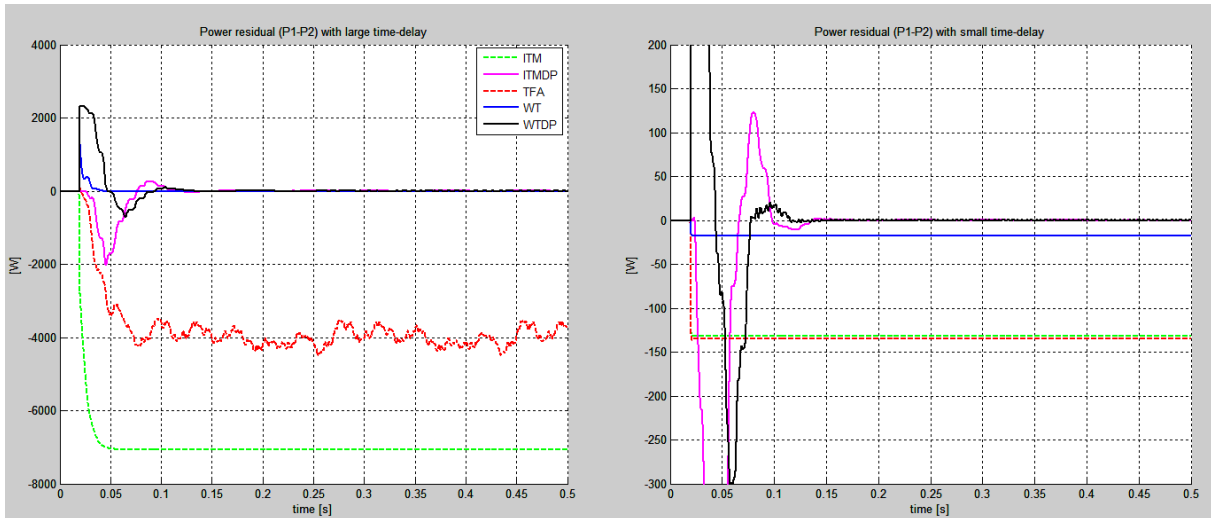


Figure 5.3.2: Power residuals for circuit A in steady state, with two different levels of time-delay

Finally, energy residuals are the metric to evaluate accuracy of the whole simulation. In steady state, interfaces based on dynamic phasors communication have a constant value of virtually added energy, which would be close to zero subtracting the initial accumulation of energy due to simulation start. TFA and ITM interfaces in time-domain have the lowest accuracy, especially with a large delay, since energy residual is continuously increasing. Overall, WT interface in time-domain allows the best accuracy in terms of energy residual, since no spikes show up at simulation start and power residual have low value, although different from zero, thus energy residual is increasing but with a low slope.

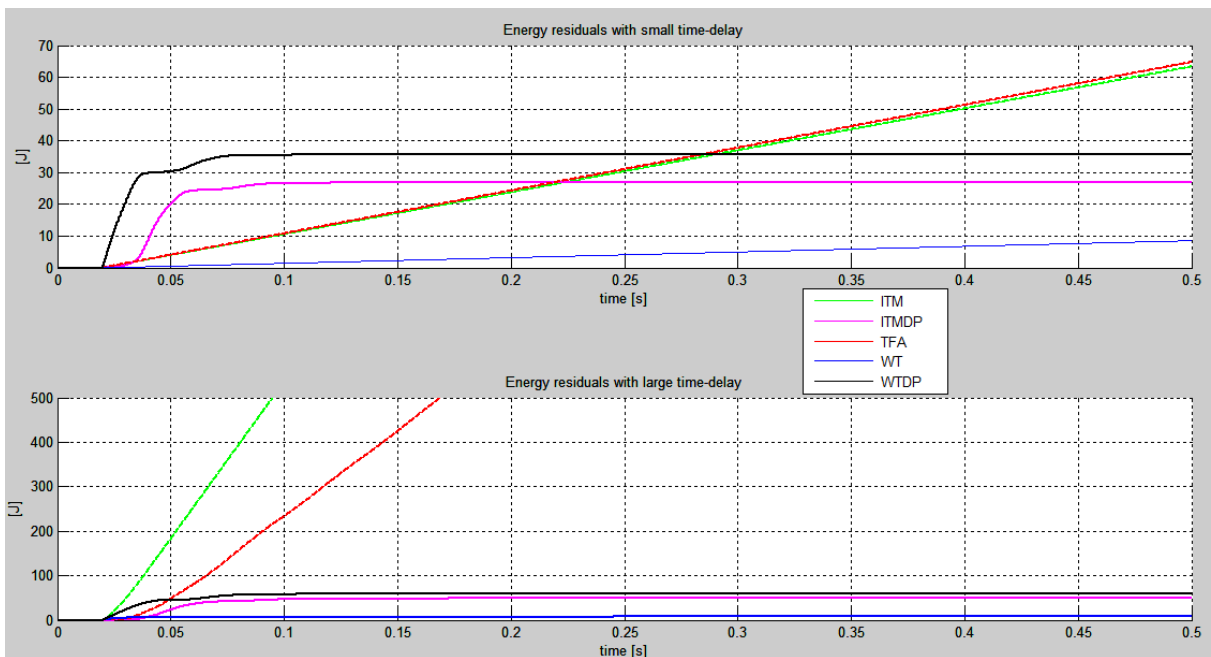


Figure 5.3.3: Energy residuals for circuit A in steady state, with two different levels of time-delay

5.3.2 Evaluation using a three-phase power system

The circuit evolves in an AC steady state, after the initial transient due to the synchronous machine and the MV/HV transformer. As in the previous subsection, the same two levels of

interface delay will be considered to calculate indexes of accuracy of the simulation, which will be reported in the following. It must be noticed that in this situation, ITM interface is not stable when using dynamic phasors to exchange coupling variables. This might happen in certain circumstances, because using dynamic phasors changes the region of stability of the interface. For this reason, results of simulation using ITM-DP interface diverge and will not be reported for accuracy evaluation in this case.

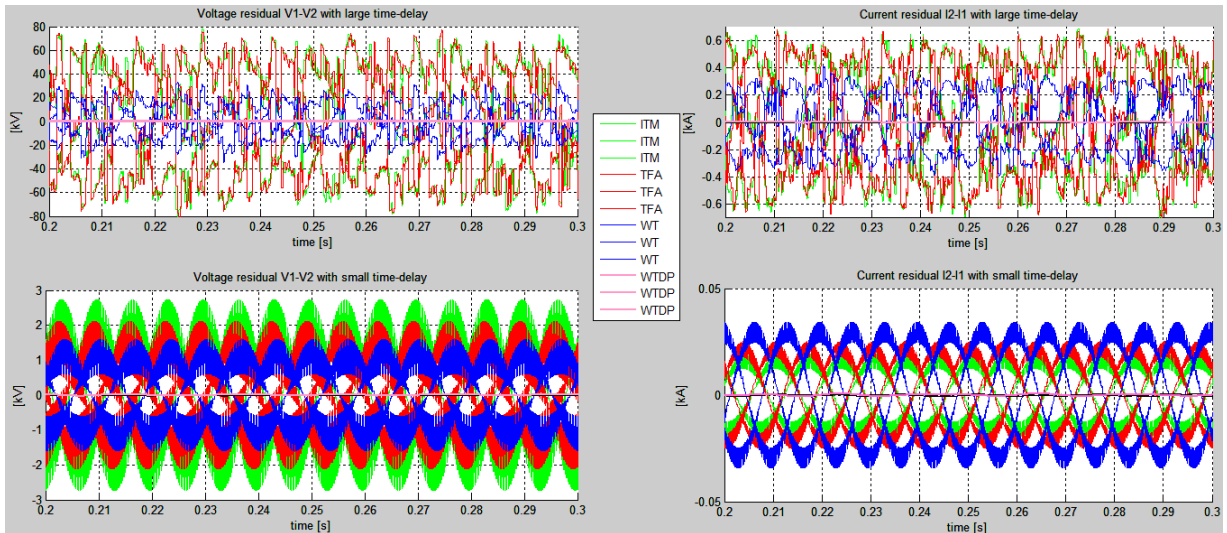


Figure 5.3.4: Signal residuals for circuit B in steady state, with two different levels of time-delay

In Figure 5.3.4, signal residuals for the simple power system, over a small time-window in steady state, show voltage and current errors using the various interface algorithms.

When a small time-delay is used for simulation, time-domain based interfaces allow different levels of accuracy for voltage and current. In fact, considering TD-interface only, ITM has the worst accuracy in voltage, followed by TFA and WT, respectively. On the other hand, ITM has the best reproduction of current, followed by TFA and WT. Hence, an opposite behavior characterizes the interfaces performance in this scenario. The wave transformation interface using dynamic phasors, instead, has signal residuals tending towards zero in steady state, as expected.

When selecting a large time-delay for simulation, signal residuals for TD-based interfaces show huge values compared to the small-delay situation, proving a poor performance when it comes to large interface-delays. However, among the three interfaces, WT presents the best accuracy. Using dynamic phasors for WT, again, allows having zero signal residuals in steady state, although time-delay is 60 times larger.

Considering now power residuals, reported in Figure 5.3.5, the same conclusions regarding accuracy of the interfaces can be derived, for both levels of time-delay.

Energy residuals, computed over the entire simulation time, are shown in Figure 5.3.6. From this plots, similar results from the evaluation using a single-phase circuit yield.

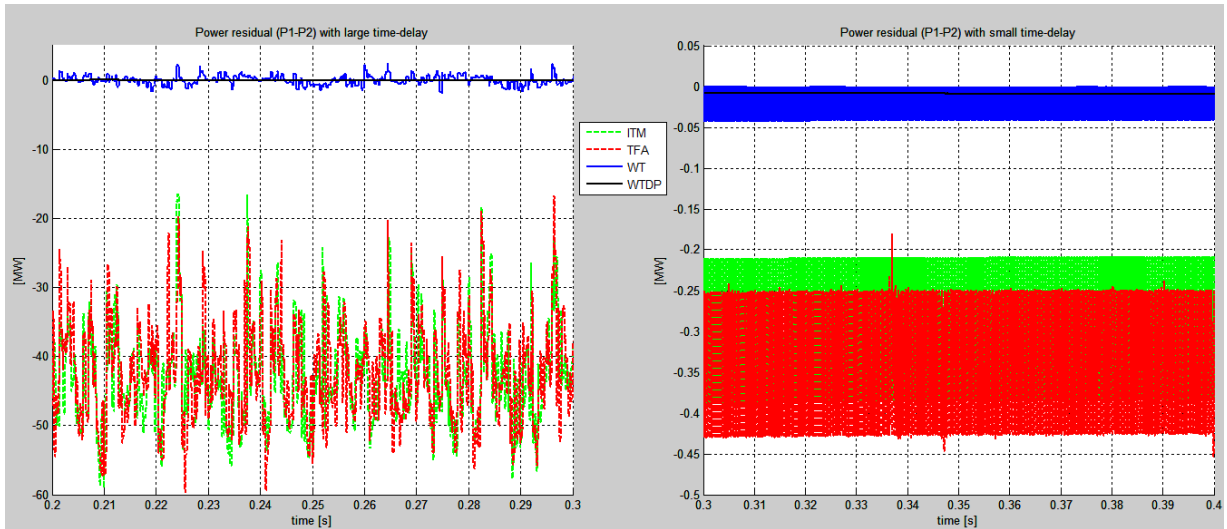


Figure 5.3.5: Power residuals for circuit B in steady state, with two different levels of time-delay

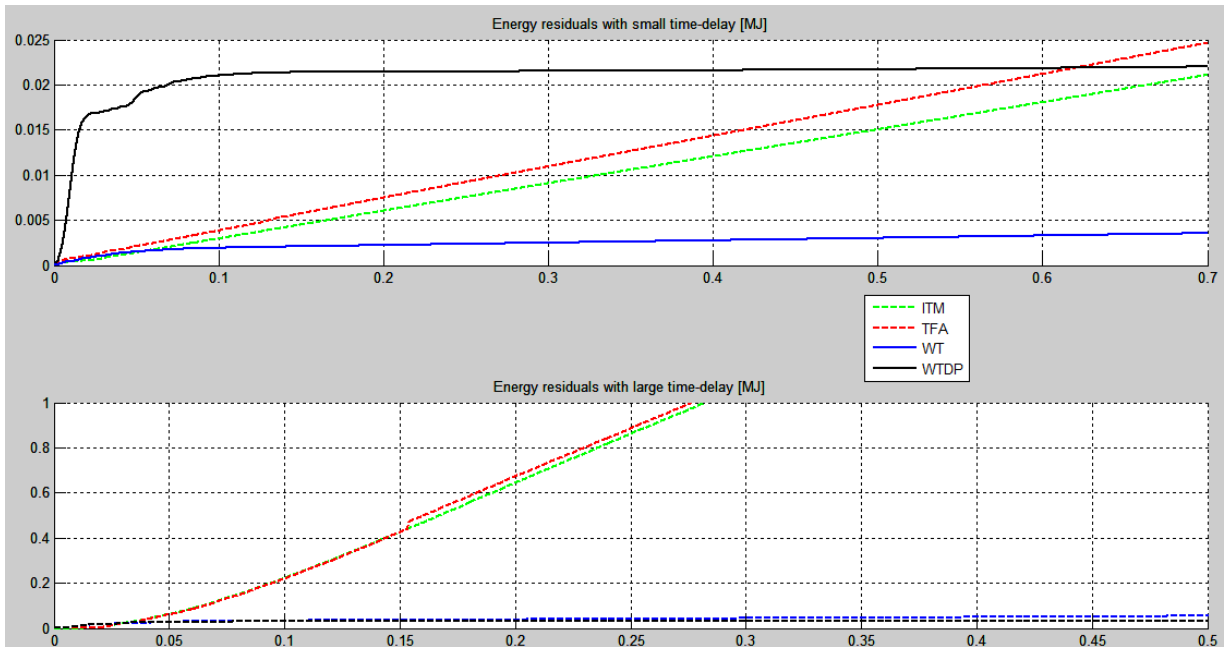


Figure 5.3.6: Energy residuals for circuit B in steady state, with two different levels of time-delay

With small value of interface-delay, WT interface with dynamic phasors shows a global energy residual larger than WT in time-domain, because of the issue with initialization of the waveforms that characterizes DP-based interfaces. Nevertheless, energy residual is almost constant using DP, whereas it keeps on increasing using instantaneous values for co-simulation. It should be noticed that in a simple circuit, it was perfectly constant; in this case, the more complex models used for simulation, such as generator and transmission line, decrease simulation accuracy.

For a larger value of time-delay, ITM and TFA interfaces have large accumulation of energy residuals compared to wave transformation based interfaces. However, using DP allows better accuracy of simulation in overall.

5.4 Transient state accuracy evaluation of interface algorithms

In this section, circuits A and B will be considered to evaluate accuracy of interface algorithms when dynamics of the circuits present some typical transients affecting electrical systems. This allows evaluation of the response of the interfaces to different types of transients and finding out for which circumstances one interface is better than another one.

5.4.1 Evaluation considering single-phase transients

Circuit A dynamics will evolve with a series of transients. The following events occur during the simulation. At $t = 0.1$ s, the magnitude of voltage source V_{s1} rises from $220 V_{pk}$ to $270 V_{pk}$ with a ramp variation, and it decreases back to $220 V_{pk}$ from $t = 0.3$ s. Finally, at $t = 0.5$ s, frequency of voltage source V_{s2} changes with a ramp from 50 Hz to 75 Hz. This scenario will be referred as simulation scenario I.

Moreover, a short-circuit transient is introduced in the decoupling point of the circuit at $t = 0.2$ s but, with this fault, the wave transformation-based interface is not stable with interface in time-domain. This shows that the wave transformation interface is not very suitable, in time-domain based communication, for fast amplitude transients. In fact, accuracy is very low during such conditions and the reason for this lays in the nature of the interface itself. Indeed, this method comes from a telerobotics background, usually implemented thus for mechanical systems that have, as known, much larger time constants than electrical systems. However, using dynamic phasors over the communication channel may help to overcome this issue. For this instability problem, the short circuit transient will be simulated in a different simulation scenario, referred as simulation scenario II, so that for the first group of transients all the interfaces can be compared.

Before showing results of accuracy evaluation, the waveforms of the integrated circuit in the decoupling point showing the transients are reported in Figure 5.4.1.



Figure 5.4.1: Waveforms of the integrated circuit A to show transients in simulation scenario I

Results for signal residuals and power residuals analysis are reported in Figure 5.4.2 and Figure 5.4.3.

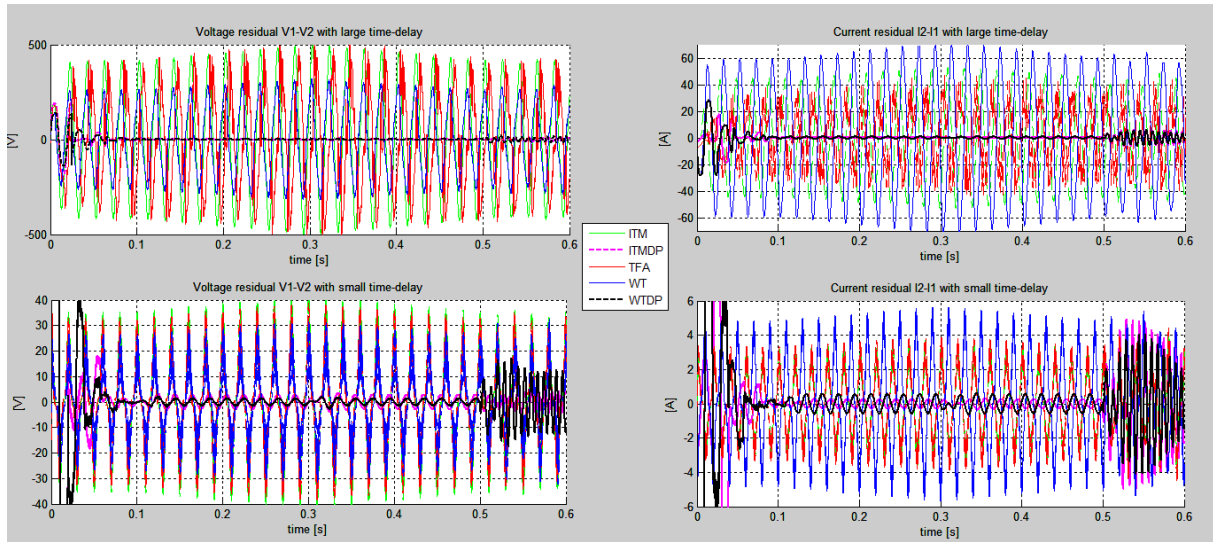


Figure 5.4.2: Signal residual errors for circuit A in simulation scenario I

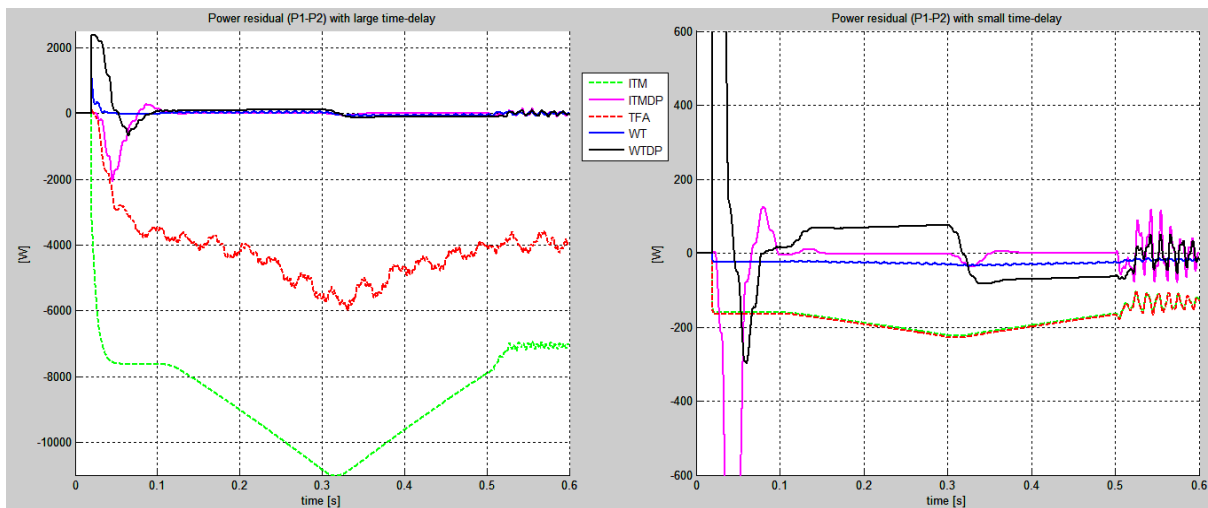


Figure 5.4.3: Power residual errors for circuit A in simulation scenario I

It is possible to see how with a small time-delay, from both signal and power residual, ITM in TD and TFA interfaces have a similar level of accuracy, although ITM shows a slightly better performance in current reproduction but lower in voltage. Regarding WT in TD, power residual is much lower than the other time-domain based interfaces, but from signal residuals, it can be seen how coupling variables have opposite response. In fact, voltage residual error is lower than for ITM and TFA. Current residual, on the other hand, is larger. This depends on the type of scheme selected for the wave transformation method: in this case, as mentioned before, an IV-type scheme has been chosen. Thus, a voltage reference is sent from subsystem 1 to subsystem 2. In the teleoperation approach, this means that accuracy of the operation is focused on voltage rather than on current, which represents the response of the “remote environment” to drive the human operator.

Results for dynamic phasors-based interfaces show that the first instants of simulation are characterized by huge spikes in both coupling variables. This might happen with such interfaces in co-simulation, so it could be helpful to saturate feedback variables before they are sent

subsystems to avoid this phenomenon. However, besides those initial transients, accuracy of DP-based interfaces is much higher, in steady state, than TD-based ones.

On the other hand, in general accuracy during transients much lower. During the voltage amplitude ramps, power residuals for WT and ITM with DP show huge errors compared to the steady state value, which tends towards zero. Instead, although frequency variation makes accuracy of both interfaces decrease, WT accuracy is better with this type of transient.

With a large interface-delay, the dynamic phasors-based interfaces have basically the same behavior, as usual, regardless of the time-delay. The WT IA in time domain shows lower levels of accuracy during transients compared to the small delay case, but overall definitely a better performance than the ITM and TFA interfaces, which have huge signal and power residuals, hence a very low accuracy. Particularly, ITM is less accurate than ITM during amplitude transients. Finally, the frequency variation is best reproduced by the WT interface in time domain, in spite of the large interface-delay.

To evaluate the overall performance of the simulation, energy residual errors will be now reported in fig. Figure 5.4.4. This last analysis confirms what has been already stated. Namely, WT interface in time-domain is the most accurate interface for simulations containing relatively slow transients like a ramp amplitude variation of voltage source and frequency transients, even with large interface-delay.

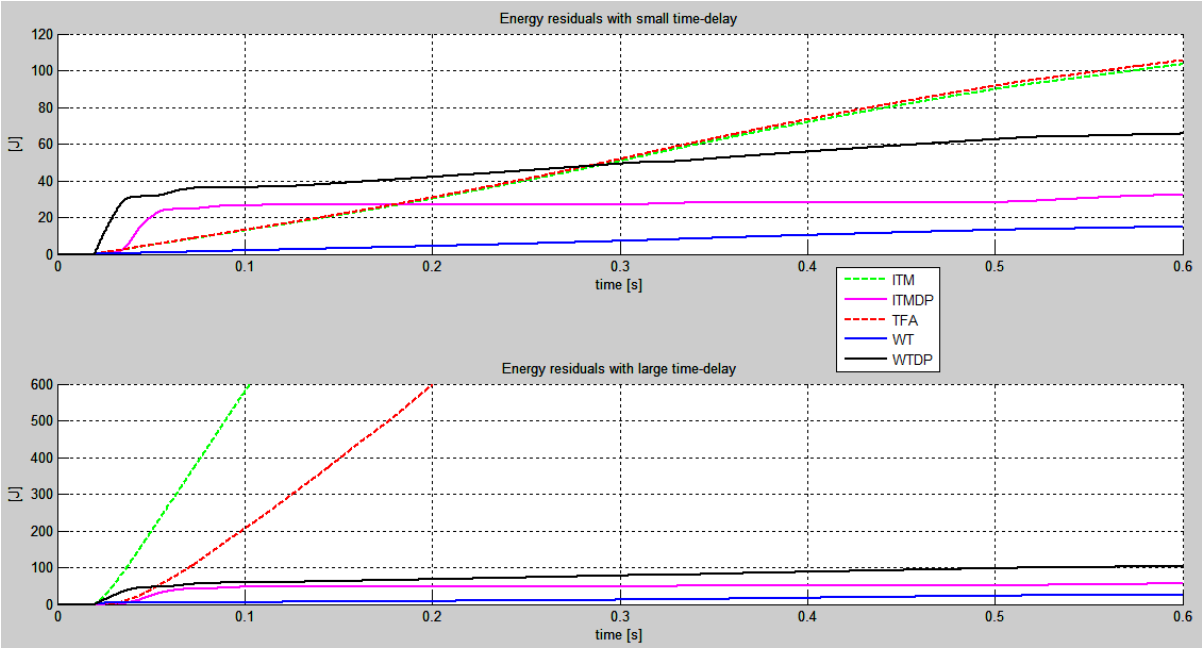


Figure 5.4.4: Residual energy and absolute energy errors for circuit A in simulation scenario I

At last, let us consider a fault in the decoupling point of the circuit at $t = 0.2$ s as transient, by analysing signal, power and energy residual errors. It is interesting to mention that with this transient, some problems of stability arise depending on the choice for number of harmonics selected for Fourier transforms of instantaneous values into dynamic phasors. As a matter of fact, with a small time delay, it was possible to choose the first 5 harmonics including the DC component. When the large 15 ms delay was selected, instead, both ITM and WT interfaces became unstable with dynamic phasors for the selected number of components of dynamic phasors. Such issue was solved selecting the first 3 harmonics including the DC component only, which allowed stable simulations.

With small time-delay, from power residuals (Figure 5.4.6), it can be seen how the fault start introduces large errors for DP-based interfaces, then it goes to zero with some oscillations, because in short-circuit voltage tends towards zero. However, even after the transient, power error for DP-based interface never reaches zero, but it oscillates around positive values over the whole duration of the fault, contrarily to what happens for TD-based interfaces.

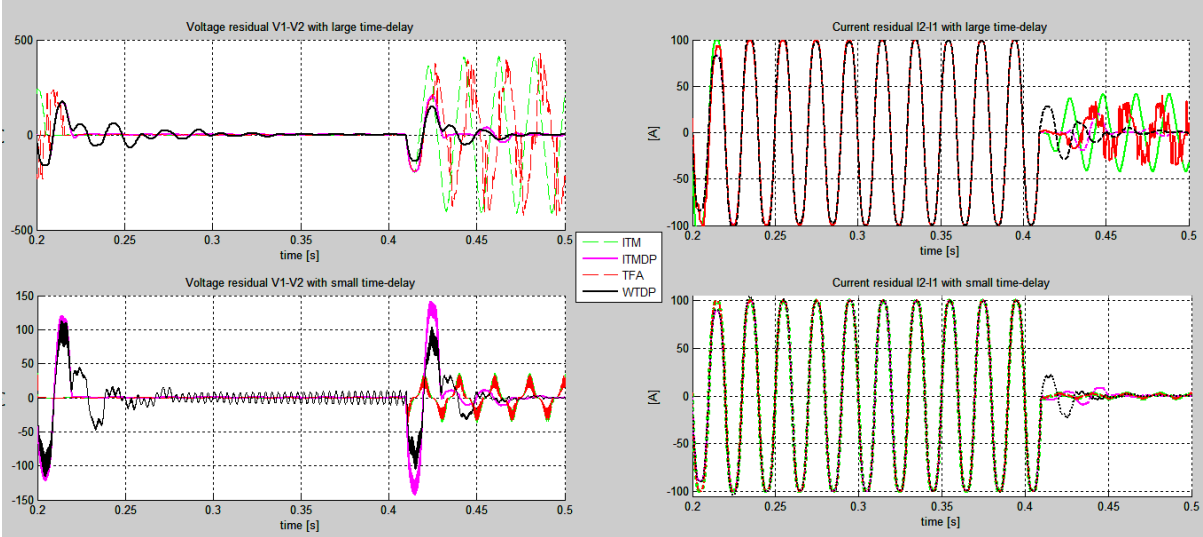


Figure 5.4.5: Signal residuals for circuit A when a short-circuit occurs in the decoupling point

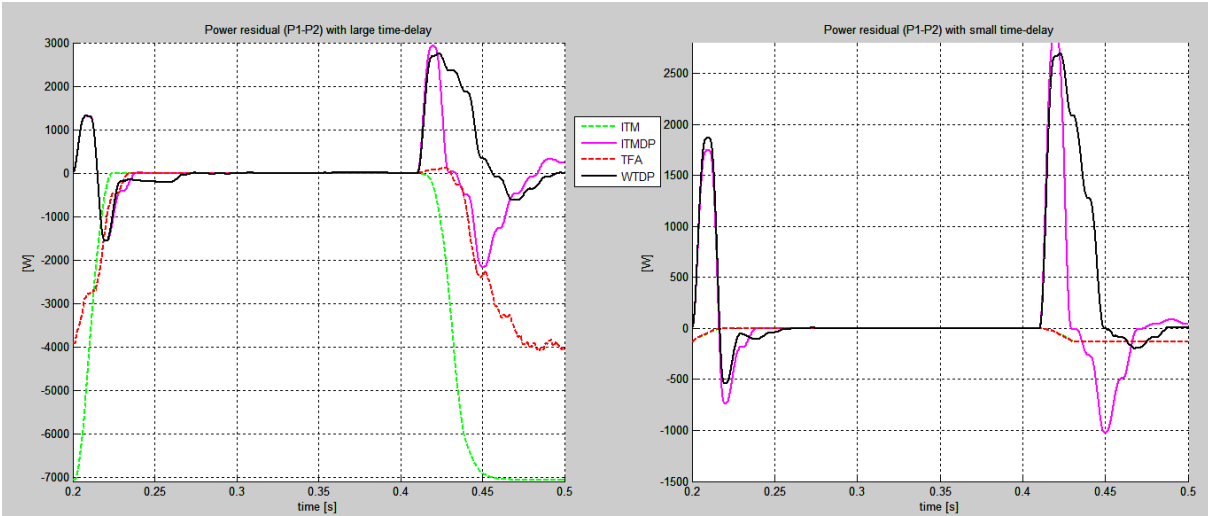


Figure 5.4.6: Power residuals for circuit A when a short-circuit occurs in the decoupling point

The reason behind this can be obtained by verifying signal residuals (Figure 5.4.5). As a matter of fact, voltage residuals for interfaces that use dynamic phasors never reach zero, although they are supposed to according to the results of previous simulations. After the fault ending, larger spikes occur in power residual waveforms, showing thus lower accuracy for switch opening transient than for the closing one. With large value of time-delay, instead, the ITM and TFA interfaces allow having zero error during the fault occurrence, even though steady state power residuals reach huge values compared to DP interfaces.

The huge errors caused by the fault have an impact on energy residuals as well. From Figure 5.4.7, it can be seen how for the same circuit and the same interface algorithms, a different transient makes the global performance of the DP-based interface the worst with a small time-

delay, since they accumulate the largest amounts of residual energy. When time-delay is large, interfaces that exchange instantaneous values have a lower accuracy during the fault occurrence.

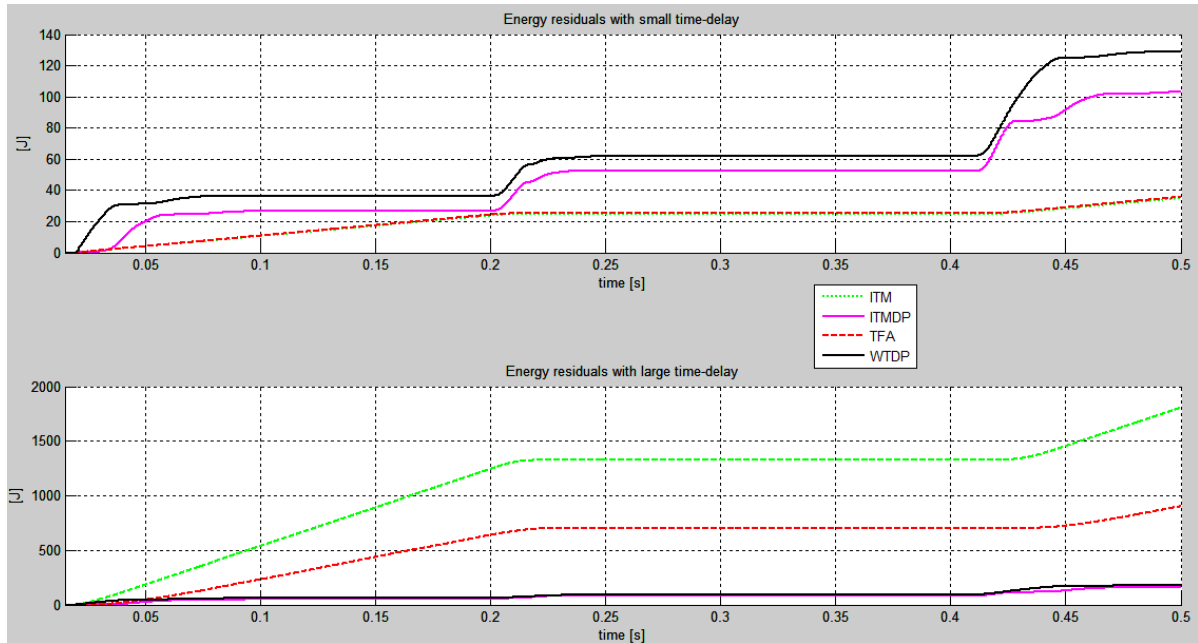


Figure 5.4.7: Energy residuals for circuit A when a short-circuit occurs in the decoupling point

5.4.2 Accuracy considering three-phase transients

In this scenario, the simple power system introduced in chapter 4 (circuit B), will be simulated when it is subjected to a single transient, in order to evaluate accuracy of interface algorithms applied to a three-phase system for the most interesting result obtained. In fact, the same transients tested in the simple single-phase circuit A have been replicated on the power system B but no further observation derived. Therefore, just a voltage source amplitude modulation will be considered. Between $t = 0.2$ s and $t = 0.4$ s, a fundamental component modulation with slow frequency (1 Hz) occurs in the generator side of the system: this is what might happen in interarea oscillations.

This type of transient, besides being typical in power systems, is interesting because it introduces a phase variation of the generator compared to the rest of the system, thus it is possible to check response of the interface algorithms to a phase variation. For the DP-based interface, only DC component and fundamental frequency have been included in Fourier transforms, since further harmonics made the simulation unstable. Results of accuracy evaluation are shown in the following figures.

In Figure 5.4.8, signal residuals are shown during the transient. For the large interface-delay case, signal and power residuals of time-domain based interfaces showed very large errors compared to interfaces using dynamic phasors, hence they are not reported, in order to focus on ITM and WT with dynamic phasors accuracy. In fact, signal residuals calculation shows that WTDP interface, during the transient, is more accurate in voltage and less accurate in current, than ITMDP, for the same reasons concerning interface topology.

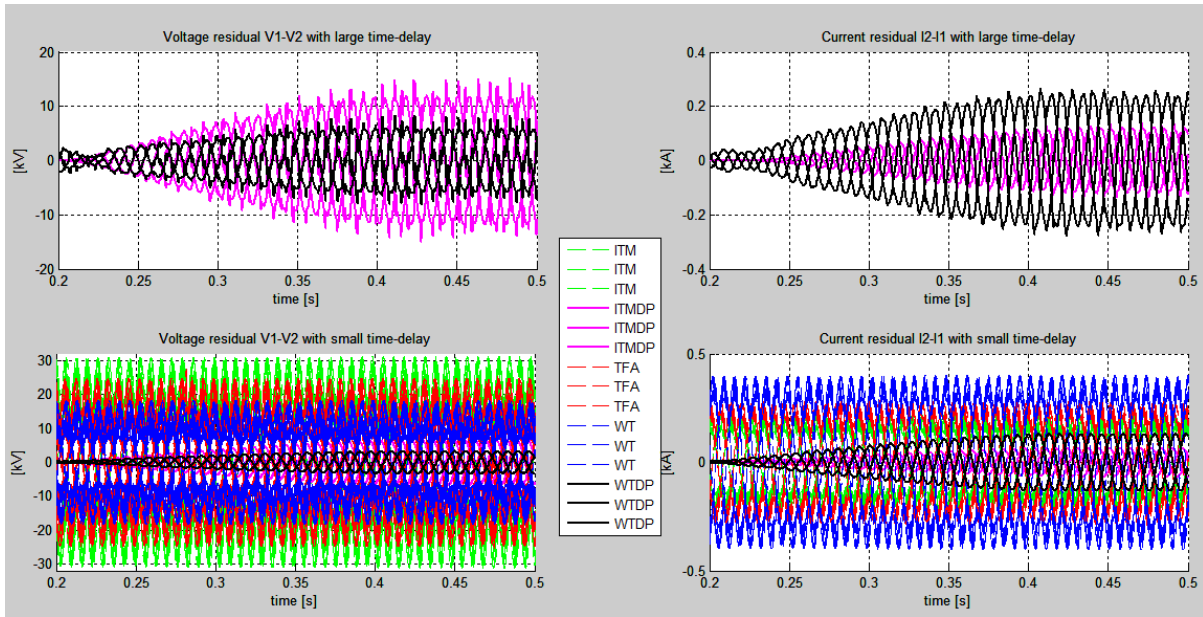


Figure 5.4.8: Signal residuals for circuit B with a voltage source slow frequency modulation transient

The same behavior appears with a small interface-delay, and in this case results are comparable to ITM, TFA and WT. From the figure, it is possible to see that ITM is the most accurate in current, WT the most accurate in voltage, and they have opposite response in terms of accuracy of the single coupling variables.

Considering power residuals (Figure 5.4.9), it can be seen, for the large time-delay case, how WT with DP is globally more accurate than ITM with DP, since it presents lower values of residual power. When instead a smaller delay is present in the communication channel, the ITMDP interface is more accurate.

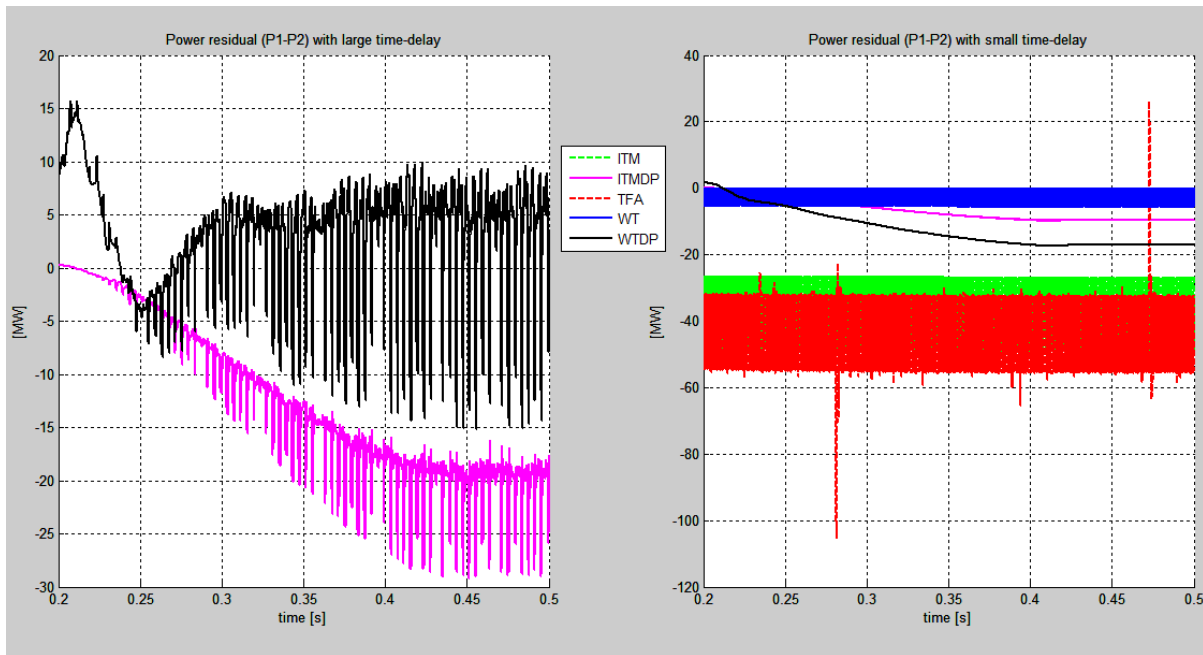


Figure 5.4.9: Power residuals for circuit B with a voltage source slow frequency modulation transient

6. Application to realistic power systems

The simple examples described in the previous chapters, allowed to understanding basic issues of implementing interface algorithms for co-simulation of power system. In fact, the most common issues have been introduced, which are:

- Instability of the simulation when using a certain interface algorithm
- Initialization and tuning of interface parameters to allow the method to converge to a correct value to represent the system properly
- Proper choice of number of harmonics for dynamic phasors-based interfaces, according to the fact that Fourier transforms might act as filters in communication, impacting simulation stability and accuracy
- Sensitivity to transients for different types of interface algorithms
- Numerical issues arising for some of implemented methods for co-simulation interface algorithm
- Different accuracy of interfaces according to different values of time delay

Especially the last point of the above list might be very challenging when it comes to apply co-simulation interfaces to simulation set-ups of real power systems. As a matter of fact, non-linear components present in such models, change the performance of the simulations. Moreover, the tests executed so far have been done off-line using MATLAB/Simulink only. As mentioned in the introduction of the thesis, the main goal of developing interface algorithms was to apply them on a simulator-to-simulator set up using digital real-time simulators, OPAL-RT and RTDS. If the former uses Simulink as GUI to model the systems to simulate in real-time, the latter has its own software environment, RSCAD. Thus, a different modelling interface control components depending on the tool can give rise to different performances of the interface algorithms in real-time simulator-to-simulator simulations.

Moreover, inherent issues of the interface algorithms can be an obstacle when it comes to implementation in a real-time simulation environment. For the wave transformation-based interfaces, the most difficult problem to solve is the algebraic loop arising on both ports of the decoupled system. This can be unwrapped adding a single time-step delay to the feedback path of the wave transformation, as mentioned in chapter 3. This method, introduced in [35], has a major drawback represented by the increase of virtually added energy in the communication channel, which might compromise passivity and thus stability of the simulation itself.

Empirical tests of the interface, however, have shown that for some systems, selecting a larger value for wave impedance, compared to the one estimated based on the circuit characteristics, is a suitable measure to preserve stability. Unfortunately, for other systems, this approach is not sufficient to provide a stable simulation. Further methods to unwrap numerically the algebraic loop should be implemented. In circumstances when the algebraic loop in the wave transformation interface cannot be solved, the code cannot be generated from the model: thus, it is not possible to run a real-time simulation which requires such a form of the mode. For this reasons, the wave transformation interface cannot be used in the RTDS-OPAL set-up until a new method to break the algebraic loop is not investigated.

In this chapter, the interface algorithms that have been described in the previous chapters will be implemented on a co-simulation set-up for two realistic power systems, in order to have an experimental proof of the obtained theoretical results. Additionally, IAs already tested in literature will be used as reference and their accuracy will be evaluated for a real-time

geographically distributed co-simulation using two different simulators, which is a new contribution for this field of real-time simulation.

The models of such power systems will be described in the following sections, together with a description of the addressed challenges that have allowed implementation.

6.1 Co-simulation of an HVDC Transmission Link

A high-voltage, direct current (HVDC) transmission system uses direct current for the transmission of electrical power, from the more utilized AC systems. For long-distance transmission, HVDC systems may be less expensive and enable lower electrical losses. For underwater power cables, HVDC avoids the heavy currents required to charge and discharge the cable capacitance each cycle.

What is more, HVDC allows power transmission between unsynchronized AC transmission systems. Since the power flow through an HVDC link can be controlled independently of the phase angle between source and load, it can stabilize a network against disturbances due to rapid changes in power. HVDC also allows transfer of power between grid systems running at different frequencies, such as 50 Hz and 60 Hz. This improves the stability and economy of each grid, by allowing exchange of power between incompatible networks.

A long distance point-to-point HVDC transmission scheme generally has lower overall investment cost and lower losses than an equivalent AC transmission scheme. HVDC conversion equipment at the terminal stations is costly, but the total DC transmission line costs over long distances are lower than AC line of the same distance. HVDC requires less conductor per unit distance than an AC line, as there is no need to support three phases and there is no skin effect.

However, many disadvantages are present in such systems, among which:

- HVDC is less reliable and has lower availability than AC systems, mainly due to the extra conversion equipment
- The required converter stations are expensive and have limited overload capacity
- HVDC circuit breakers are difficult to build because some mechanism must be included in the circuit breaker to force current to zero, otherwise arcing and contact wear would be too great to allow reliable switching

In spite of those issues, HVDC systems have found several applications throughout the last decades. As a matter of fact, the controllability of a current-flow through HVDC rectifiers and inverters, their application in connecting unsynchronized networks, and their applications in efficient submarine cables mean that HVDC interconnections are often used at national or regional boundaries for the exchange of power. Offshore windfarms also require undersea cables, and their turbines are unsynchronized. In very long-distance connections between two locations, such as power transmission from a large hydroelectric power plant at a remote site to an urban area, HVDC transmission systems may appropriately be used.

For these reasons, it might be interesting and useful to be able to simulate a detailed model of an entire HVDC system. As this short introduction to such complex power systems has illustrated, many components may be part of these systems. Thus, a higher level of detail is necessary to have a proper reproduction of actual behavior. Therefore, for the reasons already widely discussed earlier in this thesis, a co-simulation allows simulation of the entire model of a complex system with a higher level of detail.

6.1.1 Description of the model

The model used for co-simulation can be found in Mathworks Documentation, where a complete description of model is included [39]. As shown in Figure 6.1.1, a 200 MVA (+/- 100 kV DC) forced-commutated Voltage-Sourced Converter (VSC) interconnection is used to transmit power from a 230 kV, 2000 MVA, 50 Hz system to another identical AC system. The rectifier and the inverter are three-level Neutral Point Clamped (NPC) VSC converters using close IGBT/Diodes.

The Sinusoidal Pulse Width Modulation (SPWM) switching uses a single-phase triangular carrier wave with a frequency of 27 times the fundamental frequency ($F_c = 1350$ Hz). Along with the converters, the station includes on the AC side: the step down Yg-D transformer, the AC filters, and the converter reactor. On the DC side, the capacitors and the DC filters are included. The rectifier and the inverter are interconnected through a 75 km cable and two 8 mH smoothing reactors.

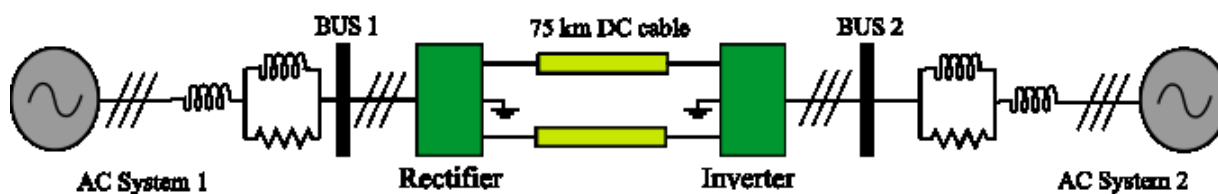


Figure 6.1.1: Single-line diagram of the HVDC transmission link model.

The system is set to start and reach a steady state. Then, at $t = 1.5$ s, the source in the AC system 1 is programmed for a step of -0.1 p.u on voltage magnitude for a duration of 7 cycles.

The power system and the control system are both discretized for a sample time $T_{sPower} = 7.406 \mu s$ and $T_{sControl} = 74.06 \mu s$ respectively. They are multiples of the carrier period $1/F_c = 740 \mu s$, in order to represent properly the rectified quantities.

6.1.2 Simulation set-up

In order to execute a co-simulation of this system, the decoupling point could be chosen either on an AC subsystem or on the DC cable. The first choice has already been done in [38], where the same system has been used to test the modified ITM interface using dynamic phasors to exchange coupling variables. In this thesis, instead, the decoupling point will be chosen in the halfway point of the DC cable to test performance of the wave transformation interfaces when DC quantities are exchanged.

The aim of this test is to evaluate accuracy and general performance of the wave transformation IA in time-domain when interface-delay is comparable to the delay in a locally distributed co-simulation. What is more, the interface will be compared to the standard ITM interface, which is known to have a good performance with DC systems (as shown in 4.3.4), in order to verify its response to a realistic power system simulation.

The modified interfaces using dynamic phasors for communication will be considered as well, although for DC quantities such transformations are just an averaging of the waveforms, unless higher harmonic orders are considered (e.g. up to 15th) so that transients can be represented. However, in this case, only the DC component and the fundamental 50 Hz frequency will be included into Fourier transforms.

As already mentioned, only one level of interface delay will be taken into account, computed as integer multiple of the simulation time-step $T_{sPower} = 7.406 \mu s$:

- $\Delta T = 5 \cdot T_s = 37 \mu s$. Moreover, a sampling rate $h = 2000 \text{ Hz}$ will be selected.

Regarding the topology of the interfaces, the ITM interface does not provide a stable simulation in none of the topologies. About the WT interfaces, particular attention must be taken when considering the power flow calculation of the system. As a matter of fact, it has already been explained multiple times in the previous chapters, that the WT interface is based on a teleoperation method where an operator commands a remote environment. In terms of electric systems, one has to consider the power flow going from one subsystem to the other selecting the first subsystem as the “master” and the second one as the “slave” of the teleoperation equivalent system. According to this approach, the subsystem where AC system 2 is located is chosen to be the master of this interface, thus a wave transformation interface with VI-type topology is selected.

When it comes to tuning of the wave impedance, the parameter value selected for the co-simulation is similar to the DC resistance of a half of cable, which is: $R_{dc} = r \cdot d/2 = 0.521 \Omega$, where r is the resistance per unit of length and d is the total length of the cable.

The following sections are organized as follows:

- Results of simulations using ITM, ITMDP, WT and WTDP interfaces, are illustrated for DC voltage and current waveforms at the decoupling point compared to the ones of the original system and for AC voltage and current waveforms at buses 1 and 2 compared to the original system ones as well.
- Accuracy evaluation, using both the above-mentioned DC quantities and AC quantities, since accuracy of the first does not ensure accuracy of the second, and vice versa.

6.1.3 Simulation results

Despite of low value of interface-delay, the ITM interface does not provide simulation stability. The use of dynamic phasors for ITM interface makes the simulation stable but simulation results are of low accuracy. For this reason, only interfaces based on wave transformation will be considered. Results using such interfaces are shown in Figure 6.1.2 and Figure 6.1.3.

Considering the DC quantities, it can be noted that the results for HV voltages in the DC cables are reproduced compared to the original response. In fact, the wave transformation acts on the voltages like an averaging function. Thus, the average values are preserved but variations are decreased. The use of dynamic phasors applies further averaging on DC variables, which decreases accuracy of the voltages reproduction.

Currents, instead, are simulated with higher accuracy using the WT interface, whereas WTDP interface has very low accuracy for currents as well. However, the first instants of simulation are characterized by a poor accuracy for both interfaces. As a matter of fact, the HVDC system has an initial fast transient that, as it has already been shown in the previous chapter, is simulated using WT-based interfaces with low degree of simulation fidelity.

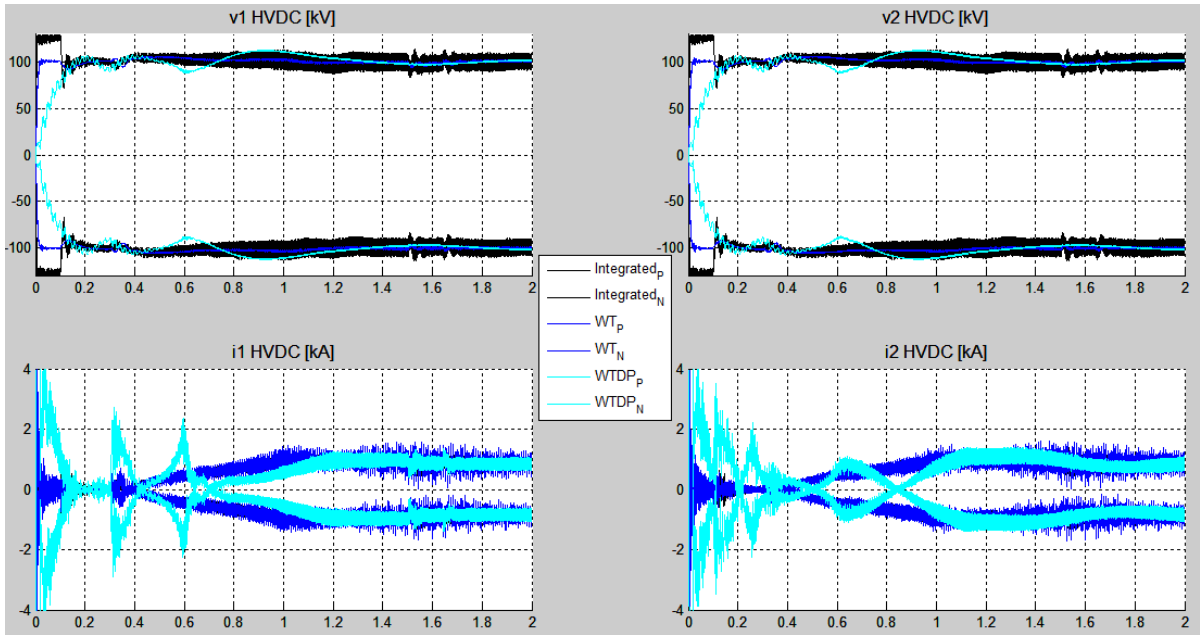


Figure 6.1.2: Results of simulation of HVDC link showing DC voltages and currents in the decoupling point

When the three-phase AC variables are considered, instead, simulation accuracy is much higher. This is possible thanks to the fact that average values are preserved in the DC cables variables. In steady state, both voltages and currents are simulated with high accuracy using wave transformation interface.

Considering the voltage transient, instead, currents are simulated with lower accuracy, even though the use of wave transformation without dynamic phasors provides better results.

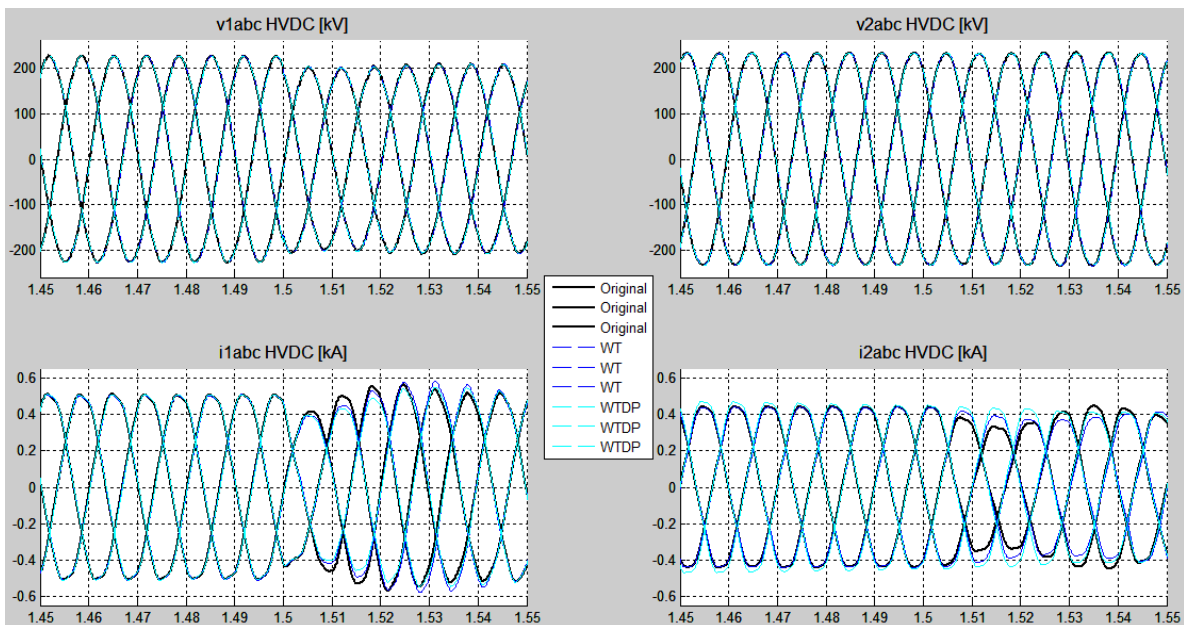


Figure 6.1.3: Zoomed results of simulation of HVDC link showing AC voltages and currents in buses 1 and 2 during the voltage amplitude transient

6.1.4 Accuracy evaluation

To evaluate accuracy of the interfaces, the same metrics used in chapter 5 will be here applied. For this scenario, it is interesting to show results coming from absolute errors analysis as well, in order to have a showcase for validity of the adopted metric using a real power system model. As VI-scheme has been adopted for the interface, residuals to evaluate accuracy for the HVDC system, will be calculated as following:

$$e_v = v_2 - v_{2D}$$

$$e_i = i_1 - i_{1D}$$

$$P_k = P_2 - P_1$$

As already mentioned before, accuracy of coupling variables, which are DC quantities, and AC quantities at the buses 1 and 2, will be evaluated separately. Regarding the AC variables, however, it is wrong to compare signals and power from AC system 1 to signals and power of AC system 2, because they are actually two different systems and there is no guarantee that they should behave in the same way. For this reason, only absolute errors will be considered to evaluate AC accuracy.

With respect to the coupling variables, signal residuals are shown in Figure 6.1.4. From this figure, it can be seen what already mentioned earlier about initialisations of simulation. Especially when using the WTDP interface, it takes almost half of the simulation time to reach a steady state. The WT interface, instead, reaches a steady state much faster, although in this case voltage residuals have higher values than WTDP interface. Current residuals, on the other hand, are more accurately simulated using WT than WTDP.

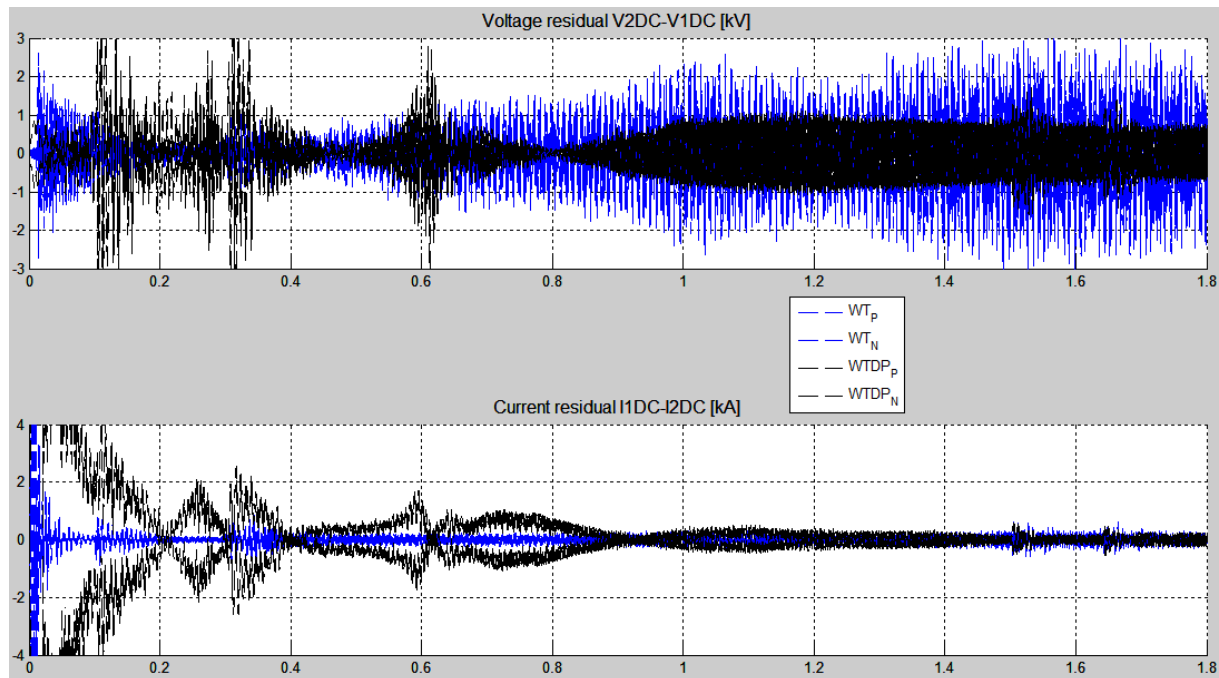


Figure 6.1.4: DC signal residuals for simulation of the HVDC transmission link using a small interface-delay

To evaluate the overall performance of simulation, power residuals are considered. For power residuals, shown in Figure 6.1.5, only power on one cable (particularly, the positive one) has been considered, since it is valid the relation: $P_{pos} = -P_{neg}$.

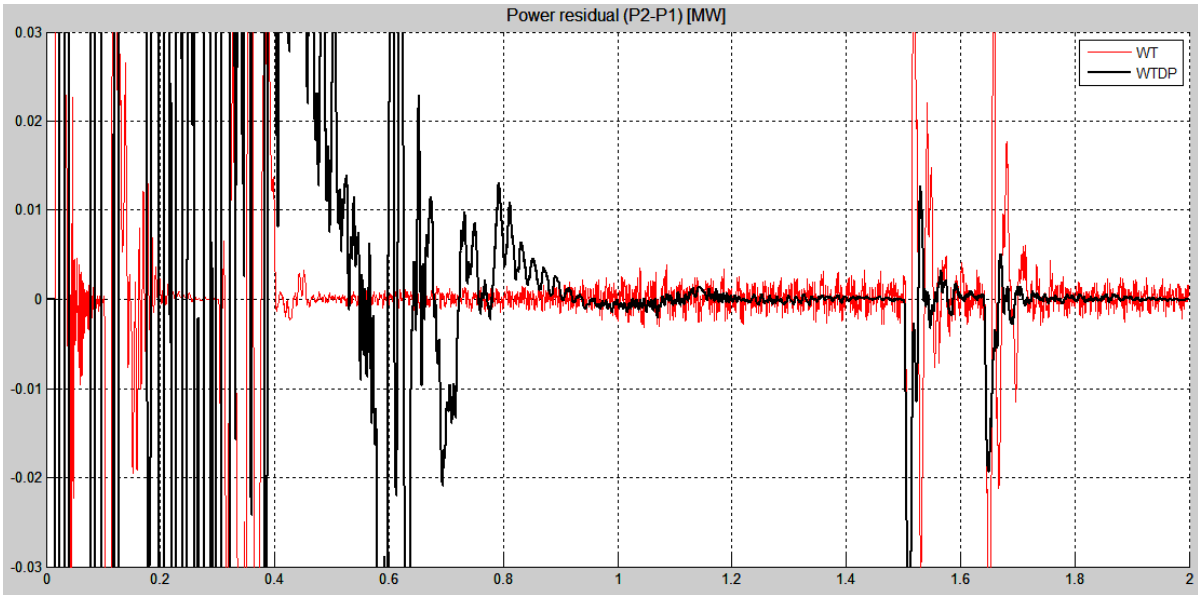


Figure 6.1.5: DC power residuals in steady state for simulation of the HVDC transmission link using a small interface-delay

The inaccuracy that characterizes the initial phase of the simulation using the WTDP interface result in large power residuals. At $t = 1.5$ s, when the voltage sag occurs, WT interface is less accurate during the transient compared to WTDP.

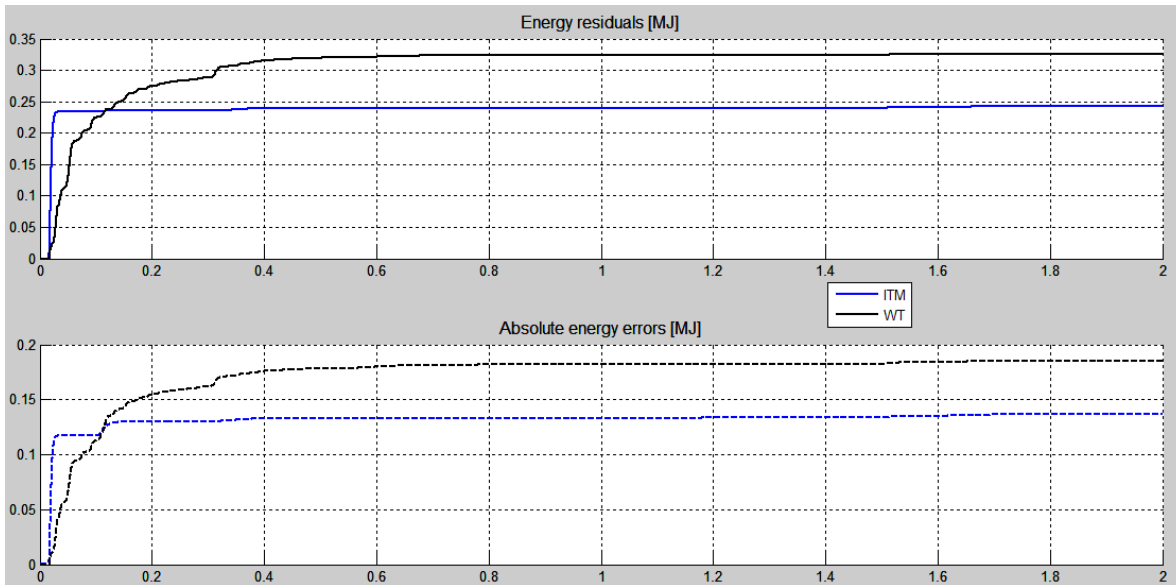


Figure 6.1.6: Energy residuals in steady state for simulation of the HVDC transmission link using a small interface-delay

However, to verify the overall accuracy of the global simulation, energy residuals are computed. In Figure 6.1.6, energy residuals are compared to absolute energy errors. First, it can be seen that the use of residual energies as metric ensures obtaining the same conclusions as the use of absolute errors.

Furthermore, it can be concluded that the WT interface provides a more accurate simulation, since only 0.23 MJ of energy is wrongly added into the communication, compared to the 0.33 MJ when the WTDP interface,

Therefore, after having concluded that wave transformation interface is the most accurate in simulating DC quantities using a small time-delay, let us evaluate the accuracy of the interfaces in the simulation of the three-phase AC variables, using absolute errors. In Figure 6.1.7, absolute signal errors are illustrated for the three-phase currents and voltages. It can be concluded that the WT interface is much more accurate in time-domain than with dynamic phasors even in reproducing the AC quantities, after the initial phase of the simulation when even WT interface generates inaccurate results.

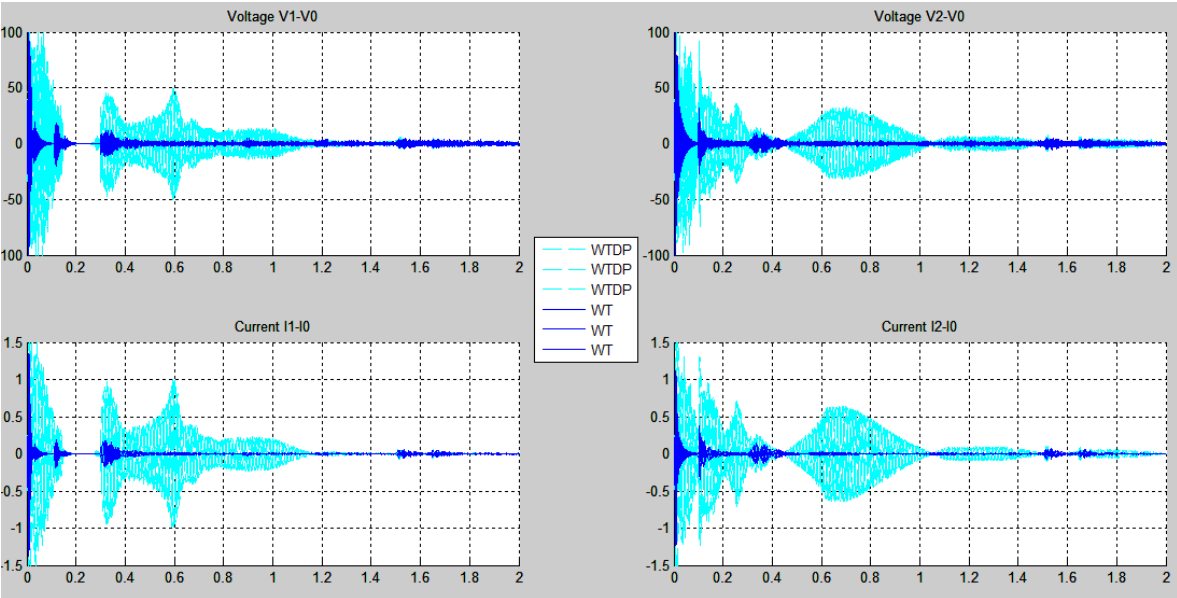


Figure 6.1.7: AC signal errors for simulation of the HVDC transmission link using a small interface-delay

These conclusions are confirmed by absolute power errors, illustrated in Figure 6.1.8.

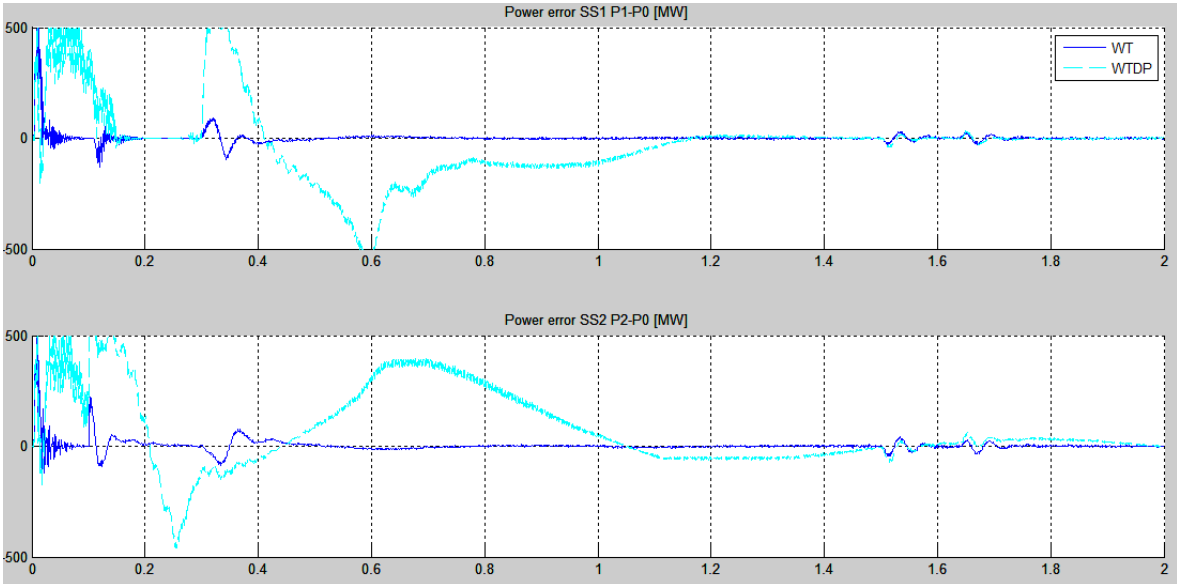


Figure 6.1.8: AC power errors for simulation of the HVDC transmission link using a small interface-delay

Finally, the accuracy of the simulation is quantified by average absolute energy errors, which show that the use of the WTDP interface in this scenario generates results that are over 10 times less accurate than using the WT interface.

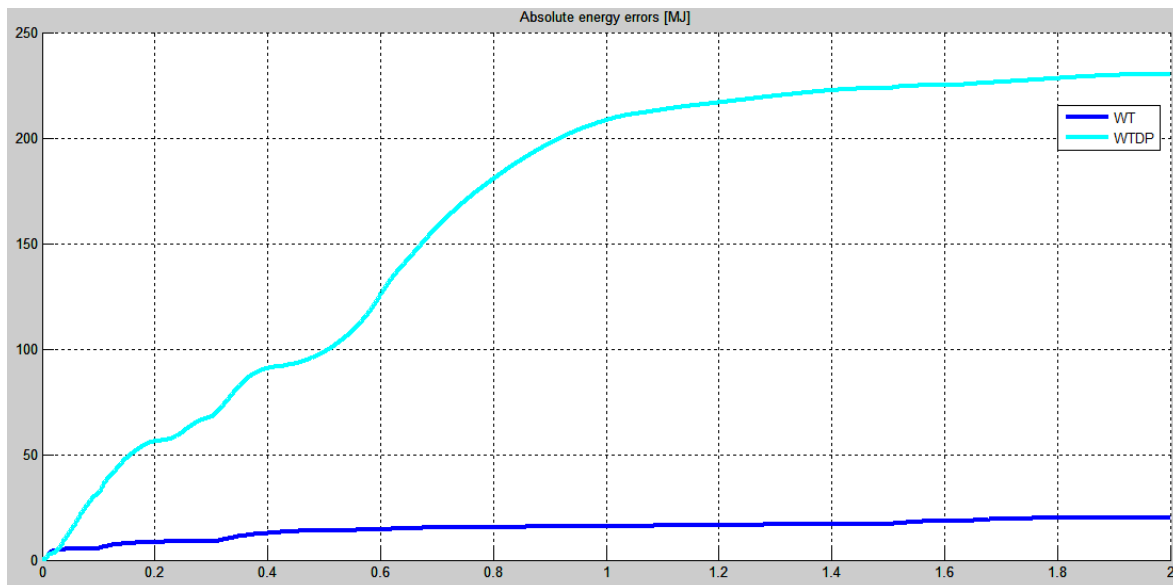


Figure 6.1.9: AC energy residuals for simulation of the HVDC transmission link using a small interface-delay

The most important result is about the stability of the wave transformation-based interfaces. Running a co-simulation of a complex power system like an HVDC transmission link, having many transients and high-frequency dynamics, and selecting the DC cable halfway as decoupling point, leads most of the IAs under study to instability. Thus, this application shows the most important feature of the WT interfaces, which is based upon the passivity concept to guarantee stable simulations.

Considering also accuracy of the simulation, it is interesting to notice that the wave transformations act on the DC quantities as averaging operations, preserving the original average value though. Therefore, accuracy in simulating the coupling variables is not high. Nevertheless, when it comes to evaluation of the accuracy of the AC three-phase quantities, high levels of accuracy are achievable.

To sum up, wave transformation has a major advantage in achieving the stable simulation, with the main obstacle of the algebraic loop inherent for the wave transformation itself. Moreover, satisfying levels of accuracy can be achieved especially for AC quantities, whereas DC quantities are reproduced with low accuracy of variations, but the average value is preserved.

6.2 Co-simulation of a Transmission Network and a Distribution Network

The necessity to simulate a transmission system and a distribution system arises from the increasing interactions between the two networks. Actually, the transition towards the widespread use of renewable and distributed energy resources (DER) in the distribution networks has led to development of new methods that allow a safe integration of DER in the existing network. In order to test those methods, benchmark models are necessary: CIGRE Task Force (TF) C6.04.02 has addressed this requirement in [9], where a common basis for testing has been developed and proposed.

In that report, benchmarks representing HV, MV and LV networks have been described in detail, with proposed application examples and indications for an appropriate simulation use. Moreover, every network has been proposed both for the North American system and the

European system. Thus, it is possible to simulate the individual systems separately, although guidelines for connecting the systems to investigate interactions are included in the report as well.

6.2.1 Description of the model used for co-simulation

In this thesis, the co-simulations include a model built to evaluate interactions between a High Voltage Transmission Network and a Medium Voltage Distribution Network only, based on the European standards. Particularly, the HV network is modelled in RSCAD, in order to be simulated with RTDS simulator. The MV network, instead, is modelled in Simulink and ARTEMIS for simulation using OPAL-RT. The connection between the two simulators, for a locally-distributed co-simulation, is realized using a Field-Programmable Gate Array (FPGA).

In detail, the high voltage transmission network benchmark is based on a physical HV network in North America covering areas of Manitoba, North Dakota, and Minnesota. Compared to the original network, the number of nodes has been decreased so that the important characteristics are preserved, with the model being suitable for simulation with EMTP-type programs as well. It includes three areas: one with surplus generation, one with excess load, and an intermediate area that is weakly connected to the remaining system.

The nominal voltage levels for the transmission are 220 kV and 380 kV, the typical for European transmission systems. Generation bus voltages are 22 kV, and the system frequency is 50 Hz. The network, showed in Figure 6.2.1, consists of 13 buses and covers three geographical areas, referred to as Areas 1, 2, and 3, marked by dashed lines.

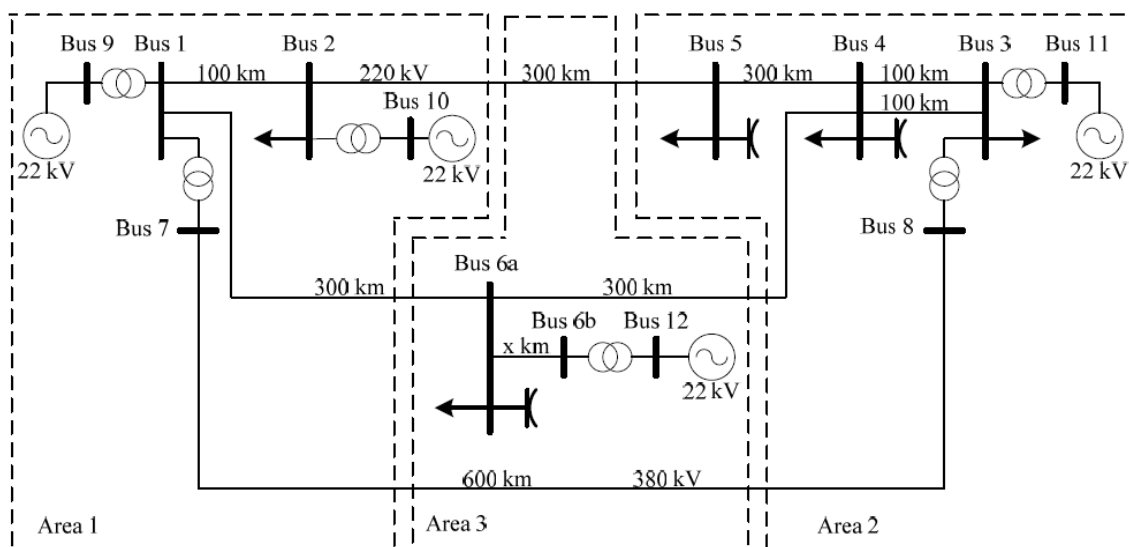


Figure 6.2.1: Topology of European Transmission Network Benchmark used for co-simulation [40]

As already mentioned, the MV network benchmarks from the same report may be introduced at the load points if more detailed representations are of interest for the study. In the models used for this thesis, the load present in the Bus 4 of the TN has been replaced with one end of the interface algorithm necessary to realize the co-simulations: therefore, bus 4 is the decoupling point used for co-simulation. For all the tested interfaces, an IV-type scheme has been adopted, thus load in Bus 4 has been replaced with a three-phase controlled current source that receives current reference from the DN.

Mean to interconnect the HV and MV voltage levels is required. While this could be done with a single transformer, a more common approach involves representation of a subtransmission network. Such a representation is integrated in the Simulink model of the MV Distribution network, using a simple subtransmission network model suggested in [9], i.e. an autotransformer connected to the subtransmission 110 kV line.

The medium voltage (MV) distribution network benchmark is derived from a physical MV network from southern Germany, which supplies a small town and the surrounding rural area. Compared with this original network, the number of nodes for the benchmark network was reduced to enhance flexibility while maintaining the realistic characteristics of the network.

European MV distribution feeders are three-phase and either of meshed or radial structure, with the latter dominating rural installations. The benchmark allows flexibility to model both meshed and radial structures. Each feeder includes numerous laterals at which MV/LV transformers would be connected. The nominal voltage is 20 kV. The system frequency is 50 Hz.

The topology of the European version of the MV distribution network benchmark is shown in Figure 6.2.2. Bordered with dashed lines are Feeders 1 and 2. Both feeders operate at 20 kV and are fed through distinct transformers from the 110 kV subtransmission network. In order to run co-simulations, the station from where the DN begins has been replaced with the other end of the interface algorithm that, as explained earlier, consists of an IV-type scheme. Therefore, a three-phase controlled voltage source that receives voltage reference coming from the TN is here located.

6.2.1 Co-simulation set-up

It has been mentioned several times that the co-simulation of the transmission and distribution networks are conducted using a simulator-to-simulator set-up using both RTDS and OPAL-RT real-time simulators. In this section, a brief description of the simulation precautions, required to run properly the co-simulation, will be given. Then, an explanation is provided which results have been collected and why will follow.

The HV transmission network benchmark is modelled using RSCAD software, which is necessary to run simulations using the RTDS simulator. As stated earlier, the load at the bus 4 of the networks has been replaced with the controlled current source to use the ITM interface algorithm. Then, voltages measured at the bus 4 are sent to the distribution network using the FPGA. In this section, the ITM interface using dynamic phasors will be used as well. In that case, voltages are transformed into dynamic phasors before being sent to the DN as magnitude-phase couples.

On the other end of the co-simulation, the MV distribution network benchmark is modelled in Simulink, in order to be run using OPAL-RT simulator. At the beginning of the DN, a controlled voltage source commands the network receiving the voltage reference coming from the FPGA. In the ITM-DP interface case, voltages are reconstructed into instantaneous values before being applied for the voltage source control. At the same time, currents are measured on this point, in order to be sent back to the TN, as already explained in detail regarding the interface algorithms concept.

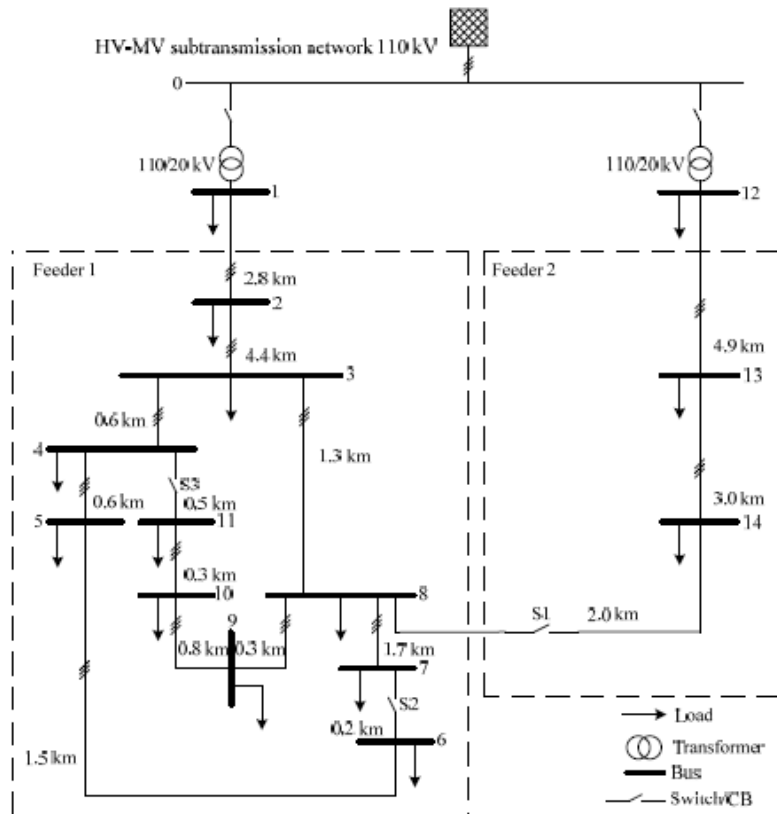


Figure 6.2.2: Topology of European Distribution Network Benchmark used for co-simulation [40]

Only a single simulation scenario will be considered in this chapter that will demonstrate certain important features of using a co-simulation. Such a scenario was automated on the TN in order to start the simulation and then, at $t = 4$ s, to simulate the disconnection of the generator located in bus 11. Thus, voltage and frequency transients occur in the TN, but this co-simulation was meant to investigate the interactions between the TN and the DN, as mentioned earlier. Indeed, when the generator disconnects, voltage profiles at all the buses decrease, and this has an impact on the distribution network, where photovoltaics (PVs) are modelled as negative loads. Such PVs are controlled following a Low Voltage Ride Through (LVRT) capability, i.e. the capability to remain connected in short periods of lower electric network voltage (voltage dips).

The original co-simulation was implemented then to study such interactions, and particularly to prove that using a complete model of both networks allows representing with higher fidelity the actual behaviour of the networks. In those cases, the co-simulation was run in a locally distributed set-up, using a standard ITM interface algorithm in time-domain. In this context, instead, some of those tests will be repeated using the modified ITM with dynamic phasors, considering a geographically-distributed co-simulation, in order to have a showcase of dynamic phasors characteristics over a co-simulation using a realistic model.

6.2.2 Simulation results

As already mentioned, this co-simulation set-up was initially implemented using an ITM interface in time-domain, since in a locally-distributed co-simulation that is enough to ensure a good level of accuracy, as long as the simulation is stable. Thus, the results obtained with that interface will be used as reference to compare the results obtained using dynamic phasors to exchange information between the two co-simulated subsystems.

Thus, in Figure 6.2.3, coupling variables, i.e. currents and voltages measured on the two ends of the decoupling point, are represented. In the same figure, active power measured on the two power ports is reported. As it can be seen, waveforms are plotted over a time windows that includes the instant when the generator in bus 11 disconnects. Following that, the voltage gap can be observed. From voltage and current waveforms, a good level of accuracy can be noticed. However, considering active powers, it can be seen how the voltage transients causes, of course, a power transient in the TN, which is not detected by the DN, where power is unchanged.

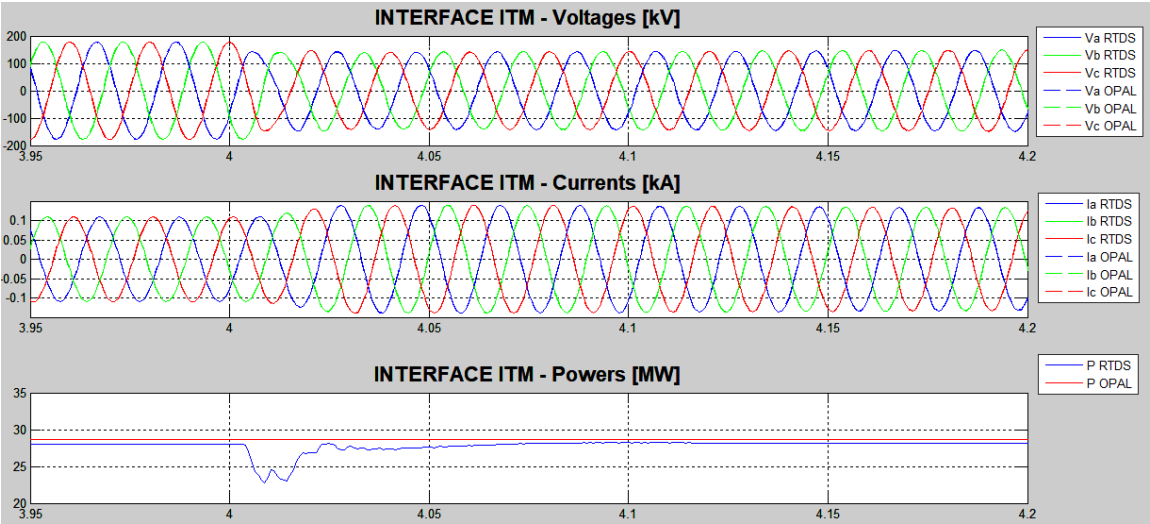


Figure 6.2.3: Coupling variables and active powers in the decoupling point using ITM-TD interface, with no additional interface delay

Before moving to the modified interface with DP, let us consider the same interface when the co-simulation is run over a communication channel that causes a large time-delay. In detail, considering $\Delta T = 15$ ms, results of simulation are now the ones in Figure 6.2.4.

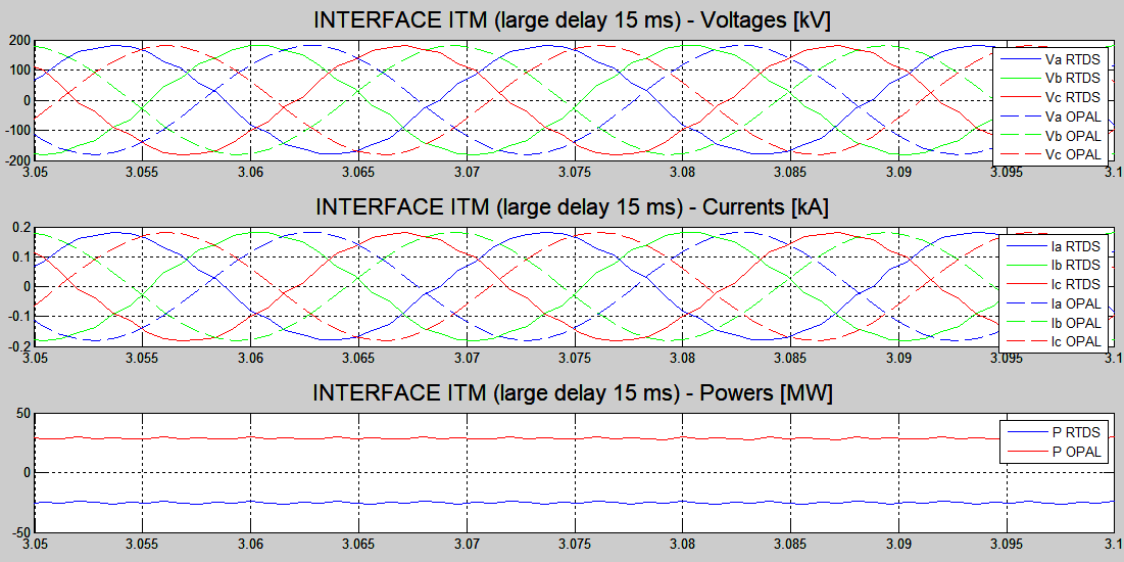


Figure 6.2.4: Coupling variables and active powers in the decoupling point using ITM-TD interface, with an additional 15 ms interface delay

The interface-delay causes a phase-shift between the waveforms in two simulators, which is not compensated by the interface algorithm. The error in this simulation is immediately

recognizable from the active powers, which have totally different values. This is interesting for what happens using DP in communication as we are going to see in the following.

As a matter of fact, in Figure 6.2.5 results of the simulation run using dynamic phasors in communication, when no further delay is introduced, are shown. Although a phase shift appears between the waveforms in the two simulators, this has a different meaning compared to the one causes by time-delay. In fact, this phase shift is due to the different phase reference that each simulator generates in order to reconstruct into time-domain the dynamic phasors. However, as it can be seen from the plotted active powers in steady state, the accuracy of simulation is even better than using standard ITM interface algorithm.

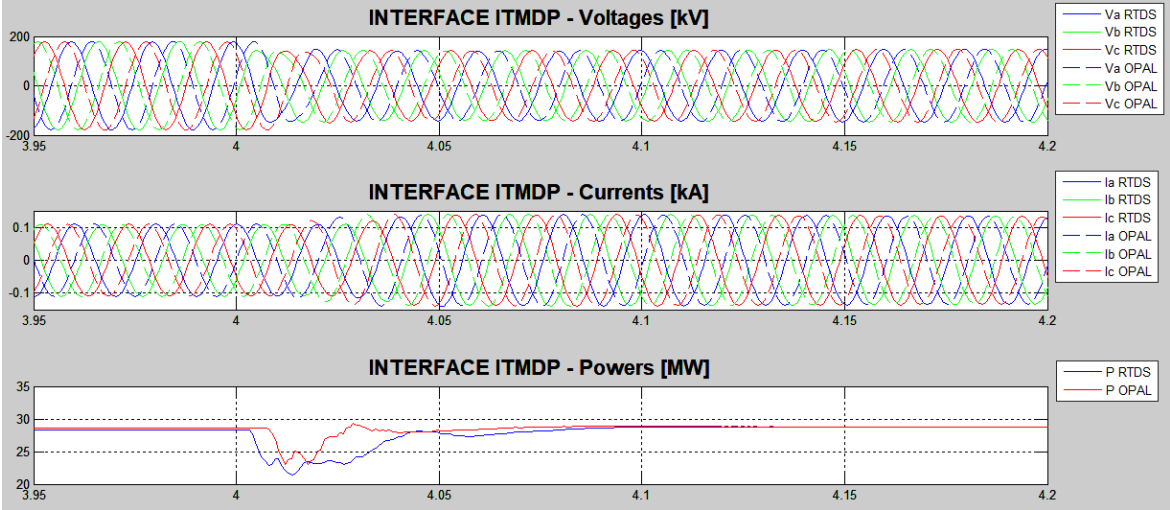


Figure 6.2.5: Coupling variables and active powers in the decoupling point using ITM-DP interface, with no additional interface delay

Moreover, compared to the time-domain-based interface, when the generator disconnects initiating a power transient in the TN (simulated in RTDS), using dynamic phasors a power transient is detected in the DN as well, whereas there was not such an interaction the standard ITM case.

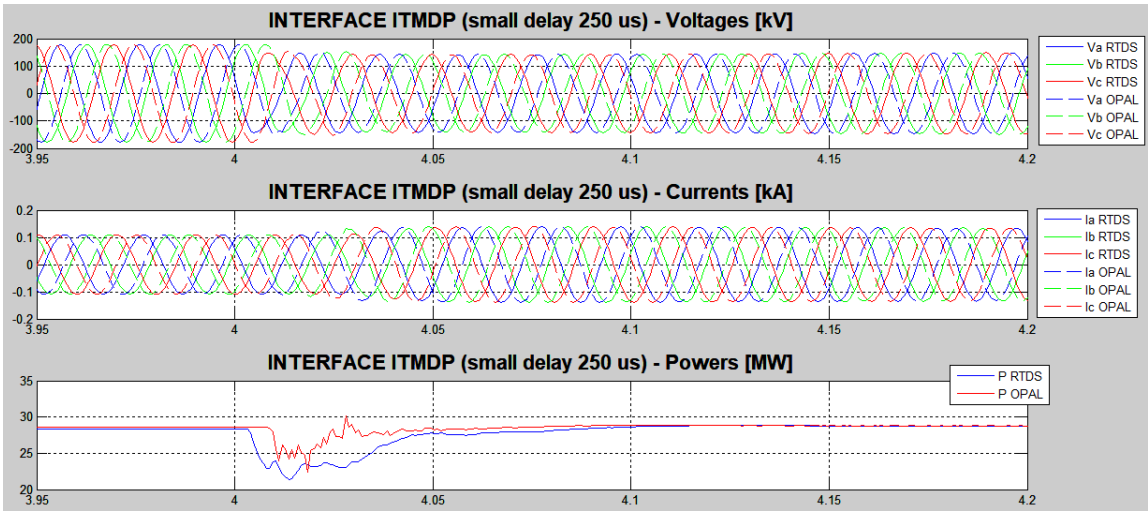


Figure 6.2.6: Coupling variables and powers in the decoupling point using ITM-DP interface, with an additional 250 us interface delay

Finally, the last considered case is using the ITM-DP interface algorithm when a further delay is present in the communication. In particular, two cases have been taken into account:

- A small interface-delay ($\Delta T = 250 \mu s$), whose results are shown in Figure 6.2.6
- A large interface-delay ($\Delta T = 15 ms$), whose results are shown in Figure 6.2.7

From those two cases, it can be seen how the same phase-shift present in the no-interface-delay case is present, as a proof that it is not caused by the communication delay. What is more, good accuracy in power values is ensured and the power transient is detected from the distribution network.

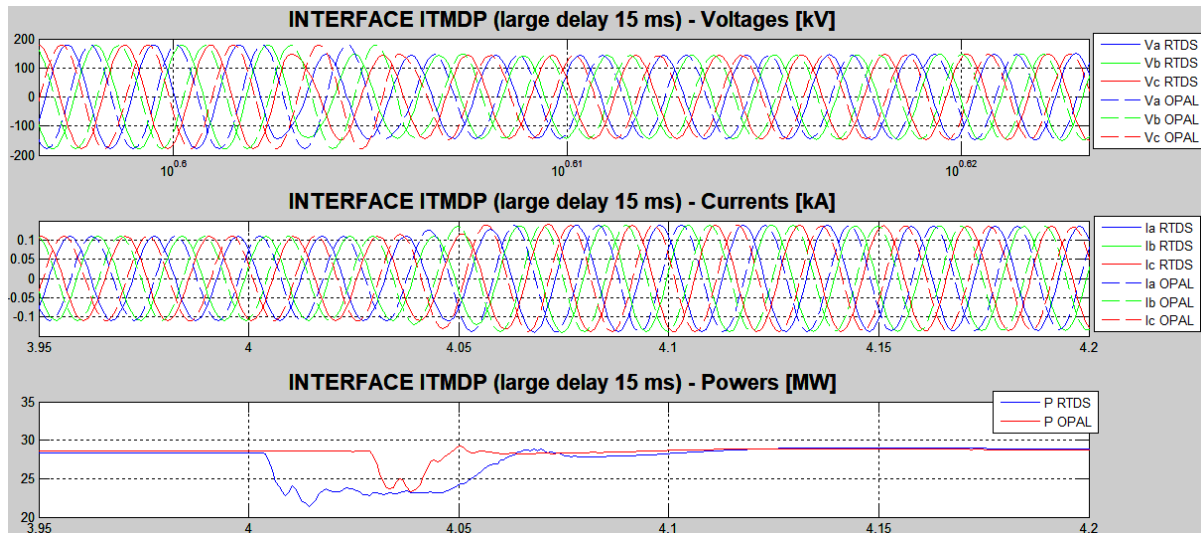


Figure 6.2.7: Coupling variables and powers in the decoupling point using ITM-DP interface, with an additional 15 ms interface delay

6.2.3 Transmission-distribution networks interaction

As already mentioned earlier, this co-simulation set-up was implemented to demonstrate the improvements in the simulation results in terms of interactions between transmission and distribution network when the distribution network is modelled and simulated with higher level of detail.

In this case, thus, it is interesting to see how such an interaction changes using DP instead of instantaneous values for communication, considering the voltage and frequency transients initiated by the generator disconnection.

From Figure 6.2.8, some observations can be done. It must be said that in this figure, results of simulation when using the ITM interface in time-domain with a large time-delay are not illustrated due to very low accuracy.

The top figure to the left shows the voltage profile in bus 3, that is the bus where the generator disconnects in the TN. All the curves represent simulation results when using the various interfaces, and they all allow simulation of the voltage transient with a satisfying accuracy.

The top picture on the right and the bottom picture on the left represent the total DN consumption, in terms of active and reactive powers, after the disconnection. From those, it can be seen how using DP, results of simulation differ during the first instants of transient.

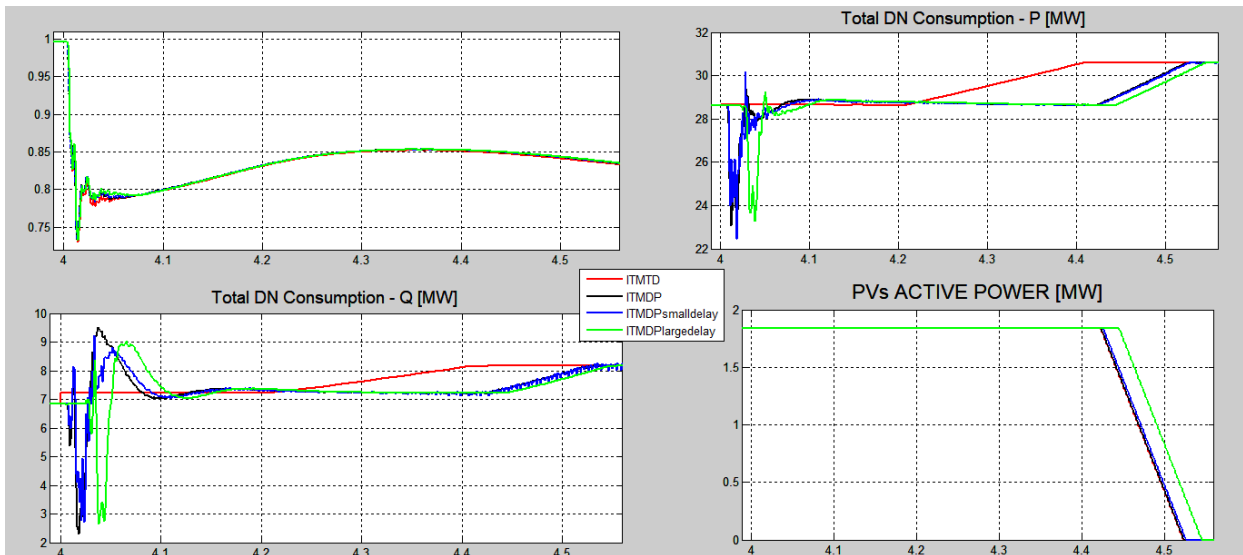


Figure 6.2.8: TN-DN interactions when generator in bus 11 of TN is disconnected at $t = 4$ s

This behavior was expected because dynamic phasors allow a high level of accuracy in steady state but, unfortunately, transients are not perfectly represented. This inaccuracy on the DN side has an impact on the simulation of power transients: in fact, total consumption increases with a different slope compared to the time-domain case, because of the different behavior during the initial transient.

Nevertheless, as shown in the bottom picture on the right, the disconnection of the PVs, which is delayed thanks to the LVRT capability, occurs in the right moment, thus this transient is well represented using dynamic phasors, except in the case with large time-delay. In this circumstance, indeed, an additional shift occurs before the PVs begin to switch off.

Finally, in Figure 6.2.9 and Figure 6.2.10, voltage profiles and frequency responses in all the TN nodes are reported. In this case, simulation results when using ITM in time-domain are illustrated, in order to show improvements when DP. As already shown in chapter 5, voltage transients are simulated with better accuracy than frequency transients when using DP is used for the interface quantities.

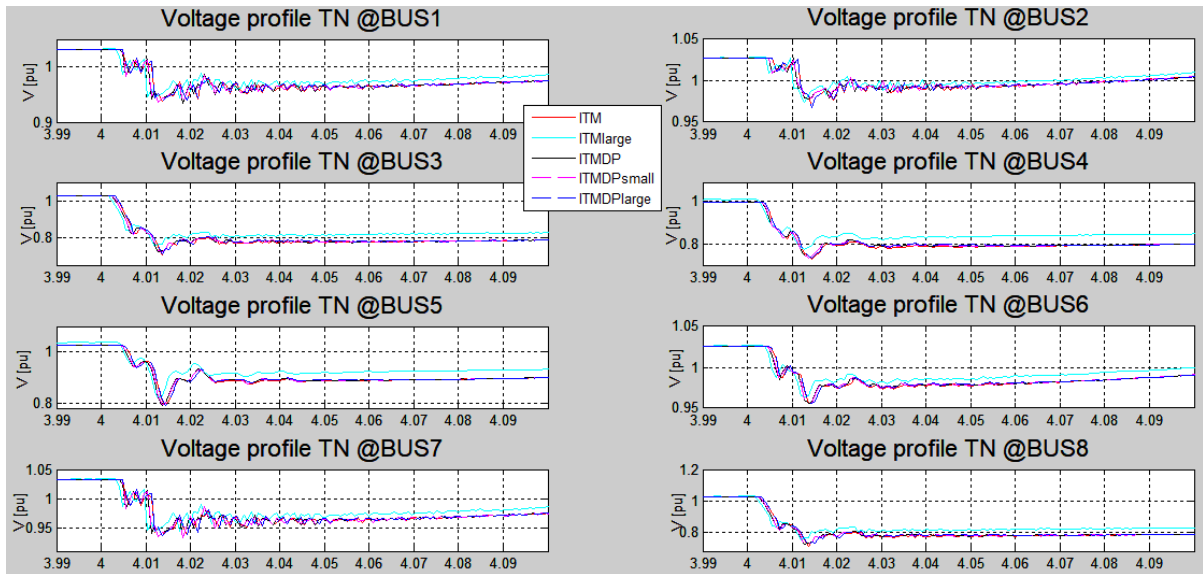


Figure 6.2.9: Voltage profiles of transmission network buses when generator in bus 3 of TN is disconnected at $t = 4$ s

In fact, the voltage gap at $t = 4$ s initiates a frequency transient response in every bus of the network, which is simulated in different fashions with the various interface algorithms.

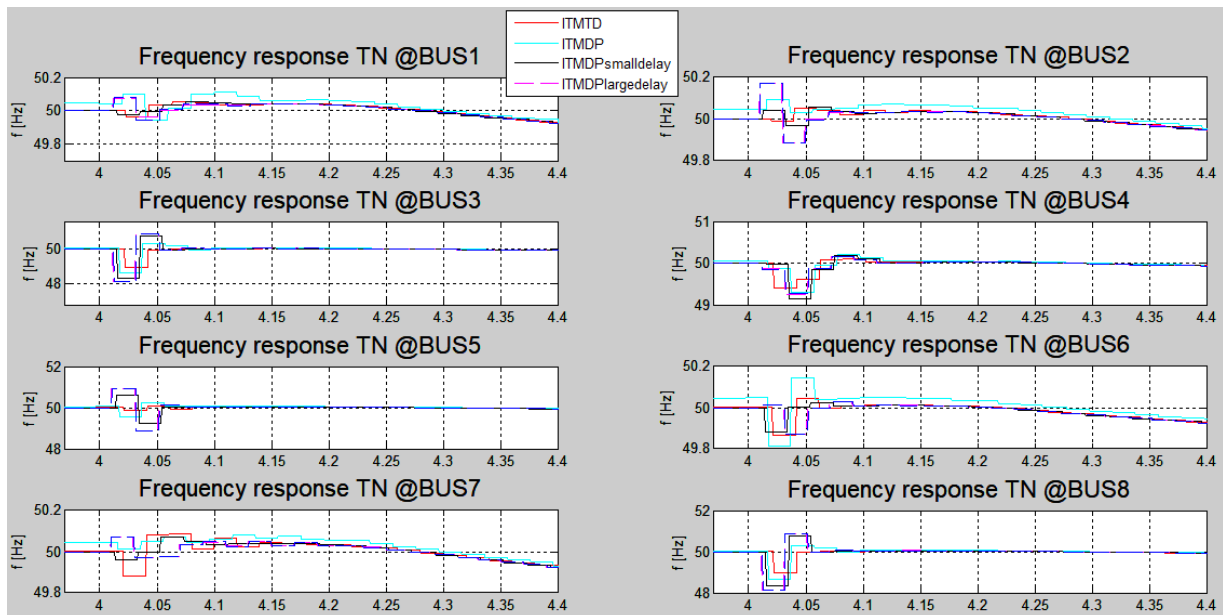


Figure 6.2.10: Frequency responses of transmission network buses when generator in bus 3 of TN is disconnected at $t = 4$ s

6.2.4 Accuracy evaluation

In this subsection, the accuracy evaluation based on metric proposed in this thesis used will be applied to the co-simulation results. In Figure 6.2.11, residual powers during the transient in the transmission network are shown.

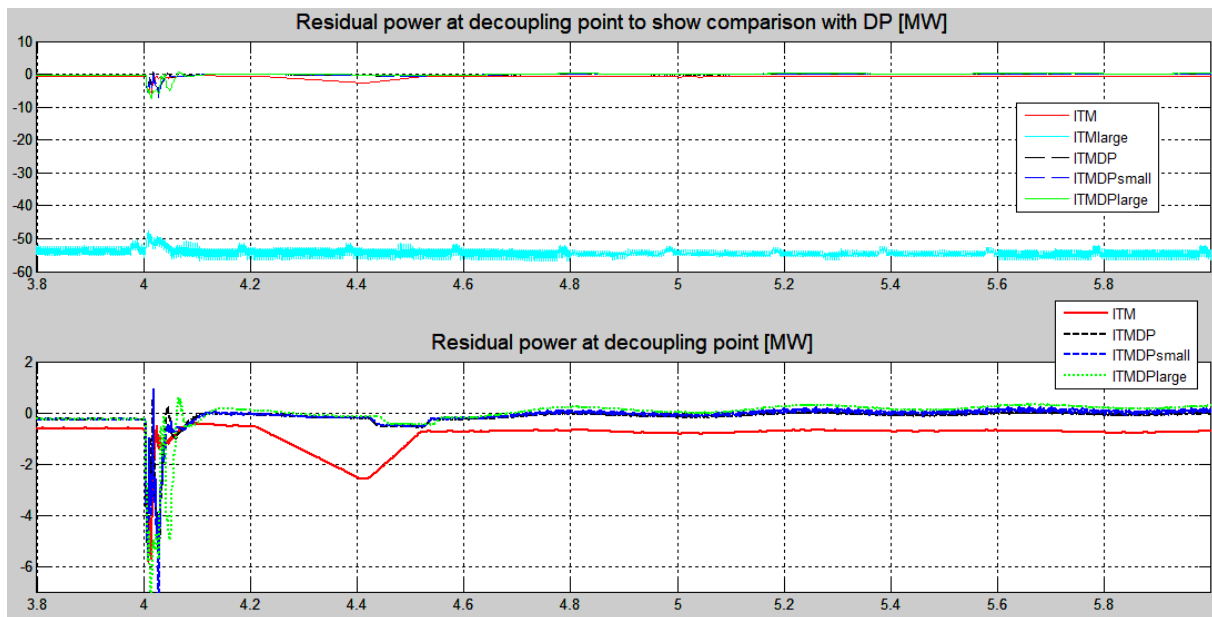


Figure 6.2.11: Residual powers using ITMTD and ITMDP interfaces with various levels of delay (top); zoom of figure to show improvements in accuracy using DP with large delay (bottom)

In detail, the top picture represents global results of the energy residuals calculation, showing the huge difference in terms of virtually added power over the co-simulation time when using the ITM interface in time-domain over a communication channel with a large 15 ms time-delay.

The bottom picture, instead, is a zoom of the top one, that shows differences between the modified ITM interfaces with DP, at the various time-delay levels, compared to the standard ITM interface, which is used as reference to make comparisons. From this picture, it can be seen the usual distortion at the beginning of the transient when using DP. Later, however, less residual energy is generated when using DP compared to instantaneous values. Finally, as expected, the steady state value of residual power for the ITM-DP interface (at every level of interface-delay) is lower than standard ITM interface case and tending towards zero with oscillations.

This last observation has a confirmation when computing residual energies over the entire co-simulation time, which are shown in Figure 6.2.12. From this picture, it can be seen how using ITM in time-domain has an accuracy, in terms of wrongly added energy, almost 5 times worse than using dynamic phasors. Also during the transient, at $t = 4$ s, the accuracy is better using DP, as it can be noticed by the lower increase in residual energies.

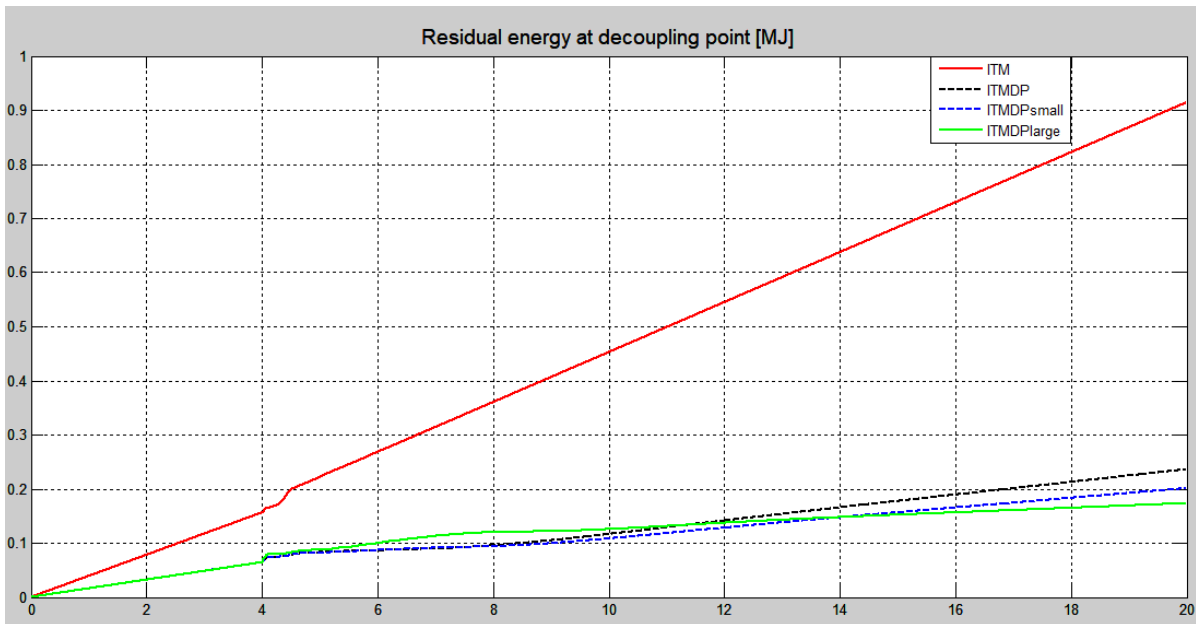


Figure 6.2.12: Residual energies using ITMTD and ITMDP interfaces with various levels of delay

Therefore, this co-simulation has allowed proving in a realistic scenario, the overall properties and improvements of using dynamic phasors in a co-simulation, especially when a large time-delay is present in the communication, which is the case in geographically distributed co-simulation.

As illustrated based on the metrics for the accuracy evaluation, the use of dynamic phasors provides in general more accurate co-simulation results compared to the time-domain-based interface.

7. Conclusions and future work

7.1 Conclusions

The results obtained have been developed starting from reviewing methods introduced in other fields of research, whose purpose is similar to the aim of this thesis. The idea was to develop a proper interface algorithm for co-simulation of power systems, in order to obtain satisfying results in terms of accuracy and stability.

In particular, approaches developed in the Power Hardware-In-the-Loop simulation and bilateral teleoperation have been implemented on simple circuits, in order to show basic characteristics of such methods. In this initial stage, the main issues of such approaches have been clarified. In detail, the common problem is to find out a way to decouple an original system and running a simulation of the two newly defined subsystems, preserving stability and accuracy. In other words, the issue is to preserve the conservation of energy at the interface between the two decoupled systems implemented for co-simulation.

Regarding the PHIL-related methods, the concept of interface algorithm has been studied and adapted to co-simulation of power systems. Both IAs that have been selected to be further explored, the ITM and the TFA interfaces, suffer from accuracy problems deriving from exchanging coupling variables in time-domain between the subsystems when time delay has large values, comparable to the ones measured in communication over the Internet. As a matter of fact, starting from previous research done in the same institute where the work for this thesis has been done, the possibility to transform the instantaneous values into dynamic phasors to improve stability and accuracy of the simulation with large values of time-delay has been addressed.

Analogous to that, the idea has been applied to the TFA interface, meaning that the equations describing the algorithm have been derived in the dynamic phasors domain. This led to a result that concerns the original IA in the first place. In fact, numerical issues are typical with such an interface, because the inversion of a matrix that tends to become singular in steady state is an issue for implementation of this algorithm. Thus, although some attempts to overcome such issues have been implemented, i.e. initialization of algorithm parameters and stop criterion for calculation, satisfying results were not achieved.

Moreover, one method coming from the bilateral teleoperation background has been further investigated, that is the so-called wave transformation. It is a variable transformation executed on the coupling variables before being exchanged with the other subsystem. This method provides stable simulation regardless of the interface time-delay, since it preserves passivity of the communication. This approach has been applied to electric systems using a mechanical-electrical domain transformation, obtaining good results in terms of accuracy and stability. In particular, the wave transformation interface allowed stable simulation results in scenarios that made the standard PHIL-based interfaces unstable.

The first issues concerning this method was the tuning of the wave impedance, which is the characteristic impedance necessary to perform the wave transformation. In fact, this impedance should be tuned according to the parameters of the circuit and the value of the time-delay of communication. As already experienced with ITM interface, a further variable transformation into dynamic phasors has been applied to wave variables, showing the same improvements in

terms of accuracy with large values of time-delay. In addition, using dynamic phasors improves some characteristic of the wave transformation itself, such as removing the dependence of the wave impedance from the time-delay.

Furthermore, it has been illustrated that the use of dynamic phasors instead of instantaneous values as interface quantities allows the best simulation performances, for all the cases under study.

Once that the mentioned IAs were implemented and their performance was tested using simple systems, the next step was to evaluate the accuracy of the simulations executed using a quantitative metric. Thus, based on the concepts of residual power and energy, a metric that does not require knowledge of the original system dynamics has been introduced and applied to various power systems of the developed interface algorithms. This analysis, conducted both in steady and in transient states, led to the conclusion that using dynamic phasors to exchange interface variables ensures the best performance in steady state. On the other hand, interface algorithms based on dynamic phasors have low accuracy during transients, particularly for amplitude and phase variations and faults in the circuit, whereas they have a better response to frequency transients. The accuracy tests have been executed considering a small values and a large value of interface delay, proving how accuracy is very low when instantaneous values are used for the case of a large time delay.

The Wave Transformation interface, overall, has the best accuracy with small interface delay, but it allows acceptable results with large values of delay if the wave impedance is properly tuned.

Finally, running the simulations using realistic power systems models led to the main conclusions of this work:

- The Wave Transformation interface has a wide region of stability for co-simulation, when compared to standard interface algorithms so far used in distributed co-simulation. On the other hand, it is not very suitable for simulation of power systems in DC State, since the variable transformation acts as an averaging operation on the variables themselves. However, the original average values are preserved, so that if the model simulates a system involving AC/DC converters, accuracy of the AC quantities simulation is very high.
- The use of dynamic phasors as means for exchanging information between two coupled simulators allows the best accuracy for every simulation scenario, especially when the communication occurs over a channel with large and variable time delay, as it is over the Internet. In fact, using instantaneous values in this circumstances leads to completely wrong results. However, it has been proved how using dynamic phasors improves the accuracy even with a small interface delay.

7.2 Future work

Although the performance of the newly developed interface algorithms has been tested and their improvements in terms of stability and accuracy of co-simulations has been proved, a number of issues remains unsolved.

First of all, the algebraic loop arising on both ends of the decoupled system when the Wave Transformation interface is used needs to be unwrapped. Otherwise, this interface cannot be used for real-time co-simulation, since the code for the system solution cannot be generated when an algebraic loop is present. As a matter of fact, the method proposed, in literature,

consisting of introducing a one time-step delay in the feedback paths of the closed-loop chain jeopardizes stability of the system. Therefore, other numerical methods should be investigated.

Regarding the TFA interface, further research should be done to adapt this method to DC state systems. As extension of this concept, even using dynamic phasors instead of AC variables in the prediction algorithm is equivalent to use DC quantities. The issue consists of the inversion of a matrix that becomes singular when DC steady state or dynamic phasors are used for simulation. Thus, a better stop criterion to maintain previous results of the algorithm calculation should be implemented.

Finally, as a general input to future research in this field, theoretical stability of the developed interface algorithms should be investigated, especially when using dynamic phasors. In fact, regions of stability for such interfaces are still unknown, and their knowledge is a necessary condition to run a co-simulation, in terms of choosing the proper interface algorithm for the case under study.

References

- [1] J. Bélanger, P. Venne and J.-N. Paquin, "The What, Where and Why of Real-Time Simulation," *IEEE PES General Meeting, Minneapolis, MN, USA*, pp. 37-49, 2010.
- [2] O. Faruque e T. S. e. al., «Real-time simulation technologies for power systems design, testing and analysis,» *IEEE Power Energy Technol. Syst. J.*, vol. 2, n. 2, pp. 63-73, Jun. 2015.
- [3] Guillaud, Xavier, M. O. Faruque, A. Teninge, A. H. Hariri, L. Vanfretti, M. Paolone e V. D. e. al., «Applications of real-time simulation technologies in power and energy systems,» *Power and Energy Technology Systems Journal, IEEE*, vol. 2, n. 3, pp. 103-115, 2015.
- [4] C. Dufour, V. Jalili-Marandi e J. Bélanger, «Real-time simulation using transient stability, ElectroMagnetic Transient and FPGA-based high-resolution solvers,» in *SC Companion: High performace computing, networking storage and analysis*, 2012.
- [5] C. F. Covrig, G. D. Santi, G. Fulli, M. Maserà, M. Olariaga, E. Bompard, G. Chicco, A. Estebasari, T. Huang, E. Pons, F. Profumo, A. Tenconi, R. W. D. Doncker, M. Grigull, A. Monti, M. Stevic e S. Vogel, «A European Platform for Distributed Real Time Modelling & Simulation of Emerging Electricity Systems,» Publications Office of the European Union, EUR, 2016.
- [6] T. Ersal, R. B. Gillespie, M. Brudnak, J. L. Stein e H. K. Fathy, «Effect of coupling point selection on distortion in Internet-distributed Hardware-in-the-Loop simulation,» in *2011 American Control Conference*, San Francisco, CA, USA, 2011.
- [7] T. Ersal, J. L. Stein, M. Brudnak, Z. Filipi, A. Salvi e H. K. Fathy, «DEVELOPMENT OF AN INTERNET-DISTRIBUTED HARDWARE-IN-THE-LOOP SIMULATION PLATFORM FOR AN AUTOMOTIVE APPLICATION,» in *Proceedings of the ASME 2009 Dynamic Systems and Control Conference*, Hollywood, California, USA, 2009.
- [8] W. Ren, M. Steurer e T. L. Baldwin, «Improve the stability and the accuracy of power Hardware-in-the-Loop Simulation by selecting appropriate interface algorithm,» *IEEE TRANSACTIONS ON INDUSTRY APPLICATIONS*, vol. 44, n. 4, pp. 1286-1294, 2008.
- [9] Task Force C6.04.02, «Benchmark Systems for Network Integration of Renewable and Distributed Energy Resources,» CIGRE, 2013.
- [10] C. Dufour, V. Jalili-Marandi, J. Bélanger e L. Snider, «Power system simulation algorithms for parallel computer architectures,» 2012.
- [11] W. Ren, Accuracy Evaluation of Power Hardware-in-the-Loop (PHIL) Simulation, 2007.
- [12] G. F. Lauss, M. O. Faruque, K. Schoder, C. Dufour, A. Viehweider e J. Langston, «Characteristics and design of power hardware-in-the-loop simulations for electrical power systems,» *IEEE Transactions on industrial electronics*, vol. 63, n. 1, pp. 406-417, 2016.

- [13] T. Ersal, M. Brudnak, A. Salvi, J. L. Stein, Z. Filipi e H. K. Fathy, «Development of an internet-distributed Hardware-in-the-Loop Simulation platform for an automotive application,» in *ASME 2009 Dynamic Systems and Control Conference*, Hollywood, California, USA, 2009.
- [14] T. Ersal, A. Tandon, M. J. Brudnak e J. L. Stein, «An observer based framework to improve fidelity in Internet-distributed Hardware-in-the-Loop simulations,» in *Proceedings of the ASME 2013 Dynamic Systems and Control Conference*, Palo Alto, California, USA, 2013.
- [15] T. Ersal, M. Brudnak, A. Salvi, Y. Kim, J. B. Siegel e J. L. Stein, «An Iterative Learning Control Approach to improving fidelity in Internet-distributed Hardware-in-the-Loop Simulation,» *Journal of Dynamic Systems, Measurements and Control*, vol. 136, 2014.
- [16] J. Zehetner, G. Stettinger, H. Kokal e B. Toye, «Real-time Co-simulation for the control of an engine test bench».
- [17] S. Sadjina, S. Skjong, E. Pedersen e L. T. Kyllingstad, «Energy conservation and power bonds in co-simulations: non-iterative adaptive step size control and error estimation,» Norwegian University of Science and Technology, Trondheim, 2016.
- [18] S. Sadjina e E. Pedersen, «Energy conservation and coupling error reduction in non-iterative co-simulations,» Department of Marine Technology, Norwegian University of Science and Technology, Trondheim, 2016.
- [19] D. Hech, «Delayed bilateral teleoperation: a direct force-reflecting control approach,» Technische Universiteit Eindhoven, Eindhoven, 2015.
- [20] «Technische Universität München - Forschung,» [Online]. Available: <https://www.lsr.ei.tum.de/forschung/>. [Consultato il giorno 27 May 2017].
- [21] G. Niemeyer e J.-J. E. Slotime, «Stable adaptive teleoperation,» *IEEE Journal of Oceanic engineering*, vol. 16, n. 1, pp. 152-162, 1991.
- [22] I. Vittorias e S. Hirche, «Stable teleoperation with communication unreliabilities and approximate human/environment dynamics knowledge,» in *American Control Conference*, 2009.
- [23] N. A. Tanner e G. Niemeyer, «Online Tuning of Wave Impedance in Telerobotics,» in *Proceedings of the 2004 IEEE Conference on Robotics, Automation and Mechatronics*, 2004.
- [24] S. Munir e W. J. Book, «Wave-Based Teleoperation with Prediction,» in *Proceedings of the American Control Conference*, Arlington, VA, 2001.
- [25] B. Hannaford e J.-H. Ryu, «Time-domain passivity control of haptic interfaces,» *IEEE Transactions on Robotics and Automation*, vol. 18, n. 1, pp. 1-10, 2002.
- [26] Y. Ye, Y.-J. Pan, Y. Gupta e J. Ware, «A power-based time domain passivity control for haptic interfaces,» *IEEE Transactions on Control Systems Technology*, vol. 19, n. 4, pp. 874-883, 2011.

- [27] M. Franken, S. Stramigioli, S. Misra, C. Secchi e A. Macchelli, «Bilateral telemanipulation with time delays: a two-layer approach combining passivity and transparency,» *IEEE Transactions on Robotics*, vol. 27, n. 4, pp. 741-756, 2011.
- [28] D. Heck, A. Saccon e H. Nijmeijer, «A two-layer architecture for force-reflecting bilateral teleoperation with time delays,» in *IEEE 54th Annual Conference on Decision and Control (CDC)*, Osaka, Japan, 2015.
- [29] J. P. Hespanha, P. Naghshtabrizi e Y. Xu, «A survey of recent results in Networked Control Systems,» *Proceedings of the IEEE*, vol. 95, n. 1, pp. 138-162, 2007.
- [30] X. Wu, S. Lentijo e A. Monti, «A novel interface for power-hardware-in-the-loop simulation,» in *Proceedings Computers in Power Electronics*, 2004 IEEE Workshop, 2004.
- [31] X. Wu e A. Monti, «Methods for partitioning the system and performance evaluation in power-hardware-in-the-loop simulation - Part I,» IEEE, 2005.
- [32] R. J. Anderson e M. W. Spong, «Asymptotic stability for force reflecting teleoperations with time delay,» in *IEEE International Conference Robotics and Automation*, Scottsdale, AZ, 1989.
- [33] R. Muradore e P. Fiorini, «A Review of Bilateral Teleoperation Algorithms,» *Acta Polytechnica Hungarica*, vol. 1, n. 13, pp. 191-208, 2016.
- [34] N. Chopra, M. W. Spong, S. Hirche e M. Buss, «Bilateral Teleoperation over the Internet: the Time Varying Delay Problem,» in *American Control Conference. Proceedings of the 2003*, Denver, CO, USA, 2003.
- [35] N. Yasrebi e D. Constantinescu, «Passive wave variable control of haptic interaction with an unknown virtual environment,» in *IEEE International Conference on Robotics and Automation*, Shanghai, China, 2011.
- [36] M. A. Kulasza, Generalized dynamic phasor-based simulation for power systems, Winnipeg: Department of Electrical and Computer Engineering, University of Manitoba, 2014.
- [37] T. H. Demiray, «Simulation of power system dynamics using dynamic phasor models,» Swiss Federal Institute of Technology, Zurich, 2008.
- [38] M. Stevic, A. Monti e A. Benigni, «Development of a simulator-to-simulator interface for geographically distributed simulation of power systems in real time,» in *IECON 2015 - 41st Annual Conference of the IEEE Industrial Electronics Society*, Yokohama, Japan, 2015.
- [39] Mathworks, «VSC-Based HVDC Transmission System (Detailed Model),» [Online]. Available: <https://de.mathworks.com/help/phymod/sps/examples/vsc-based-hvdc-transmission-system-detailed-model.html>.